University of Pennsylvania
ScholarlyCommons

Publicly Accessible Penn Dissertations

1-1-2016

Monocyte and Macrophage Apoptosis and Activation During HIV-1 Infection and Antiretroviral Therapy

Sean Christopher Patro
University of Pennsylvania, patro@mail.med.upenn.edu

Follow this and additional works at: http://repository.upenn.edu/edissertations

 Part of the Allergy and Immunology Commons, Immunology and Infectious Disease Commons, Medical Immunology Commons, and the Virology Commons

Recommended Citation
Patro, Sean Christopher, "Monocyte and Macrophage Apoptosis and Activation During HIV-1 Infection and Antiretroviral Therapy" (2016). *Publicly Accessible Penn Dissertations*. 1936.
http://repository.upenn.edu/edissertations/1936

This paper is posted at ScholarlyCommons. http://repository.upenn.edu/edissertations/1936
For more information, please contact libraryrepository@pobox.upenn.edu.

Monocyte and Macrophage Apoptosis and Activation During HIV-1 Infection and Antiretroviral Therapy

Abstract
Monocytes and macrophages represent a cell lineage integral to multiple aspects of HIV-1 infection, dissemination, and pathogenesis. They also play a fundamental role in innate host defense and may act as a tissue-privileged viral reservoir during all stages of infection. In the current ART-era of the HIV pandemic, HIV-seropositive patients can maintain undetectable viral loads for years. Nevertheless, this population faces central nervous system, cardiovascular, and other HIV-related co-morbidities, many of which are characterized by underlying monocyte/macrophage contributions. To investigate the regulation of the survival and activation profiles of monocytes/macrophages during HIV-1 infection in vivo, we performed the following sets of experiments: (1) we determined monocyte apoptosis profiles in previously uncharacterized highly viremic HIV (+) donors and assessed monocyte gene expression associated with monocyte apoptosis outcome; (2) we tested the impact of ART and CCR5 antagonism during advanced HIV-1 infection on the reversal of monocyte/macrophage activation; (3) we tested the impact of the interferon stimulated genes (ISGs) IFI6 and IFI27 as an underlying mechanism regulating monocyte apoptosis in the context of HIV-1 infection. Our results indicate both constitutive and oxidative stress-induced monocyte apoptosis are elevated in HIV (+) individuals with viral loads above 40,000 HIV-1 copies/mL and are associated with decreasing CD4 count. Furthermore, elevated apoptosis is associated with a shift in interferon stimulated gene and Bcl-2 family gene expression. Longitudinal analysis of ART treatment during advanced HIV-1 infection (nadir CD4 count < 100 cells/mm3) demonstrated differential reversal of cell-associated and soluble biomarkers of monocyte/macrophage activation. We show the addition of CCR5 antagonism (Maraviroc) does not impact the reversal of monocyte/macrophage activation beyond the impact of standard ART alone. Finally, we investigate the roles of the ISGs IFI6 and IFI27 in the regulation of monocyte apoptosis in vitro. Our work demonstrates the impact of viral and host pressures on monocyte survival/apoptosis and activation state during distinct stages of HIV-1 infection.

Degree Type
Dissertation

Degree Name
Doctor of Philosophy (PhD)

Graduate Group
Cell & Molecular Biology

First Advisor
Luis J. Montaner

Keywords
Activation, Apoptosis, HIV, Macrophage, Monocyte, Therapy

This dissertation is available at ScholarlyCommons: http://repository.upenn.edu/edissertations/1936

Subject Categories
Allergy and Immunology | Immunology and Infectious Disease | Medical Immunology | Microbiology | Virology

This dissertation is available at ScholarlyCommons: http://repository.upenn.edu/edissertations/1936

MONOCYTE AND MACROPHAGE APOPTOSIS AND ACTIVATION DURING HIV-1 INFECTION AND ANTIRETROVIRAL THERAPY

Sean C. Patro

A DISSERTATION

in

Cell and Molecular Biology

Presented to the Faculties of the University of Pennsylvania

in

Partial Fulfillment of the Requirements for the

Degree of Doctor of Philosophy

2016

Supervisor of Dissertation

_____
Luis J. Montaner, D.V.M., D.Phil.
Professor of Medicine

Graduate Group Chairperson

_____
Daniel S. Kessler, Ph.D
Associate Professor of Cell and Developmental Biology

Dissertation Committee
Michael R. Betts, Ph.D., Associate Professor of Microbiology
Ronald G. Collman, M.D., Professor of Medicine
Dennis L. Kolson, M.D., Ph.D., Professor of Neurology
Louise C. Showe, Ph.D., Professor of Molecular and Cellular Oncogenesis

MONOCYTE AND MACROPHAGE APOPTOSIS AND ACTIVATION

DURING HIV-1 INFECTION AND ANTIRETROVIRAL THERAPY

COPYRIGHT

2016

Sean Christopher Patro

This work is licensed under the
Creative Commons Attribution-
NonCommercial-ShareAlike 3.0
License

To view a copy of this license, visit

http://creativecommons.org/licenses/by-ny-sa/2.0/

This thesis is dedicated to my family.

Thank you for your unwavering support and love.

ACKNOWLEDGEMENTS

I want to thank my partner Brittany Good for walking with me on this journey towards a PhD.

I want to thank my mentor, Luis. J. Montaner, for the opportunity to be a part of this team. His commitment, guidance, and enthusiasm have been critical in my maturation as a scientist. I thank all the members of the Montaner lab for providing a stimulating environment for the growth of the scientific mind.

Beth Peterson
Jennifer Dubin
Costin Tomescu
Emmanouil (Manolis) Papasavvas
Matthew Fair
Shaheed Abdulhaqq
Brian Ross
Jocelin Joseph
Charity Calloway
Farzaneh Sabahi
Livio Azzoni
Agnieszka (Agnes) Mackiewicz

I would like to thank and acknowledge the contributors to the work performed in this dissertation: researchers at Wistar, clinical coordinators and physicians, rotation students, and the HIV-patients who volunteered to participate in these studies.

I would also like to thank my thesis committee, Michael R. Betts, Ronald G. Collman, Dennis L. Kolson, and Louise C. Showe for their guidance along the way.

Wistar Institute:
Deborah D. Davis
Ramana V. Davuluri
Sharmistha Pal
Yingtao Bi
David Schultz
Henry Hoff
Andrew V. Kossenkov
Celia Chang
Jeffrey Faust

Coordinators/ Physicians:
Kenneth Lynn
Karam C. Mounzer
Jay R. Kostman

UPENN/Wistar Rotation Students:
Megan Wise
Amanda Versace
Alana Sharp

The CADIRIS Study:
Juan G. Sierra-Madero
Mohammed S. Rassool
Ian Sanne

UPENN CFAR:
Ronald G. Collman
James A. Hoxie
Farida Shaheen
Steven Bryan

I. ABSTRACT

MONOCYTE AND MACROPHAGE APOPTOSIS AND ACTIVATION DURING HIV-1 INFECTION AND ANTIRETROVIRAL THERAPY

Sean C. Patro

Dr. Luis J. Montaner

Monocytes and macrophages represent a cell lineage integral to multiple aspects of HIV-1 infection, dissemination, and pathogenesis. They also play a fundamental role in innate host defense and may act as a tissue-privileged viral reservoir during all stages of infection. In the current ART-era of the HIV pandemic, HIV-seropositive patients can maintain undetectable viral loads for years. Nevertheless, this population faces central nervous system, cardiovascular, and other HIV-related co-morbidities, many of which are characterized by underlying monocyte/macrophage contributions. To investigate the regulation of the survival and activation profiles of monocytes/macrophages during HIV-1 infection *in vivo*, we performed the following sets of experiments: (1) we determined monocyte apoptosis profiles in previously uncharacterized highly viremic HIV (+) donors and assessed monocyte gene expression associated with monocyte apoptosis outcome; (2) we tested the impact of ART and CCR5 antagonism during advanced HIV-1 infection on the reversal of monocyte/macrophage activation; (3) we tested the impact of the interferon stimulated genes (ISGs) IFI6 and IFI27 as an underlying mechanism regulating

monocyte apoptosis in the context of HIV-1 infection. Our results indicate both constitutive and oxidative stress-induced monocyte apoptosis are elevated in HIV (+) individuals with viral loads above 40,000 HIV-1 copies/mL and are associated with decreasing CD4 count. Furthermore, elevated apoptosis is associated with a shift in interferon stimulated gene and Bcl-2 family gene expression. Longitudinal analysis of ART treatment during advanced HIV-1 infection (nadir CD4 count < 100 cells/mm^3) demonstrated differential reversal of cell-associated and soluble biomarkers of monocyte/macrophage activation. We show the addition of CCR5 antagonism (Maraviroc) does not impact the reversal of monocyte/macrophage activation beyond the impact of standard ART alone. Finally, we investigate the roles of the ISGs IFI6 and IFI27 in the regulation of monocyte apoptosis *in vitro*. Our work demonstrates the impact of viral and host pressures on monocyte survival/apoptosis and activation state during distinct stages of HIV-1 infection.

Table of Contents

II. Abbreviations

HIV-1: Human immunodeficiency virus type 1

ART: Anti-retroviral therapy

CDC: Centers for disease control and prevention

AIDS: Acquired immune deficiency syndrome

HTLV-III: Human T-lymphotropic virus type III

LAV: Lymphadenopathy-associated virus

AZT/ZDV: Azidothymidine/Zidovudine

NRTI: Nucleoside reverse transcriptase inhibitor

NNRTI: Non-nucleoside reverse transcriptase inhibitor

NtRTI: Nucluotide reverse transcriptase inhibitor

cART/HAART: combined/highly-active anti-retroviral therapy

NHP: Non-human primate

SIV: Simian immunodeficiency virus

BrdU: Bromodeoxyuridine (5-bromo-2'-deoxyuridine)

PHA: Phytohaemagglutinin

PBMC: Peripheral blood mononuclear cells

APOBEC: Apolipoprotein B mRNA editing enzyme, catalytic polypeptide-like

HIVE/SIVE: HIV/SIV encephalopathy

HIV-2: Human immunodeficiency virus type 2

SAMHD1: SAM domain and HD domain-containing protein 1

miRNA: micro RNA

ISG: Interferon stimulated gene

Viperin/RSAD2: Virus Inhibitory Protein, Endoplasmic Reticulum-Associated, Interferon-Inducible /Radical S-Adenosyl Methionine Domain Containing 2

MDM: Monocyte-derived macrophage

CNS: Central nervous system

sCD14/sCD163: Soluble CD14/CD163

CSF: Cerebrospinal fluid

GI: Gastrointestinal

LPS: Lipopolysacharride

DC: Dendritic cell

FasL: Fas-ligand

TUNEL: Terminal deoxynucleotidyl transferase dUTP nick end labeling

ESN: Exposed seronegative

STAT-1: signal transducer and activator of transcription 1

TRAIL: TNF-related apoptosis-inducing ligand; sTRAIL, mTRAIL: soluble, membrane TRAIL

mDC: myeloid dendritic cell

M-CSF/CSF1: Macrophage colony-stimulating factor/Colony stimulating factor 1

IRF: Interferon regulatory factor

IFN-α: Interferon alpha; IFN-γ: Interferon gamma

STI: scheduled treatment interruption

SN/Sialoadhesin/SIGLEC1: Sialic acid-binding immunoglobulin-type lectin type 1

TLR: Toll-like receptor

BAFF: B cell-activating factor

IFITM1-3: Interferon-induced transmembrane protein 1-3

ADAM17/TACE: A disintegrin and metalloproteinase domain 17/ tumor necrosis factor-α-converting enzyme

ERK/MAPK: Extracellular-signal-regulated kinases/Mitogen-activated protein kinases

c-FLIP/CFLAR: FLICE-like inhibitory protein/CASP8 and FADD-like apoptosis regulator

HIC: Human immunology core

LVL: Low viral load (Viral load < 100,000 copies/mL in Section 2.2; viral load < 40,000 copies/mL in Section 2.3 onward)

HVL: High viral load (Viral load > 100,000 copies/mL in Section 2.2; viral load > 40,000 copies/mL in Section 2.3 onward)

NLR: NOD-like receptor

U/mL: units/mL (IFN-α)

RT-PCR: Reverse transcription polymerase chain reaction

mRNA/cDNA/rRNA: messenger RNA/complimentary DNA/ribosomal RNA

HUP/FIGHT: Hospital of the University of Philadelphia/ Philadelphia Field Initiating Group for HIV-1 Trials

ELISA: Enzyme-linked immunosorbent assay

CADIRIS: CCR5 antagonism to decrease the incidence of immune reconstitution inflammatory syndrome

IRIS: immune reconstitution inflammatory syndrome

MVC: Maraviroc

EFV: Efavirenz

TDF: Tenofovir

FTC: Emtricitabine

MFI: Mean fluorescence intensity

HLA-DR: Human leukocyte antigen-D related

NK: Natural killer cell

MM1: Monomac1

MCS: Multiple cloning site

VSV: Vesicular stomatitis virus

TREmin: Tet-response element

IRES: Internal ribosome entry site

eGFP: Enhanced green fluorescent protein

hPGK promoter: Human phosphoglycerate kinase promoter

III. List of Tables

IV. List of Illustrations

V. Preface: Publications and Presentations

Publications

Patro SC, Azzoni L, Joseph J, Fair M, Sierra-Madero JG, Rassool MS, Sanne I, Montaner LJ. Antiretroviral therapy in HIV-1-infected individuals with CD4 count below 100 cells/mm^3 results in differential recovery of monocyte activation. *J Leukoc Biol.* **Accepted Nov 1 2015.**

Patro SC, Pal S, Bi Y, Lynn K, Mounzer KC, Kostman JR, Davuluri RV, Montaner LJ. Shift in Monocyte Apoptosis with Increasing Viral Load and Change in Apoptosis-related ISG/Bcl2-family Gene Expression in Chronic HIV-1 Infected Subjects. *J Virol.* **2015 Jan**; 89(1):799-810. doi: 10.1128/JVI.02382-14. Epub 2014 Oct 29.

Patro SC, Montaner LJ. Editorial: Is HIV-1 induction of macrophage expression of PD-L1 and PD-L2 its weakest or strongest link to disease? HIV-1 plays both sides by augmenting and limiting T cell activation to survive in vivo. *J. Leukoc Biol.* **2011 Apr**; 89 (4). p. 495-498.

Wilen CB, Wang J, Tilton JC, Miller JC, Kim KA, Rebar EJ, Sherrill-Mix SA, **Patro SC**, Secreto AJ, Jordan AP, Lee G, Kahn J, Aye PP, Bunnell BA, Lackner AA, Hoxie JA, Danet-Desnoyers GA, Bushman FD, Riley JL, Gregory PD, June CH, Holmes, MC, Doms RW. Engineering HIV-resistant human CD4+ T cells with CXCR4-specific zinc-finger nucleases. *PLoS Pathog.* **2011 Apr**. 7 (4).

Presentations

2014 Shift in Monocyte Apoptosis with Increasing Viral Load and Change in Apoptosis-related ISG/Bcl2-family Gene Expression in Chronic HIV-1 Infected Subjects. Poster Presentation. *2014 Penn CFAR Annual Research Retreat.* Philadelphia, Pennsylvania, United States. Dec 12, 2014.

2012 Differential ISG12 family gene expression is associated with monocyte apoptosis sensitivity in high HIV-1 viremic patients versus monocyte apoptosis resistance in low viremic patients. Poster Presentation. *45th Annual Meeting of the Society for Leukocyte Biology.* Maui, Hawaii, United States. Oct 23-28, 2012.

2012 Differential ISG12 family gene expression is associated with monocyte apoptosis sensitivity in high HIV-1 viremic patients versus monocyte apoptosis resistance in low viremic patients. Oral and Poster Presentation. *8th International Workshop: HIV, Cells of Macrophage/Dendritic Lineage, and Other Reservoirs: Pathogenic and Therapeutic Implications.* Stresa, Italy, May 11, 2012.

CHAPTER 1: Introduction

1.1 The HIV-1 pandemic: The early years, infection, and treatment

The earliest clinical reports of HIV in the United States occurred in the summer of 1981 (1, 2). Unusual presentations of *Pneumocystis carinii* pneumonia, Kaposi's sarcoma, and other infections typically associated with immunosuppression were documented in previously healthy homosexual men in California and New York City (3-6). In September 1982, the CDC coined the term AIDS (acquired immune deficiency syndrome) to describe the growing epidemic (7). In 1983, two research groups isolated a retrovirus from AIDS patients, Robert Gallo and colleagues in the United States (termed HTLV-III, human T-lymphotropic virus type III) and Françoise Barré-Sinoussi, Luc Montagnier, and colleagues in France (termed LAV, lymphadenopathy-associated virus) (8, 9). This retrovirus would become known as HIV and the etiological agents of AIDS.

The natural disease course of HIV-1 infection can be divided into three stages: acute, chronic, and advanced infection/AIDS (Figure 1.1 (10), Reviewed in (11)). Acute infection typically lasts 9 to 12 weeks and can present clinically as a flu-like acute retroviral syndrome. This period is characterized by peak viral replication, viral seeding of host lymphoid tissue, and severe CD4 depletion of gut-associated lymphoid tissue (12). During chronic infection, viremia is partially controlled by host immune responses, reaching a relatively stable viral load set-point (13, 14). The length of chronic infection is highly variable, and viral set point is predictive of time to progression to AIDS (15, 16). Progression to AIDS (advanced infection) occurs when CD4 count decreases below 200 cells/mm^3 or

with the onset of AIDS-associated opportunistic infections, as defined per CDC guidelines.

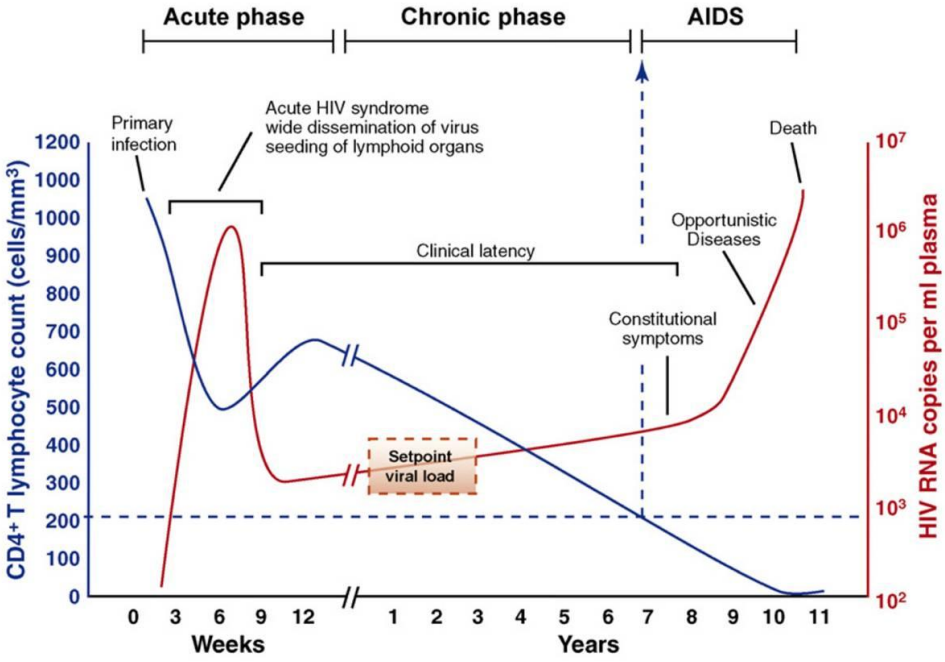

Figure 1.1: HIV-1 natural disease course.
HIV-1 viral load (red, HIV-1 copies/mL) and CD4 count (blue, CD4 T-cells/mm^3) during untreated HIV-1 infection. The infection stages are acute, chronic, and advanced infection/AIDS. [10]

The first drug to treat HIV infection, azidothymidine (AZT/ZDV), was approved by the FDA on March 19, 1987 and belongs to the reverse transcriptase inhibitor class of anti-retroviral drugs, specifically a nucleoside reverse transcriptase inhibitor (NRTI). The current arsenal of anti-retroviral drugs targets multiple stages of the viral life cycle and includes reverse transcriptase inhibitors (nucleoside (NRTI), non-nucleoside (NNRTI), and nucleotide (NtRTI)), protease inhibitors, integrase inhibitors, and entry inhibitors (Table 1.1). By the

mid 1990s, combination therapy (multiple anti-retroviral drugs, with at least two from different classes) began the era of cART/HAART (combined/highly active anti-retroviral therapy), drastically extending the lifespan and improving prognosis of HIV-infected individuals.

Drug	Abbreviation	Year Approved	Company
NUCLEOSIDE/TIDE REVERSE TRANSCRIPTASE INHIBITORS (NRTIs)			
Zidovudine	ZDV	1987	Gilead
Didanosine	ddI	1991	Bristol-Myers Squibb
Stavudine	d4T	1994	Bristol-Myers Squibb
Lamivudine	3TC	1995	ViiV
Abacavir	ABC	1998	ViiV
Tenofovir disoproxil fumarate	TDF	2001	Gilead
Emtricitabine	FTC	2003	Gilead
Tenofovir alafenamide	TAF	2015	Gilead
NON-NUCLEOSIDE REVERSE TRANSCRIPTASE INHIBITORS (NNRTIs)			
Nevirapine	NVP	1996	Boehringer Ingelheim
Efavirenz	EFV	1998	Bristol-Myers Squibb
Etravirine	ETR	2008	Tibotec
Rilpivirine	RPV	2011	Tibotec
PROTEASE INHIBITORS (PIs)			
Saquinavir	SQV	1995	Roche
Indinavir	IDV	1996	Merck
Ritonavir	RTV	1996	Abbot
Nelfinavir	NFV	1997	Pfizer
Lopinavir	LPV	2000	Abbot
Atazanavir	ATV	2003	Bristol-Myers Squibb
Fosamprenavir	FPV	2003	ViiV
Tipranavir	TPV	2005	Boehringer Ingelheim
Darunavir	DRV	2006	Tibotec
INTEGRASE INHIBITORS (INSTIs)			
Raltegravir	RAL	2007	Merck
Elvitegravir	EVG	2012	Gilead
Dolutegravir	DTG	2013	ViiV
FUSION INHIBITOR			
Enfuviritide	T20	2003	Roche
CCR5 ANTAGONIST			
Maraviroc	MVC	2007	Pfizer

Table 1.1: HIV antiretroviral therapy (ART).
ART drugs, abbreviations, year approved, and company sorted by class.

1.2 HIV target cells: CD4 T-cells and monocytes/macrophages

1.2.1 HIV CD4 T-cell infection and activation

HIV viral particles target host immune cells expressing the receptor CD4 and one of two co-receptors, CCR5 and CXCR4 (17). As it follows, the primary targets of HIV-1 infection are CD4 T-cells (CCR5/CXCR4) of the adaptive immune system and monocytes and macrophages (CCR5) of the innate immune system.

Depletion, activation, and dysfunction of CD4 T-cells have come to be the signature of HIV-1 infection (12, 18, 19). CD4 T-cell loss during HIV-1 infection is mediated by multiple mechanisms including cytopathic effects by viral replication, immune clearance of infected cells by CD8 T-cells and natural killer cells (13, 14, 20, 21), and bystander killing of uninfected CD4 T-cells by interactions with viral proteins and apoptotic ligands on antigen presenting cells (Figure 1.2, Reviewed in (18, 22)). In addition, the activation state of CD4 and/or CD8 T-cells (defined by the expression of CD38 and/or HLA-DR) is associated with both disease progression and poor immunological response to therapy (16, 23-25). It is also appreciated that sustained viremia, immune activation, and exposure to microbial products during HIV infection leads to a state of T-cell exhaustion in both CD4 and CD8 compartments mediated by chronic stimulation and induction of inhibitory ligands and receptors such as PDL-1/PDL-2-PD-1, among others (26-28).

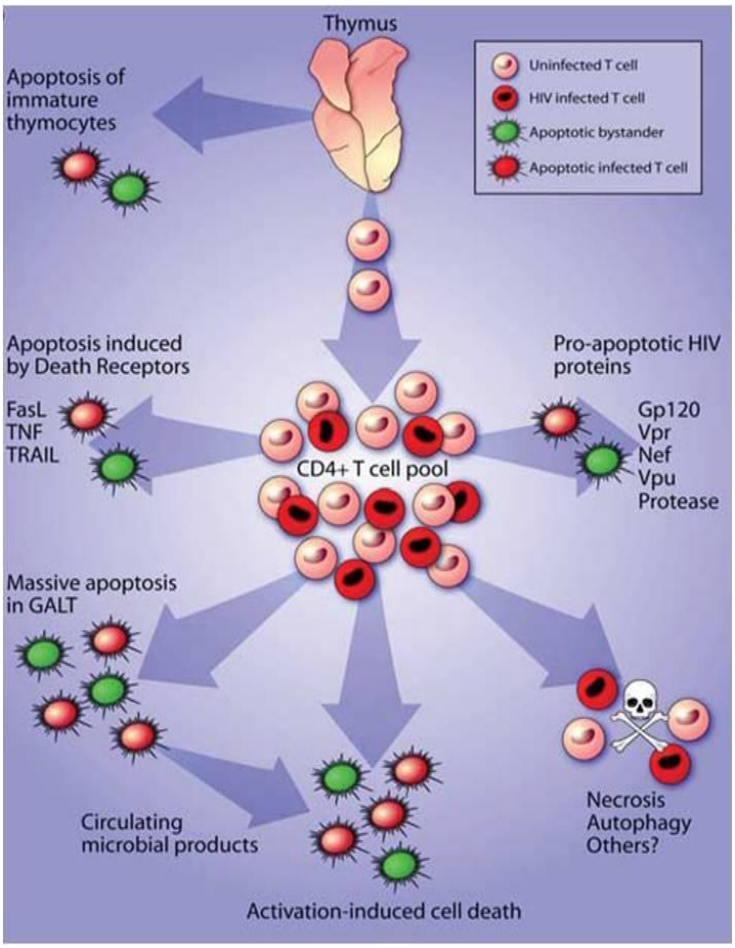

Figure 1.2: Mechanisms of CD4 T-cell death during HIV-1 infection. During untreated infection, CD4 T-cell death results from apoptotic pressure of HIV-1 proteins, activation-induced death, and extrinsic apoptosis mediated by death ligands, often presented by on antigen presenting cells (APC). (Adapted from [22].)

1.2.2 Monocyte heterogeneity and infection by HIV/SIV

Monocytes are phagocytic cells that are generated from myeloid progenitors in bone marrow, circulate in blood, and migrate into tissue, maturing into macrophages in response to chemotactic and inflammatory signals (29). Blood monocytes exist in heterogeneous populations, similar in both humans and rhesus macaques, and much of our understanding of monocyte heterogeneity

and phenotypes in both healthy and HIV/SIV-infected conditions has been obtained from non-human primate (NHP) models (29-31). Classical monocytes ($CD14^{++}CD16^{-}$) represent the largest subset under normal conditions while the intermediate ($CD14^{++}CD16^{+}$) and non-classical ($CD14^{+}CD16^{++}$) subsets are expanded during HIV/SIV-infection and other inflammatory conditions (30, 32-36) (Figure 1.3). Separate transcriptional profiles have been described for $CD16^{-}$ and $CD16^{+}$ subsets (37), and BrdU pulse-chase has demonstrated that maturation of monocytes in blood progresses from classical to intermediate to non-classical monocytes upon differentiation (29). Furthermore, the $CD16^{+}$ subsets bear significance based on permissiveness to infection (30, 38-40) and immunophenotypic similarity to infected macrophages in tissue (41, 42). In light of such heterogeneity, subset composition and phenotype are an important consideration of monocyte studies regarding all stages of HIV-infection.

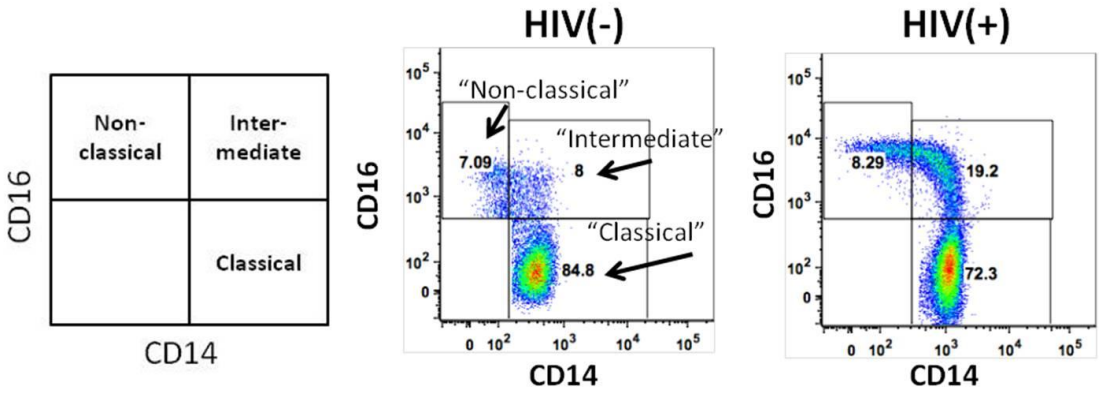

Figure 1.3: Human monocyte subsets.
Human blood monocytes are divided into classical ($CD14^{++}CD16^{-}$), intermediate ($CD14^{++}CD16^{+}$), and non-classical ($CD14^{+}CD16^{++}$) subsets by expression of CD14 and CD16 (left). Shown are representative HIV (-) (middle) and HIV (+) (right) donors.

Among HIV-infected individuals (both viremic and ART-suppressed), it is estimated that less than 0.1% of circulating monocytes harbor HIV-1 DNA (38, 43, 44). The degree of ongoing replication in monocytes *in vivo* is a source of debate as early studies found monocytes from HIV (+) patients could seed infection of PHA-stimulated PBMC co-culture *in vitro* (45) while more recent studies have proposed the hypothesis that tissue macrophages may reflect phagocytosed infected T-cells rather than macrophage infection (46).Additionally, viral sequence analysis has suggested low levels of monocyte virus production (38). The $CD16^+$ subsets of blood monocytes has been proposed to be permissive to infection as they harbor higher levels of HIV DNA when compared to the $CD16^-$ fraction, explained by higher expression of CCR5 and expression of high molecular weight APOBEC3G (compared to restrictive, low molecular weight APOBEC3G in $CD14^+CD16^-$ monocytes) (40). Similarly, intermediate monocytes are reported to have the highest levels of SIV DNA in acutely infected rhesus macaques (30). The most direct evidence for the importance of infection of $CD16^+$ monocytes is supported by the detection of p28/p24-positive, $CD16^+$ macrophages in brain of SIVE macaques and autopsy of HIVE patients (41, 47).

The resistance of monocytes to infection compared to tissue macrophages has been assigned to the activity of a number of host intrinsic factors and other mechanisms that limit infection and replication in monocytes (Figure 1.4, Reviewed in (48, 49)). Restriction of monocyte infection is considered to occur post-entry and pre-integration (50). Transcriptional profiling of monocytes

suggests expression of the cytidine deaminases APOBEC3G and APOBEC3A, which are downregulated with macrophage differentiation, may contribute to restriction of replication in monocytes (51). A low level of nucleotide precursors, limiting reverse transcription, may contribute to low infection in monocytes, macrophages, and dendritic cells; however, this block is removed by the SIV/HIV-2 accessory protein Vpx (52, 53). The restriction factor responsible for this activity was discovered to be the deoxynucleoside triphosphate phosphohydrolase SAMHD1 (54, 55). In addition to host restriction factors, microRNA activity may also limit HIV-1 transcription in monocytes, either directly targeting viral mRNA or indirectly by the repression of CycT1 (56, 57). Together, factors above and the recently described interferon stimulated gene (ISG) viperin/RSAD2 (58) limit HIV-1 infection in monocytes.

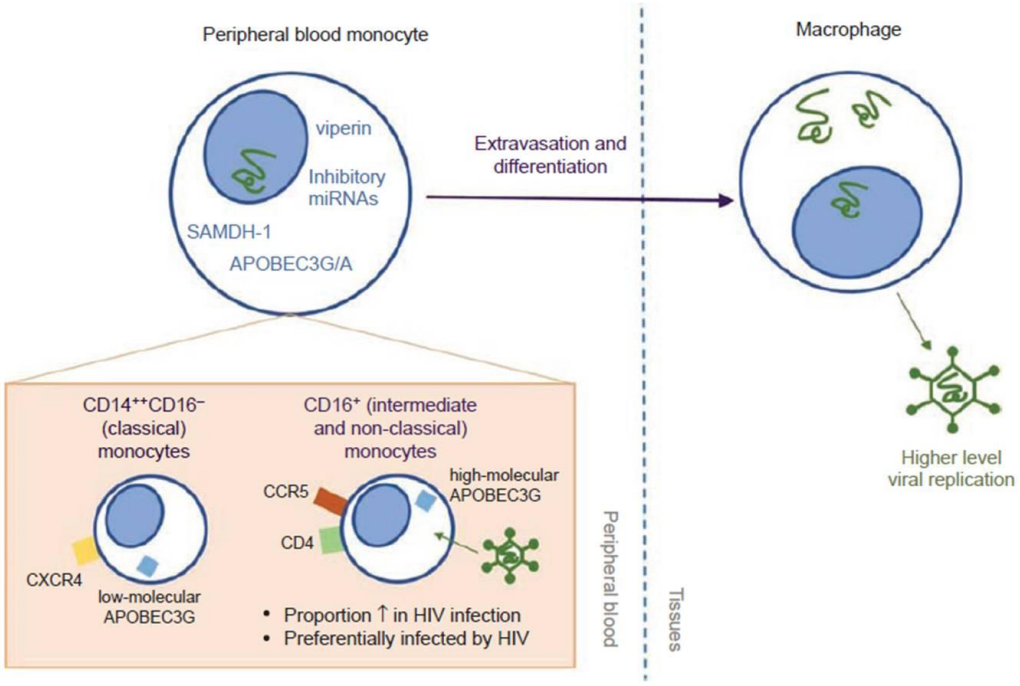

Figure 1.4: Barriers to HIV-1 replication in monocytes.
Shown are intrinsic host restriction factors that contribute to restriction of HIV-1 replication in monocytes (top left) and differences in susceptibility of select monocyte subsets (bottom left) and tissue macrophages (right). [49]

1.2.3 Role of macrophages as viral reservoirs

Although macrophages are typically ascribed a secondary role compared to resting memory CD4 T-cells in discussions of HIV/SIV persistence and viral reservoirs, multiple observations over the past 20 years makes a strong argument for their involvement. This argument is based on evidence of productively infected macrophages in lymphoid tissue (59) and macrophage sequence evolution in AIDS patients (60). In non-human primates models, rhesus macaques that are severely CD4-depleted, by either natural progression or severely pathogenic SHIV infection, maintain high levels of viral replication through macrophage sources of virus (61-63). This evidence is supported by

studies of SIV infection with antibody-mediated CD4 T-cell-depletion, in which high levels of $CD68^{+}$ macrophage infection are observed in rectal biopsies (64) and high proportions of viral RNA-positive macrophages are observed in lymphoid tissue and brain (65). This concept of macrophages as an immune-privileged reservoir in various tissue sites is reviewed in (49). As noted above, these observations stand in contrast to recent data that suggests macrophages acquire viral DNA by phagocytosis of infected CD4 T-cells and therefore do not reflect productive infection (46).

1.2.4 Role of monocytes and macrophages in HIV CNS and gut pathogenesis

CNS Pathogenesis

Macrophage infection within the CNS has been appreciated since the early years of the HIV-1 epidemic, described in post-mortem HIV patients with CNS pathology (66, 67). SIV models have demonstrated that the virus enters the brain early during acute infection (41, 68) and the primary target of HIV/SIV infection within the brain is the perivascular macrophage ($CD68^{+}CD163^{+}$), which are immunophenotypically similar to expanded $CD14^{+/-}CD16^{+}$ monocytes observed during infection, suggesting a mechanism of CNS entry (41, 47, 69). This population is distinct from resident microglia and “recently infiltrated” macrophages ($MAC387^{+}$) recruited from peripheral blood during inflammatory conditions (70-73). The association of monocyte activation and CNS recruitment with direct measurements of neuronal injury and neurocognitive dysfunction in

both HIV-infection and SIV-models supports a vital role of the monocyte/macrophage in CNS pathogenesis (Figure 1.5, Reviewed in (49, 73, 74)). These include an expansion of activated subsets in blood and brain (32, 47, 69, 75, 76), increased monocyte turnover in blood (71), monocyte ISG expression (Discussed in **Section 1.4**), and soluble markers of monocyte/macrophage activation, including sCD14 in blood (77, 78) and cerebrospinal fluid (CSF) (47, 79) and sCD163 in blood (80). Once virus and inflammatory/activated macrophages reach the brain, the cellular mechanisms of neuronal injury include the activity of viral proteins, activating chemokines and cytokines, and neurotransmitters (Reviewed in (49, 81, 82)).

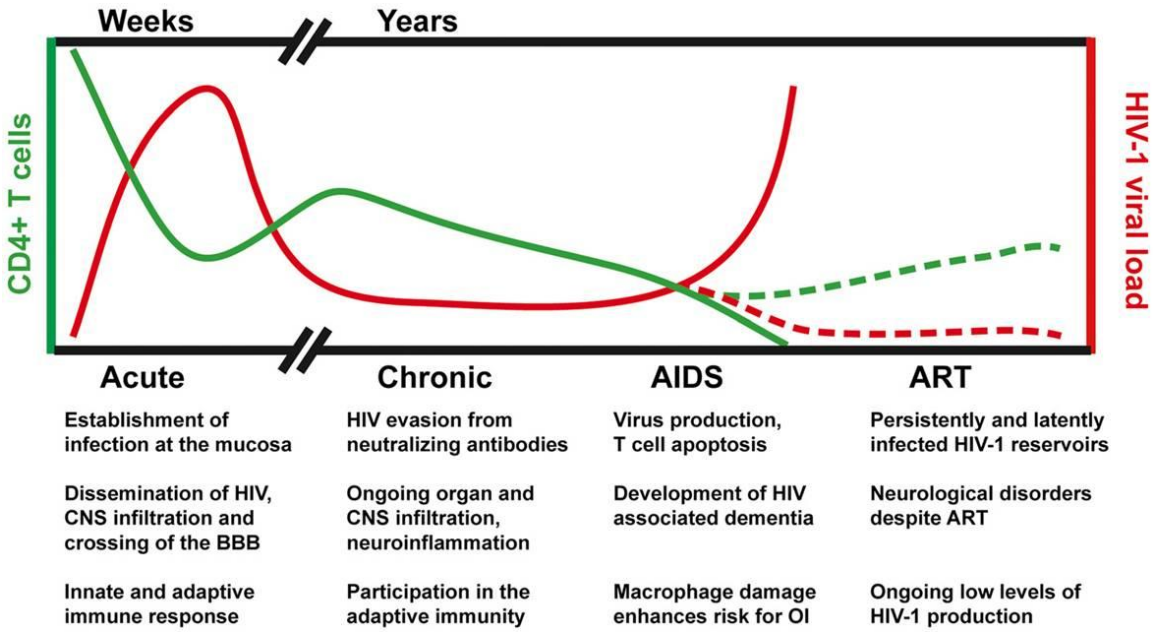

Figure 1.5: Monocytes and macrophages in HIV-1 pathogenesis.
Shown is an overview of the contribution of monocytes/macrophages to HIV-1 pathogenesis, including CNS, during acute, chronic, and advanced infection (AIDS) and ART treatment. [74]

Gut Pathogenesis

Under normal conditions, macrophages within the gastrointestinal mucosa are maintained in an anti-inflammatory, functionally inert state (though still functionally competent) despite the presence of GI bacteria through TGF-β production by resident stromal cells (83). This mechanism also downregulates CD4 and CCR5 expression conferring a resistance to HIV-1 infection in gut macrophages not observed in other tissue macrophages, such as vaginal macrophages (84, 85). However, during chronic, untreated SIV/HIV infection, gut epithelial barrier dysfunction results in leakage of microbial products that drive TLR-mediated activation and overall increases in immune activation (86-90). Tissue macrophage activation is proposed to be an important determinant of outcome as markers of plasma LPS (sCD14) predict mortality in HIV-1 infected individuals (91). Plasma sCD14 and markers of gut epithelial dysfunction also predict mortality among ART-suppressed individuals (92, 93). During chronic HIV-1 infection, high levels of $CD68^{+}CD163^{+}$ macrophages are recruited to gut mucosa by CCL2/CCR2 and integrin-β7-mediated mechanisms (94). Within gut mucosa, these macrophages may contribute to epithelial barrier dysfunction and microbial translocation by increased production of pro-inflammatory cytokines and chemokines (TNF-α, IL-1β, CCL5, CXCL9, CXCL10) and impaired phagocytic activity (88, 94).

1.3: Modulation of monocyte and macrophage apoptosis during HIV-1/SIV infection

Unlike CD4 T-cells, the apoptotic fate of monocytes during chronic infection and elevated HIV/SIV viremia is less clear, as different *ex vivo* and *in vitro* studies have reported both anti-apoptotic and pro-apoptotic mechanisms and outcomes. HIV-1/SIV can directly impact apoptosis in monocyte and macrophages (Figure 1.6) and monocyte/macrophage-mediated apoptosis of non-myeloid bystander cells, particularly CD4 T-cells (Reviewed in (18, 22)).

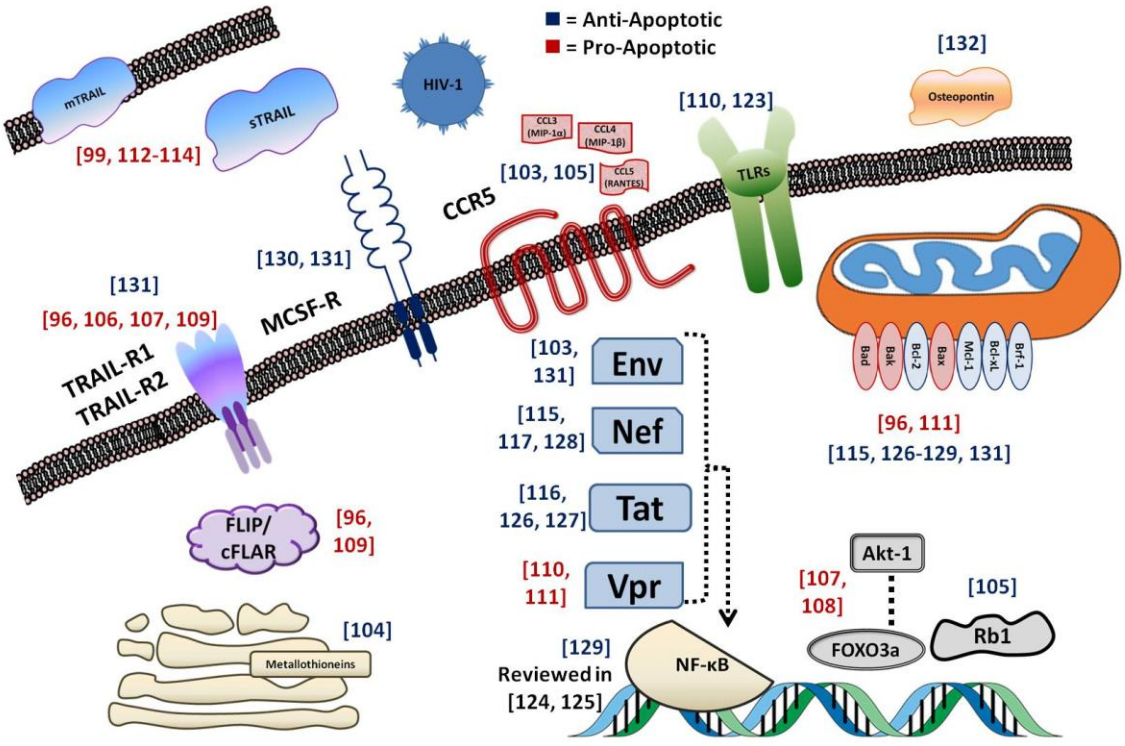

Figure 1.6: Pro- and anti-apoptotic pressures on monocytes/macrophages during HIV-1 infection/exposure.
Summary of apoptotic impacts of HIV-1 infection/exposure observed *ex vivo* and with infection/exposure of monocytes/MDM *in vitro*.

1.3.1: SIV infection of NHP models *in vivo*

The NHP model of SIV-infected rhesus macaques has generated significant insight regarding HIV-1 pressure on monocyte and macrophage apoptosis. Early descriptions of macrophage apoptosis (macrophages and microglia) within the brain were observed with CNS pathology of rhesus macaques infected with neurovirulent SIV (95). The ability of *in vivo* SIV infection to sensitize monocytes and dendritic cells (DC) to constitutive and receptor-mediated apoptosis has been well-characterized (96). Interestingly, elevated plasma FasL (Fas ligand) observed in rhesus macaque infection was not observed in the non-pathogenic model of SIV infection in African green monkeys (AGM). Furthermore, *in vivo* BrdU labeling of monocytes in SIV-infection showed that elevated monocyte turnover is associated with macrophage apoptosis in lymph nodes ($CD163^{+}TUNEL^{+}$) and faster progression to AIDS (70). Elevated monocyte turnover has also been associated with the severity of SIV CNS pathology and the monocyte/macrophage activation marker, sCD163 (71). The association of sCD163 with monocyte turnover offers additional insight when interpreting monocyte/macrophage activation reflected by elevated sCD163 during HIV-1 infection (Discussed in **Section 1.4**). Indeed, turnover of monocytes in NHP models (70, 71) may suggest a contribution of cell death and monocyte/macrophage dysfunction in compromised host defense during advanced SIV/HIV infection (97). The relationship between monocyte activation and soluble markers of activation during viremia and ART-mediated viral suppression will be addressed in this thesis.

1.3.2: Monocyte regulation in HIV infection: Pro-apoptotic

While findings in NHP models have demonstrated pro-apoptotic impacts of SIV-infection, *in vitro* studies of HIV-1 exposure/infection of monocytes and macrophages and *ex vivo* studies on monocytes from HIV-infected patients have yielded both pro- and anti-apoptotic findings. It is of paramount importance to interpret *ex vivo* HIV-1 monocyte apoptosis data in the context of clinical status (HIV-1 viral load and CD4 count). In a study of HIV-exposed seronegative (ESN), HIV (+), and HIV (-) individuals, Velilla et al described increased constitutive and *in vitro* HIV-1 induced monocyte apoptosis in the ESN and HIV (+) group relative to the HIV (-) group (98). However, viral load, CD4 count, and ART-status were not reported in the HIV (+) group. A study of STAT1 expression demonstrated elevated constitutive monocyte apoptosis and plasma TRAIL in the HIV (+) viremic group (off-ART, median viral load = 94,000 copies/mL) relative to the HIV (-) group and an association of STAT1 protein expression and monocyte apoptosis in the HIV (+) viremic group (99). Regarding myeloid dendritic cells (mDC), decreased Bcl-2 expression and increased apoptosis (Caspase-3^{+}) was observed in HIV (+) (mean viral load=89,700 copies/mL) relative to HIV (-) donors, and apoptosis was associated with viral load CD8 T-cell activation ($CD38^{+}$) and decreased with ART (100). Taken together, pro-apoptotic outcomes in monocyte studies in HIV infection have pointed to a relationship between high viral load and cell death.

1.3.3: Monocyte regulation in HIV infection: Anti-apoptotic

However, *ex vivo* HIV-1 studies have also demonstrated mechanisms of HIV-1 induced monocyte apoptosis resistance. Cosenza et al observed evidence of apoptosis resistance in HIVE-CNS, as $p24^+$ cells had lower percentages of $TUNEL^+$ cells than the overall CNS macrophage/microglia population (101). Furthermore, *ex vivo* analysis of gene expression from circulating monocytes and *in vitro* HIV-1 exposure/infection of whole PBMC supported gene modulation consistent with anti-apoptotic regulation (Reviewed in (102)). Specifically, a stable 38-gene anti-apoptosis gene signature was noted in monocytes from viremic HIV (+) donors (mean VL=32,000 copies/mL) compared to HIV (-) donors and was associated with resistance to induced apoptosis (103). Gene and protein expression data evidence engagement of CCR5 contributing to pro-survival signaling (p38/ERK/MAPK) by viral envelope interactions and/or natural CCR5 ligands (i.e., β-chemokines). Additional investigation of target apoptosis gene families from the parent array confirmed the apoptosis resistance phenotype in monocytes of additional HIV (+) patients and demonstrated the contribution of elevated intracellular zinc content, zinc importer expression, metallothionein expression (mean VL=39,294 copies/mL) (104) and Rb1 protein activity (mean VL=59,269 copies/mL) (105) to HIV-1 mediated monocyte apoptosis resistance. These data suggest viral replication and CCR5 ligands may promote monocyte survival, which stands in contrast to pro-apoptotic findings reviewed above. The relationship between pro- and anti-apoptotic regulation of monocytes in HIV infection will be addressed in this thesis.

1.3.4: MDM HIV infection *in vitro*: Pro-apoptotic

HIV-1 infection of MDM *in vitro* increases sensitivity to TRAIL-mediated apoptosis. Recombinant TRAIL and TRAIL-receptor agonists were initially explored *in vitro* as a means of purging HIV-1 infected CD4 T-cells and macrophages (106). *In vitro* HIV-1 infection of MDM and comparison of primary peripheral blood lymphocytes in HIV (-) and HIV (+) donors demonstrated higher TRAIL-receptor expression in HIV (+) conditions, and MDM from HIV (+) donors (relative to HIV (-) donors) were more sensitive to recombinant TRAIL-mediated apoptosis. Downstream of receptor expression, HIV infection/exposure was shown to sensitize macrophages to apoptosis by inhibiting Akt-1 activity in the Akt-1-FOXO3a pathway (107, 108). Furthermore, Laforge et al provided an extensive *in vitro* characterization of HIV-1 induced monocyte and dendritic cell apoptosis sensitization (96). Infection of MDM increased both activation induced (LPS+IFN-γ) and ligand mediated apoptosis (TRAIL) by the down-regulation of the anti-apoptotic molecules FLIP and Mcl-1 and up-regulation of the pro-apoptotic Bax and Bak. Similarly, Zhu et al demonstrated infection with a HIV-pseudotype sensitized MDM to TRAIL-mediated apoptosis by down-regulation of the TRAIL decoy receptors DcR1 and DcR2 (TNFRSF10C and TNFRSF10D) and the anti-apoptotic protein FLIP (109). Additionally, the accessory protein Vpr has been shown to induce apoptosis in monocytes *in vitro* (110, 111).

In vivo and *in vitro* evidence has accumulated of HIV-induced TRAIL (both membrane and soluble) production by monocytes and macrophages as a

mechanism of bystander apoptosis induction. In a study of 107 HIV (+) individuals, sTRAIL was elevated in viremic and suppressed patients relative to HIV (-) donors, and sTRAIL and mTRAIL was highly inducible in monocytes *in vitro* in a CD4-dependent mechanism by a type-I interferon/STAT pathway (112). The ability of HIV-infection and type-I interferons to induce MDM sTRAIL/mTRAIL has been further characterized to be IRF-1/IRF-7-dependent (113). Finally, Kim et al demonstrated robust TRAIL induction in MDM in pathogenic infection settings (SIV-RM *in vivo*, HIV *in vitro*) but not in non-pathogenic systems (SIV-chimpanzee, SM, AGM), suggesting a TRAIL-mediated role of monocytes and macrophages in CD4 T-cell depletion (114). Overall, induction of apoptosis after MDM infection is primarily associated with external regulation of activation (TRAIL, LPS, IFN-γ).

1.3.5: MDM HIV infection *in vitro*: Anti-apoptotic

One the other hand, anti-apoptotic impact has been demonstrated by infection and HIV-1 proteins *in vitro*, including Tat, Nef, and Env (115-117) (Reviewed in (118, 119)). This impact is complimented by the notion that viral or disease pressures that drive monocyte activation and/or differentiation mediate an increasingly pro-survival phenotype (110, 120-125). Specifically, Zhang et al demonstrated HIV-1 infection of MDM resulted in increased Bcl-2 expression, and treatment with exogenous HIV-Tat (126) was able to recapitulate apoptosis resistance to TRAIL-mediated apoptosis (127). Furthermore, it was demonstrated that HIV-Nef could mediate apoptosis resistance in MDM, mediated by Bad

inactivation by hyper-phosphorylation (128). HIV-1 infection of MDM was also described to upregulate anti-apoptotic Bcl2 and Bcl2L1 and downregulate Bad and Bax, the former through a TNF-α-dependent mechanism (129). HIV-induced M-CSF production has been implicated in monocyte/macrophage-associated pathogenesis (Reviewed in (130)). Specifically, Env expression induced an anti-apoptotic macrophage state, characterized by increased Mcl-1 and Bcl2-A1 expression and decreased TRAIL-R1 expression by a M-CSF dependent mechanism (131). Additionally, as noted above, *in vitro* engagement of CCR5 by virus can mediate Rb1 protein activity resulting in apoptosis resistance (103, 105). Interestingly, osteopontin, elevated during SIVE, also protects human monocytes from induced apoptosis *in vitro* (132). Overall, apoptosis resistance is primarily associated with virus/receptor interactions, intrinsic, and/or paracrine regulation.

1.4: Modulation of monocyte interferon gene expression during HIV-1 infection

The predominance of ISG expression in monocytes and macrophages is a hallmark of HIV-1 infection and has been well described in both *in vitro* studies and patient populations spanning all stages of infection.

Early studies demonstrated elevated plasma interferons in HIV-1 infected patients during both acute (133) and advanced (134) infection as well as the impact of ART on plasma IFN-α (135). Additionally, plasma IFN-α has been

associated with plasma LPS (but not viral load), suggesting that microbial translocation may serve as a source of sustained type-I interferon-driven activation (86). Monocyte ISG expression in the context of HIV-1 exposure or infection has been demonstrated both *ex vivo* and *in vitro*. Early studies established HIV-1 treatment of monocytes could induce IFN-α production independent of productive infection (136). Microarray studies have extensively characterized ISG induction from HIV-1 infection/exposure of MDM *in vitro*, (113, 137-140), temporal phases of ISG induction (138, 139), and an overlap of type-I ISG expression profiles between patient derived monocytes and *in vitro* stimulated monocytes (140). Additionally, the HIV-1 accessory proteins Tat and Vpr are independently sufficient to induce ISG expression in MDM *in vitro* (141, 142). Microarray and gene expression studies of primary patient monocytes have also demonstrated robust ISG expression during chronic infection associated with viremia (140, 143-146) that is decreased with viral suppression (147). ISG expression has also been characterized relative to infection stage in human lymphoid tissue in a cross-sectional study (148) and longitudinally in PBMC in the SIV NHP model (149).

This ISG profile is further supported by the detection of ISGs at the protein level, including both monocyte/macrophage cell-associated and plasma soluble proteins. Plasma CXCL10 is a well-characterized marker of ISG expression during HIV-1 infection, as it is elevated in viremic patients (144, 146, 150-152) and associated with HIV-1-associated neuronal injury (144, 146) in a manner

similar to monocyte ISG expression (145). Additionally, *ex vivo* culture of duodenal tissue, enriched for macrophage infiltrate in viremic HIV (+) donors, has demonstrated elevated CXCL10 production relative to tissue from HIV (-) donors (94). Longitudinal studies have described increased plasma CXCL10 during STI (scheduled treatment interruption) (153) and decreased CXCL10 during ART (135); however, cross-sectional studies suggest viremic suppression is not accompanied by complete reversal, as plasma CXCL10 is elevated in ART-treated patients (150, 152) and elite controllers (152) relative to HIV (-) donors. CD169 (Sialoadhesin, SN, SIGLEC1) is a surface-expressed ISG (IFN-α, IFN-γ inducible) on monocytes, macrophages, and dendritic cells and is highly expressed during HIV-1 infection (143, 146, 154-156) and other inflammatory diseases (155, 157). CD169 can facilitate trans-infection of target cells by both monocytes and dendritic cells (156, 158, 159). CD169 expression was elevated in progressive stages of infection a HIV-1 cross-sectional study (154) and reversed with ART in a SIV longitudinal study (160).

Monocyte/macrophage ISG expression also has a significant bystander effect on T-cells and other immune cells. As noted above, *ex vivo* and *in vitro* studies suggests HIV-1 can induce monocyte/macrophage TRAIL expression (membrane and soluble) by an IFN-dependent mechanism that may contribute to bystander CD4 T-cell apoptosis (22, 112, 113). Monocyte/macrophage ISG expression may also play a role in T-cell exhaustion during HIV-1 infection. Specifically, the ligands, PD-L1 and PD-L2 are expressed on monocytes and

macrophages during HIV-1 infection and can be up-regulated by factors present during infection including virus particles, TLR-agonists, and type-I interferons (27, 28, 161) (Reviewed in (162)). PD-L1/L2 ligand interactions with PD-1 on activated T-cells can mediate CD4 and CD8 T-cell exhaustion during HIV-1 infection (26, 27, 163). Finally, type-I interferon driven BAFF (B cell-activating factor) expression and secretion by monocytes may also drive B-cell dysfunction observed during HIV-1 infection (164).

While ISG expression is associated with disease progression in HIV/SIV infection (165, 166), ISGs also include HIV restriction factors that inhibit/limit replication in monocytes (48, 49, 167, 168). While comprehensive study is not a focus of this thesis, we will briefly highlight major HIV-1 restriction factors described to date. The APOBEC3 family of cytidine deaminase hypermutates incoming HIV proviral DNA (169), and SAMHD1 limits the pools of dNTPs available for reverse transcription (54, 55). IFITM proteins (IFITM1-3), members of the ISG12 family, have also been shown to inhibit HIV replication (170). Tetherin (BST2, CD317) restricts budding of virus particles (171). Finally, Mx2 has recently been ascribed post-entry/pre-integration restriction activity (172). The overall benefit (HIV restriction) or burden (association with disease progression and persistence by PD-L1/IL-10 (27, 161, 173)) of ISG expression remains in debate. This thesis will address whether ISG induction in monocytes relative to viral load is related to changes in monocyte apoptosis.

1.5: Cell-associated and soluble biomarkers of monocyte and macrophage activation during HIV-1 infection and ART

It is established that sustained T-cell activation during HIV-1 infection is associated with disease progression and sub-optimal CD4 T-cell recovery after ART (16, 23-25). Nonetheless, the significance of monocyte and macrophage activation, independent of infection, has returned to prominence due to the association with gut epithelial barrier dysfunction and microbial translocation (77, 86-89, 91-93, 174, 175). The phases of this activation sequela, gut barrier dysfunction (apoptosis, I-FABP, zonulin) (91-93), microbial translocation (plasma LPS, plasma 16S rDNA) (77, 86, 87, 91, 174, 175), and biomarkers of innate activation (sCD14) (77, 78, 86, 91, 174, 175), have been investigated for their association with one another and predictive value of clinical and therapeutic outcome. Furthermore, activation of monocytes and macrophages (by virus, microbial translocation, immune cross-talk, and other sources) remains a potential source of inflammation that may not be fully reversed during ART (Figure 1.7) (80, 86, 91, 150, 174, 176-179). We will address the relationship between markers of innate monocyte/macrophage activation and ART-mediated viral suppression in advanced infection.

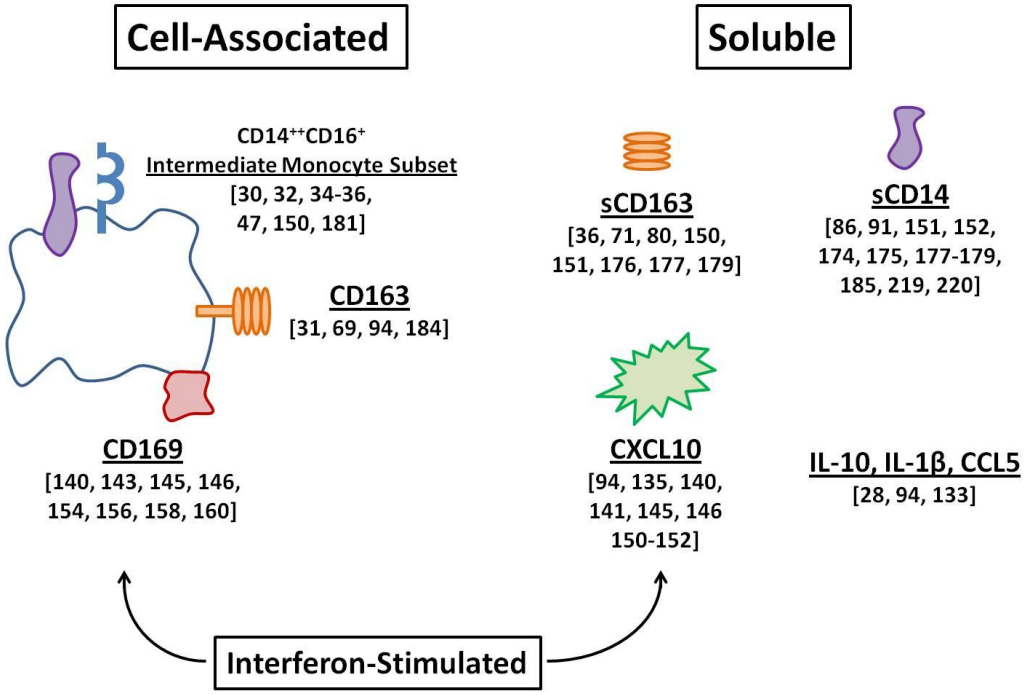

Figure 1.7: Biomarkers of monocyte and macrophage activation during HIV-1 infection.
Shown are major cell-associated biomarkers of monocyte/macrophage activation during SIV/HIV-1 infection.

1.5.1: Cell Associated Biomarkers

The expansion of $CD16^+$ monocyte subsets, including $CD14^{++}CD16^+$ intermediate monocyte subset, has been described during HIV-1 (32-36) and SIV viremia (30) and are associated with HIV pathogenesis (32, 47, 150). Elevated $CD16^+$ monocyte subsets may indicate long-term inflammation as similar elevations have been described in patients with cardiovascular disease in HIV (-) (35) and ART-suppressed cohorts (180). $CD14^{++}CD16^+$ monocytes are also elevated in elite controllers compared to HIV (-) controls, supporting evidence of ongoing innate activation despite viral control (181). Regarding ART, the intermediate monocyte subset was decreased in patients treated during early

infection, but not chronic infection (177), and cross-sectional comparisons have demonstrated suppressed patients reach comparable levels to HIV (-) donors (35).

CD163, the hemoglobin/haptoglobin receptor, is expressed on blood monocytes tissue macrophages (182) and can be shed, as sCD163, by ADAM17/TACE-cleavage during activated/TLR-stimulated conditions (177, 183). CD163 expression is increased on intermediate monocytes of HIV (+) individuals (31) and is highly expressed on macrophage infiltrates of CNS, cardiac, and gut tissue during HIV/SIV infection (69, 72, 94, 184).

1.5.2: Soluble Biomarkers

Soluble biomarkers of monocyte/macrophage activation are also well-characterized during HIV infection, including sCD14 and sCD163. Elevated sCD14 has been described as a marker of HIV-associated microbial translocation and increased plasma LPS (86, 152, 185). Longitudinal ART studies have found elevated sCD14 levels persist despite viral suppression (86, 174, 177) and are only partially resolved after extended ART (174, 175). In addition, cross-sectional comparisons have demonstrated ART patients do not resolve sCD14 to the level of HIV (-) donors (91, 152, 174, 178, 179).

Soluble CD163, shed from activated monocytes and macrophages, is elevated during SIV/HIV infection and associated with both cardiac and CNS

pathogenesis (36, 71, 80, 150, 152, 176, 177, 179). Soluble CD163 was reduced to HIV (-) levels in patients treated during early infection but not in those treated during chronic infection (177); however, unlike the intermediate monocyte subset, cross-sectional studies suggest sCD163 does not reach levels of HIV (-) donors upon viral suppression (80, 150, 176, 179).

The relationship between monocyte subsets, viral load, monocyte apoptosis, soluble markers of activation, and ART-mediated viral suppression will be addressed in this thesis.

1.6 Scope of Thesis

This thesis provides new data on monocyte biology during HIV-1 infection addressing regulation of monocyte apoptosis, innate immune activation, viral load, and ART-mediated viral suppression. We investigate the presence of activated monocyte subsets in patients with high viral load/low CD4 count and examine modulation of monocyte apoptosis sensitivity and transcription profiles (ISG expression) relative to viral load/CD4 count. We characterize the induction of genes associated with apoptosis regulation as well as the impact of over-expression of target genes on apoptotic outcome *in vitro*. Additionally, we investigate the impact of ART-mediated viral suppression on monocyte/macrophage activation profiles in HIV-1 patients initiating therapy during advanced HIV-1 infection (CD4 count less than 100 cells/mm^3). We also

investigate the impact of CCR5 antagonism during ART on the reversal of monocyte/macrophage activation profiles.

CHAPTER 2: Shift in monocyte apoptosis with increasing viral load and change in apoptosis-related ISG/Bcl2 family gene expression in HIV-1 infected patients during chronic infection

2.1 Introduction

While HIV-1 infection is characterized by compromised adaptive immunity with CD4 T-cell loss in tissue (12) and peripheral blood (18, 19), the loss of monocytes and macrophages is less evident. The impact of HIV-1 viremia on monocyte gene expression (103, 140, 147, 161, 186) and function (32, 33, 40, 143, 153) is largely independent of productive infection, as less than 0.1% of circulating monocytes are estimated to harbor integrated HIV-1 DNA (38, 43, 44). However, exposure to viral particles and proteins, microbial products, and host products (inflammatory cytokines) can modulate monocyte function (27, 102, 140, 147, 158, 161, 187) and apoptosis (96, 99, 103, 109, 127, 131) during HIV-1 infection.

Unlike CD4 T-cells, the apoptotic fate of monocytes during elevated HIV/SIV viremia is less clear, as *ex vivo* and *in vitro* studies have reported both anti-apoptotic (103-105, 127, 131) and pro-apoptotic (96, 99, 109) mechanisms and outcomes (Figure 1.6, **Section 1.3**). Gene expression studies have identified a predominant anti-apoptosis gene signature in monocytes during chronic HIV-1 infection (103), and multiple studies have described anti-apoptosis mechanisms *ex vivo* and *in vitro* including: engagement of CCR5 and pro-survival signaling (p38/ERK/MAPK) (103), elevated intracellular zinc content, metallothionein expression (104), elevated Rb1 protein activity (105), and M-CSF mediated protection from TRAIL-induced apoptosis (131). Based on oxidative stress (188) and increased expression of apoptotic ligands (22, 112, 113) observed during

HIV infection, resistance to apoptosis has been tested by multiple induction mechanisms ($CdCl_2$, sFasL) in cross-sectional studies (103-105, 131). By contrast, NHP SIV studies have characterized longitudinal changes under high viremic settings and have shown higher monocyte turnover and elevated activation markers in animals with rapid disease progression and neuropathogenesis (69-71, 73, 75), suggesting a shift in monocyte viability upon the onset of advanced infection. Other SIV and *in vitro* HIV-1 studies have demonstrated pro-apoptotic outcomes of viral exposure based on modulation of Bcl2 family genes (Bax, Bak, Mcl-1), downregulation of anti-apoptotic c-FLIP proteins, and downregulation of TRAIL decoy receptors (96, 109). While the impact of elevated viremia on monocyte activation has been characterized, no HIV-1 study, to date, has measured monocyte apoptosis concurrently with monocyte/macrophage activation to identify functional changes relative to one another and elevated viral load. In addition, reports on anti-apoptotic outcomes in monocytes from HIV-1 patients *ex vivo* have examined a limited range of viral load (mean viral load, 32,000, 39,294, and 59,269 HIV-1 copies/mL for (103-105)), requiring a more extensive analysis across a wider viral load distribution.

Herein, we reconcile data between independent reports of pro- and anti-apoptotic gene expression and apoptosis outcomes by the *ex vivo* characterization of circulating monocytes from a broad clinical spectrum of HIV-1 viremia in the absence of anti-retroviral therapy.

2.2 *Ex vivo* HIV (+) monocyte apoptosis characterization and RNA sequencing

2.2.1 Pilot RNA sequencing

A pilot experiment was designed to utilize RNA sequencing in isolated CD4 T-cells and monocytes from viremic HIV-1 patients to investigate gene expression in order to confirm and expand upon previous microarray findings (Reviewed in (102)). Apoptosis characterization and RNA-sequencing was performed on two samples of each HIV (-), HIV (+) LVL (low viral load), and HIV (+) HVL (high viral load) group (Table 2.1). (LVL and HVL defined below/above 100,000 HIV-1 copies/mL in pilot.) Patients with low viral load were selected to match previously reported profiles of monocyte apoptosis resistance in chronic HIV (+) individuals (103-105). Patients with high viral load were chosen to the investigate the unstudied monocyte apoptosis and gene expression profiles in patients with viral load > 100,000 HIV-1 copies/mL.

ID	Group	Viral Load	Log Viral Load	CD4 Count (cells/mm^3)
APN2	HIV(-)	-	-	-
APN4	HIV(-)	-	-	-
APH1	HIV(+) Low	36,096	4.56	425
APH6	HIV(+) Low	9,196	3.96	283
APH3	HIV(+) Hi	150,442	5.18	202
APH7	HIV(+) Hi	439,508	5.6	26

Table 2.1: Pilot donor characteristics.
Study group, viral load (and log viral load), and CD4 T-cell count of pilot study cohort.

Gene expression was examined in pooled samples of two donors from each group. The CD4 T-cell expression profile was not available in the HVL group due to low CD4 T-cell recovery. The sequencing analysis pipeline and read-purity is shown for each group, and mRNA reads represented 79-83% of the sequences (Figure 2.1). Sequencing analysis was used to highlight candidate genes regulating monocyte apoptosis (ISG/Bcl2 family) at different levels of HIV-1 viremia (Pursued in **Sections 2.2.2**, **2.2.3**, and **2.3**).

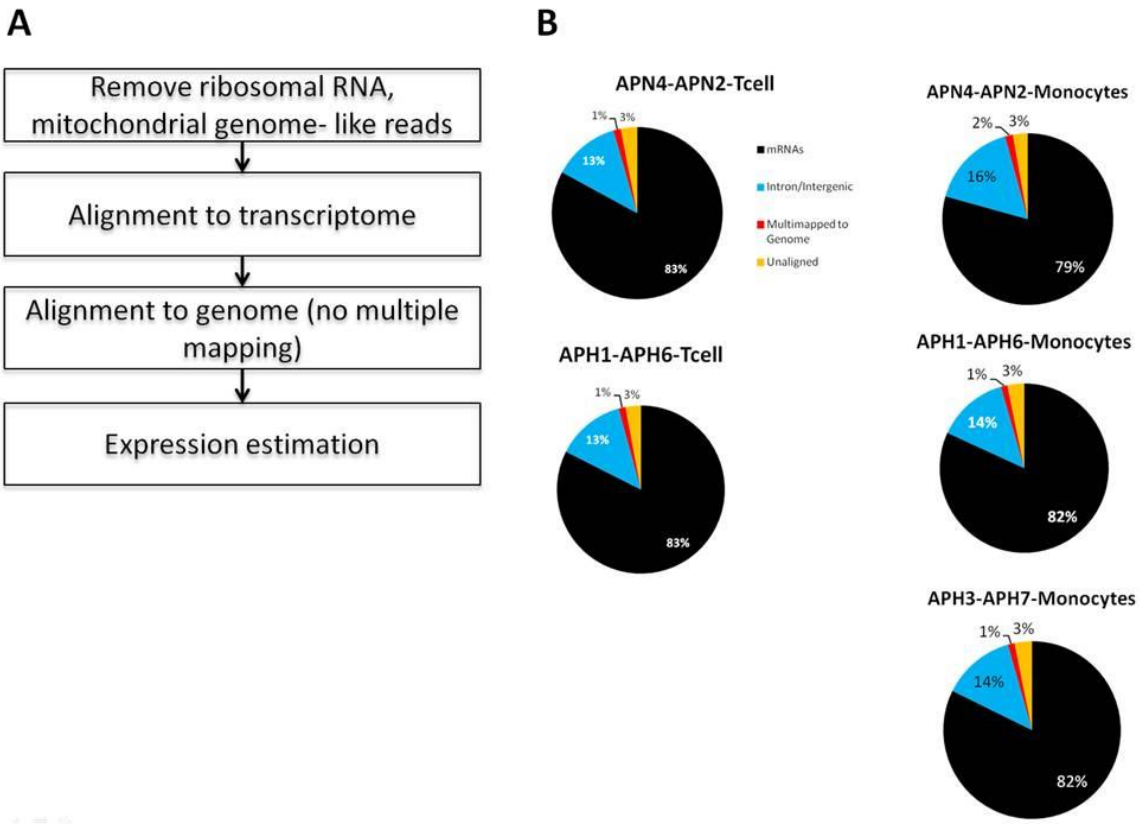

Figure 2.1: RNA sequencing analysis.
Shown is RNA sequencing analysis (A) and quality control/read purity (B) of the two CD4 T-cell and three monocyte sequencing groups.

We targeted ISG expression as a set of genes expected to be induced in monocytes from high viral load patients. Indeed, the HVL (+) monocytes demonstrated the expected ISG induction, including Mx1, IFITs, OAS1, etc (Figure 2.2, green box). Additionally, we observed differences in monocyte p53/Bcl2 family gene expression, with a predominance for pro-apoptotic gene expression at high viral load, and selected candidate genes for follow-up in an expanded cohort (Figure 2.3; Follow-up **Section 2.3**).

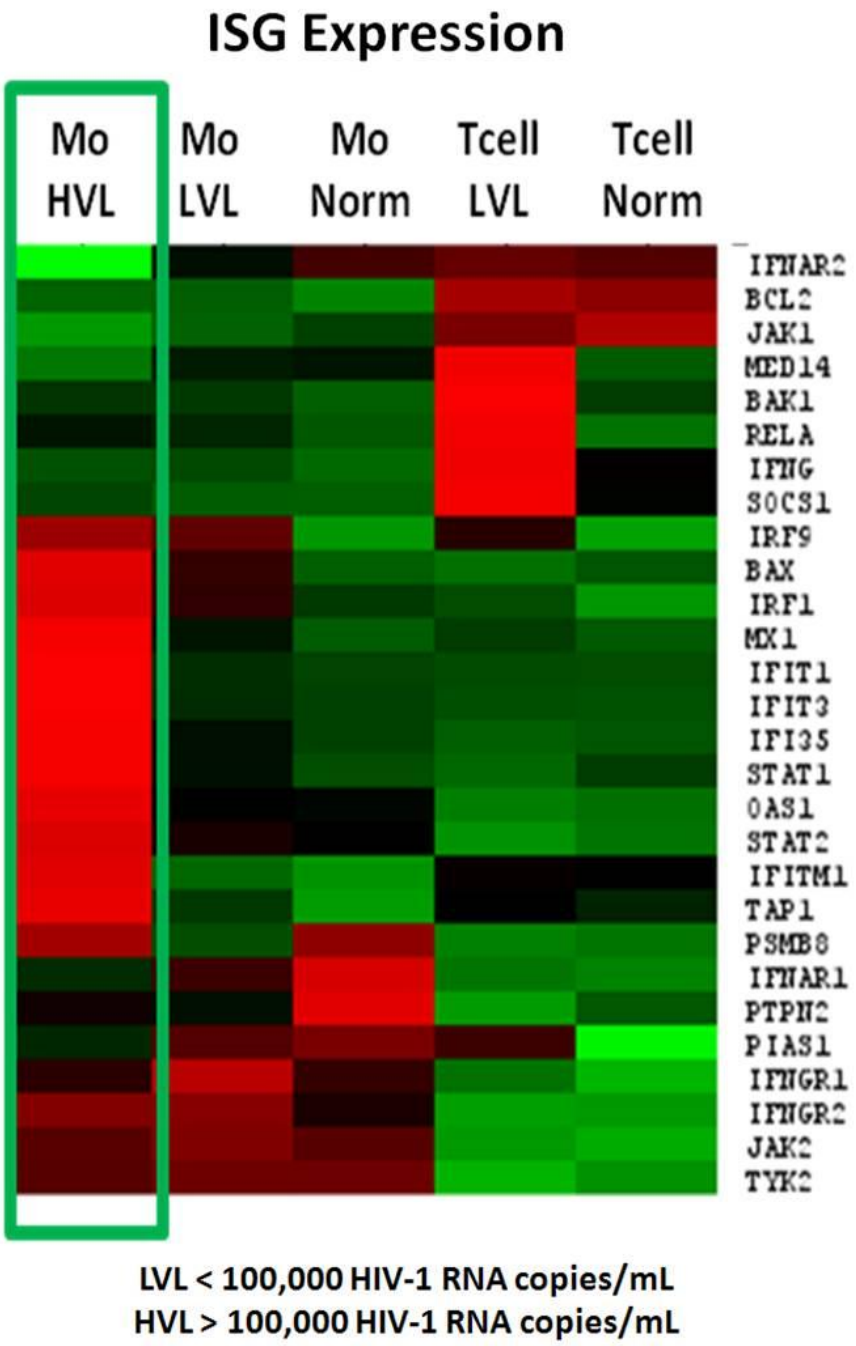

Figure 2.2: Interferon stimulated gene expression during HIV-1 infection. ISG expression profile of monocytes (left three columns) and CD4 T-cells (right two columns) from HIV (-) and HIV (+) (low and high viremia) individuals.

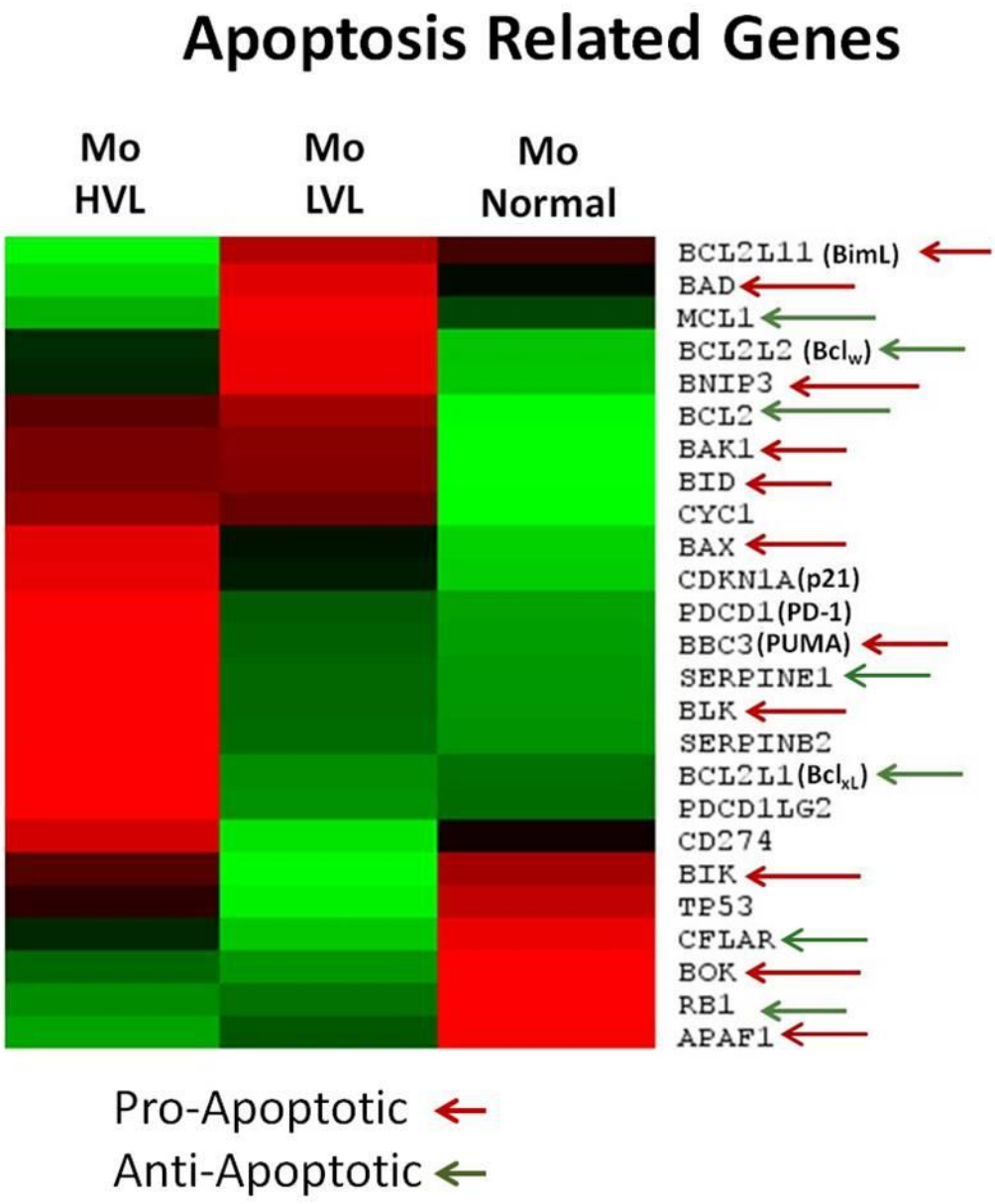

Figure 2.3: Monocyte apoptosis-related gene expression during HIV-1 viremia.
Apoptosis-regulatory gene expression profiles in monocytes of HIV (-) and HIV (+) (low and high viremia) individuals. Pro-apoptotic genes designated with red arrow, anti-apoptotic genes designated with green arrow.

2.2.2 *Ex vivo* expression of the ISG12 family highlights candidate ISG/apoptosis-regulatory genes

A primary goal of the RNA sequencing pilot was to highlight gene targets that may regulate apoptosis in monocytes during HIV-1 infection. The ISG12/FAM14 family was a lead of particular interest. This family is a group of small, hydrophobic, interferon-inducible proteins, upregulated during viral infection, with roles in both apoptosis regulation and virus-host interactions (Reviewed in (189, 190)). IFI6 (G1P3, ISG6-16) has demonstrated inhibition of mitochondrial-associated apoptosis in cancer cell lines (191, 192). Two other members of the ISG12 family, IFI27 (ISG12) and IFITM2 (I-8D), have demonstrated pro -apoptotic properties, mitochondrial localization, and induction during viral infection (193-195). Interestingly, IFITM2 (along with IFITM1, IFITM3) has been described to inhibit HIV-1 infection (170) and other viral infections (196). The RNA sequencing expression illustrates that the ISG12 family is highly expressed in the HIV (+) patient groups relative to the HIV (-) group like the prototypic ISG, Mx1 (Figure 2.4). Of note, expression of the pro-apoptotic IFI27 expression was elevated in the HVL (+) group (relative to HIV (-)) by over 1000-fold. Based on elevated expression in the pilot dataset and reported apoptosis-regulatory function, we selected candidate ISG12 genes to characterize gene regulation *in vitro* and gene expression in an expanded HIV (+) patient cohort.

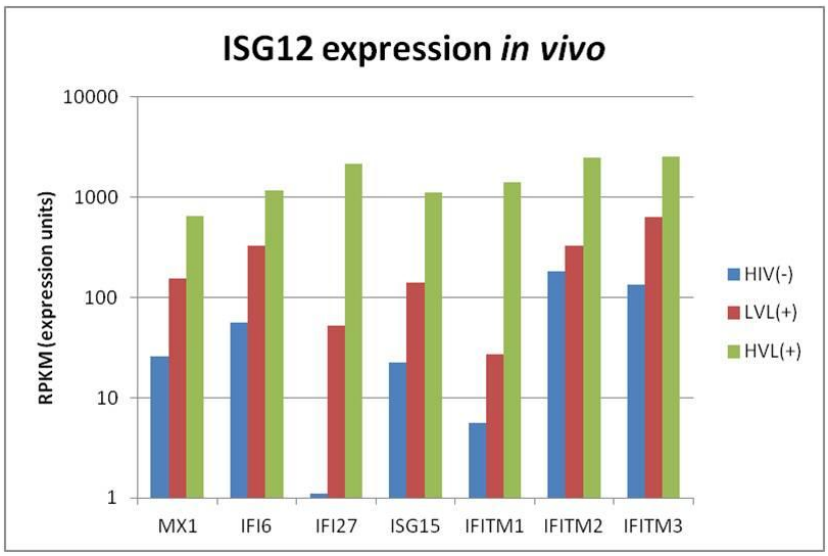

Figure 2.4: Monocyte ISG12 gene family expression during HIV-1 viremia. Expression values of the prototypic ISG, Mx1, and the ISG12 gene are shown for HIV (-) (blue), HIV (+) LVL (green), and HIV (+) HVL (red). (n=2 patient per group) (RPKM=Reads Per Kilobase of transcript per Million mapped reads)

2.2.3 *In vitro* regulation of IFI6 and IFI27 expression in primary human monocytes

Based on the ISG expression in HVL (+) monocytes, we first investigated the regulation of the apoptosis-regulatory ISG12 genes, IFI6 and IFI27, in primary human monocytes by IFN-α and HIV-1 treatment *in vitro*. IFI6 and IFI27 were robustly induced after 48 hours incubation with high-dose exogenous IFN-α (0 to 5000 units/mL) (Figure 2.5, left column). IFN-α treatment induced a 2-log fold induction for IFI6 (similar to Mx1) and a 4-log fold induction for IFI27 over unstimulated conditions (Figure 2.5E). We also investigated induction at lower levels of stimulation (0 to 50 U/mL) (Figure 2.6, right column) and observed IFI6 expression at very low doses (1-10 U/mL) (Figure 2.5B) and comparable IFI6 and IFI27 raw expression at 25 to 50 U/mL (Figure 2.5B, D, representative of n = 2).

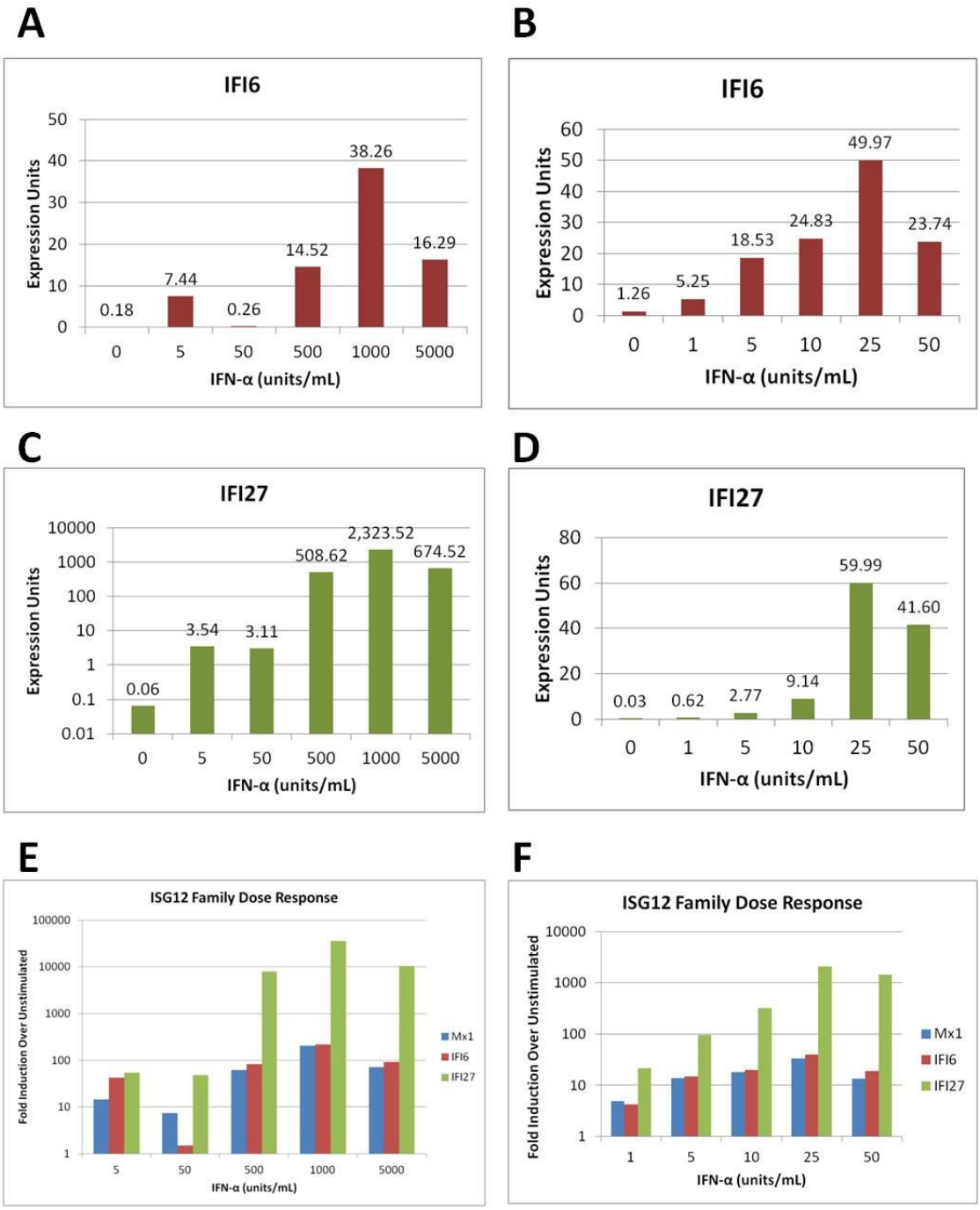

Figure 2.5: Dose response of IFI6 and IFI27 expression in primary monocytes.

Primary monocytes were treated with high-dose (0-5000 U/mL) (left) or low-dose (0-50 U/mL) (right) IFN-α for 48 hours and gene expression was measured by RT-PCR. Expression of IFI6 (A, B) and IFI27 (C, D) are shown. Fold-induction over unstimulated (E, F) is shown for Mx1 (blue), IFI6 (red), and IFI27 (green).

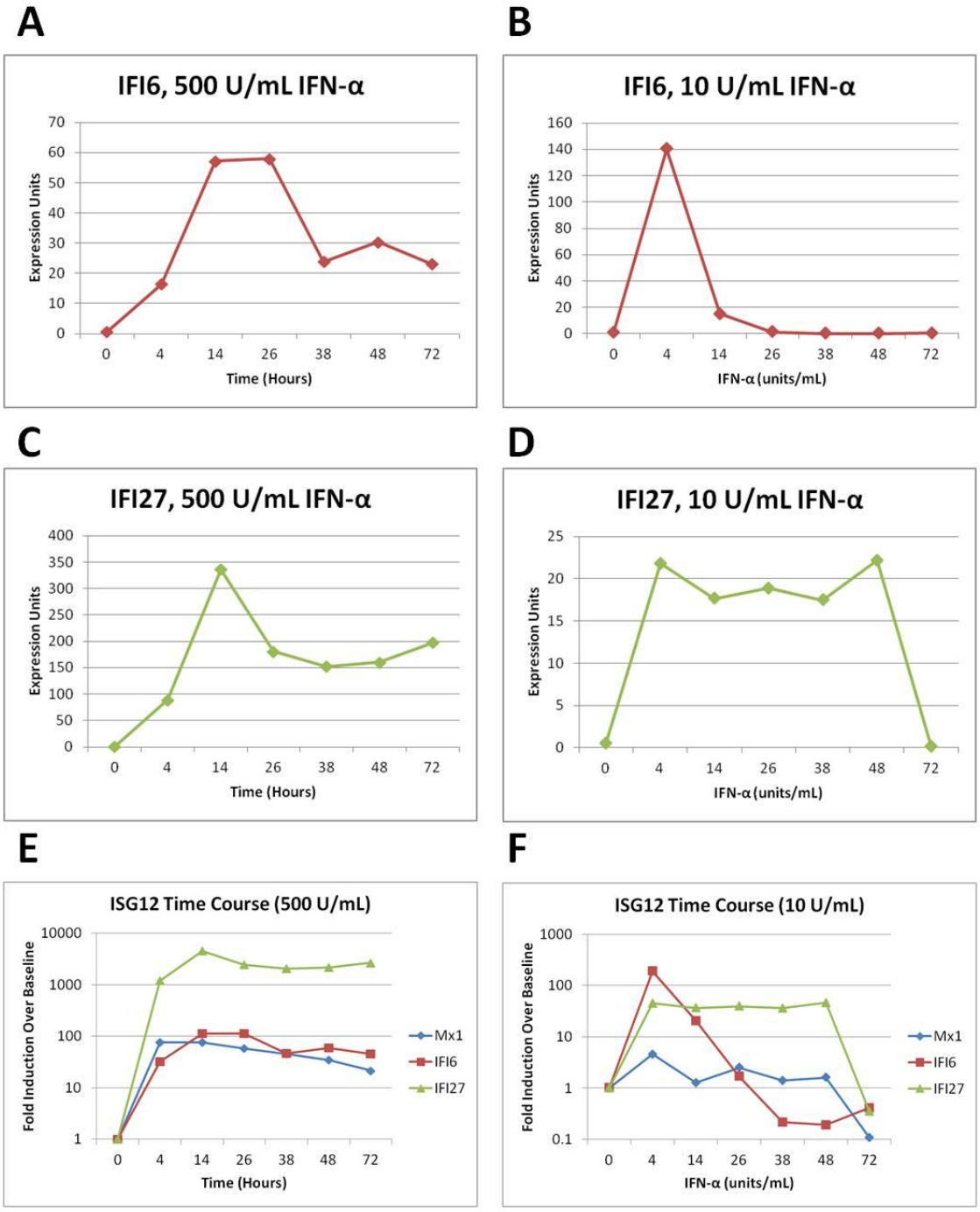

Figure 2.6: Kinetics of IFI6 and IFI27 expression in primary monocytes. Primary monocytes were treated with high-dose (500 U/mL) (left) or low-dose (10 U/mL) (right) IFN-α for 72 hours and gene expression was measured by RT-PCR. Expression of IFI6 (A, B) and IFI27 (C, D) are shown. Fold-induction over baseline (E, F) is shown for Mx1 (blue), IFI6 (red), and IFI27 (green).

Appropriate temporal regulation of IFI6 and IFI27 expression may be essential for a concerted antiviral response. We conducted a 72 hour time course of gene expression at two IFN-α doses (10 and 500 U/mL) (Figure 2.6). IFI6 expression peaked early, at 4 hours in the low-dose titration (Figure 2.6A) and 14-26 hours in the high-dose titration (Figure 2.6B), while IFI27 expression persisted for 48 hours or longer post-stimulation (Figure 2.6C, D). Our findings suggest IFI6 may be upregulated with lower stimulation (Figure 2.5B) and at early time points (Figure 2.6A, B) compared to IFI27, which is highly expressed with strong IFN-α stimulation and persistent at later time points *in vitro* (Figure 2.5C, Figure 2.6C, D), supporting a sequential regulation of ISG12 family expression (190).

We then tested whether or not HIV-1 exposure would induce IFI6 and IFI27 expression in monocytes similar to that of exogenous IFN-α treatment (Figure 2.7). The experiment was designed to test the impact of exposure (and limit productive infection) with monocytes cultured in the absence of differentiating cytokines and in Teflon pots to prevent adherence-induced differentiation. Monocytes were cultured for 48 hours and treated with IFN-α (500 U/mL), HIV-1 Bal, a lab-adapted CCR5-tropic lung isolate (50 ng p24/mL), HIV-1 Jago, a primary CCR5-tropic CSF isolate (50 ng p24/mL), and IFN-α plus HIV-1 combinations. HIV-1 Bal induced IFI6 and IFI27 to levels slightly lower than IFN-α alone (Figure 2.7A, B) while HIV-1 Jago did not induce comparable ISG induction. Interestingly, the combination of HIV-1 Bal and IFN-α induced IFI27

expression one log higher than IFN-α alone, suggesting a potential additive or synergistic induction. Such conclusions are limited due to the lack of replicates and detailed follow-up; however, these data and pilot experiment data (**Section 2.2.2**) suggest HIV-1 can upregulate monocyte ISG12 family gene expression and support follow-up in a comprehensive HIV (+) viremic cohort.

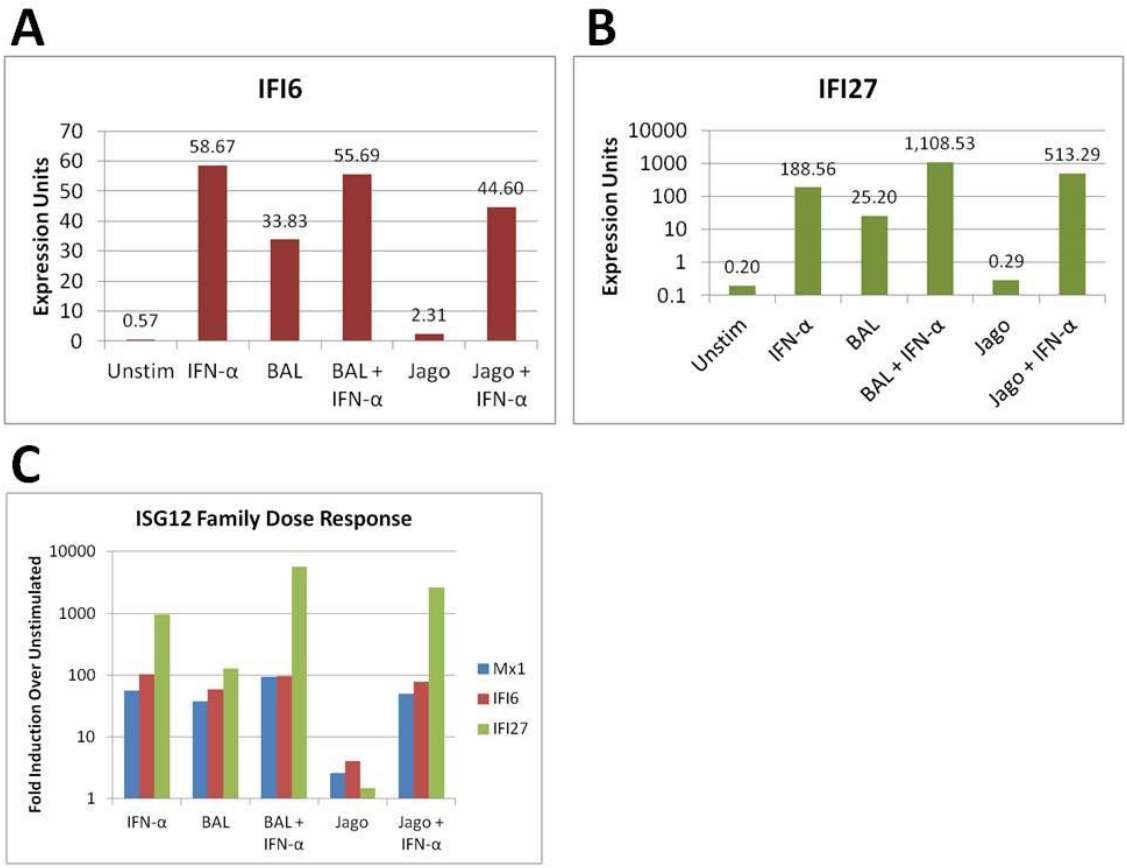

Figure 2.7: Monocyte IFI6 and IFI27 expression is induced by HIV-1 Bal, but not Jago *in vitro*.
Primary monocytes were treated with IFN-α (500 U/mL), HIV-1 Bal or Jago (50 ng p24/mL), or a combination of IFN-α and HIV-1 for 48 hours gene expression was measured by RT-PCR. Expression of IFI6 (A) and IFI27 (B) are shown. Fold-induction over baseline (C) is shown for Mx1 (blue), IFI6 (red), and IFI27 (green).

2.3 Shift in monocyte apoptosis with increasing viral load and change in apoptosis-related ISG/Bcl2 family gene expression in HIV-1 infected patients during chronic infection

2.3.1 Monocyte apoptosis is elevated in HIV-1 patients with high viremia

Constitutive and induced monocyte apoptosis were examined in a cohort of viremic patients (Table 2.2, 2.3) that included a wide range of viral load (2,243-1,355,998 copies/mL) and CD4 count (26-801 cells/mm^3). As expected, CD4 count was negatively associated with viral load (P = 0.0012, R = –0.5255). Flow cytometry gating is shown in Figure 2.8.

ID#	Gender	Age	Log Viral Load (copies/mL)	CD4 Count (Cells/mm^3)
1	M	46	5.44	26
3	M	23	4.97	773
4	M	44	3.35	801
5	M	33	5.67	380
7	M	48	3.72	209
8	M	33	4.38	428
9	M	52	4.93	497
10	M	37	3.97	620
11	M	40	6.13	61
12	M	41	4.56	425
13	M	54	3.96	483
14	M	56	5.64	27
15	M	40	5.49	264
16	M	27	5.18	202
17	M	49	4.31	289
18	M	24	4.18	653
19	M	27	5.54	99
20	M	43	4.61	329
22	M	56	4.59	293
23	M	24	4.85	464
24	M	22	4.15	370
25	M	60	5.45	107
26	M	30	4.64	605
27	F	52	4.41	142
28	M	47	5.00	333
29	M	52	5.07	133
30	F	49	4.58	309
31	M	45	4.61	163
32	F	47	5.29	101
33	M	36	4.64	617
34	M	28	4.62	515
35	M	27	4.10	325
36	M	24	5.04	225
37	F	84	4.29	190
40	M	44	5.76	186
Median		43	4.64	309
IQR		30-49	4.31-5.29	163-464

Table 2.2: HIV (+) patient population.
Gender, age, log viral load, and CD4 T-cell count are shown (n=35).

Category	n	Female/Total	% Female	Age (Med, IQR)
HIV(-)	33	8/33	0.242	43.5 (28.5-54)*
HIV(+) Lo (<Log4.6)	14	3/14	0.214	46 (30-53)
HIV(+) Hi (>Log4.6)	21	1/21	0.048	40 (27.5-47)

Table 2.3: Gender and age of study groups.
Gender and age distribution of HIV (-) and HIV (+) sub-groups. *Age information in the HIV (-) group available for 22/23 donors.

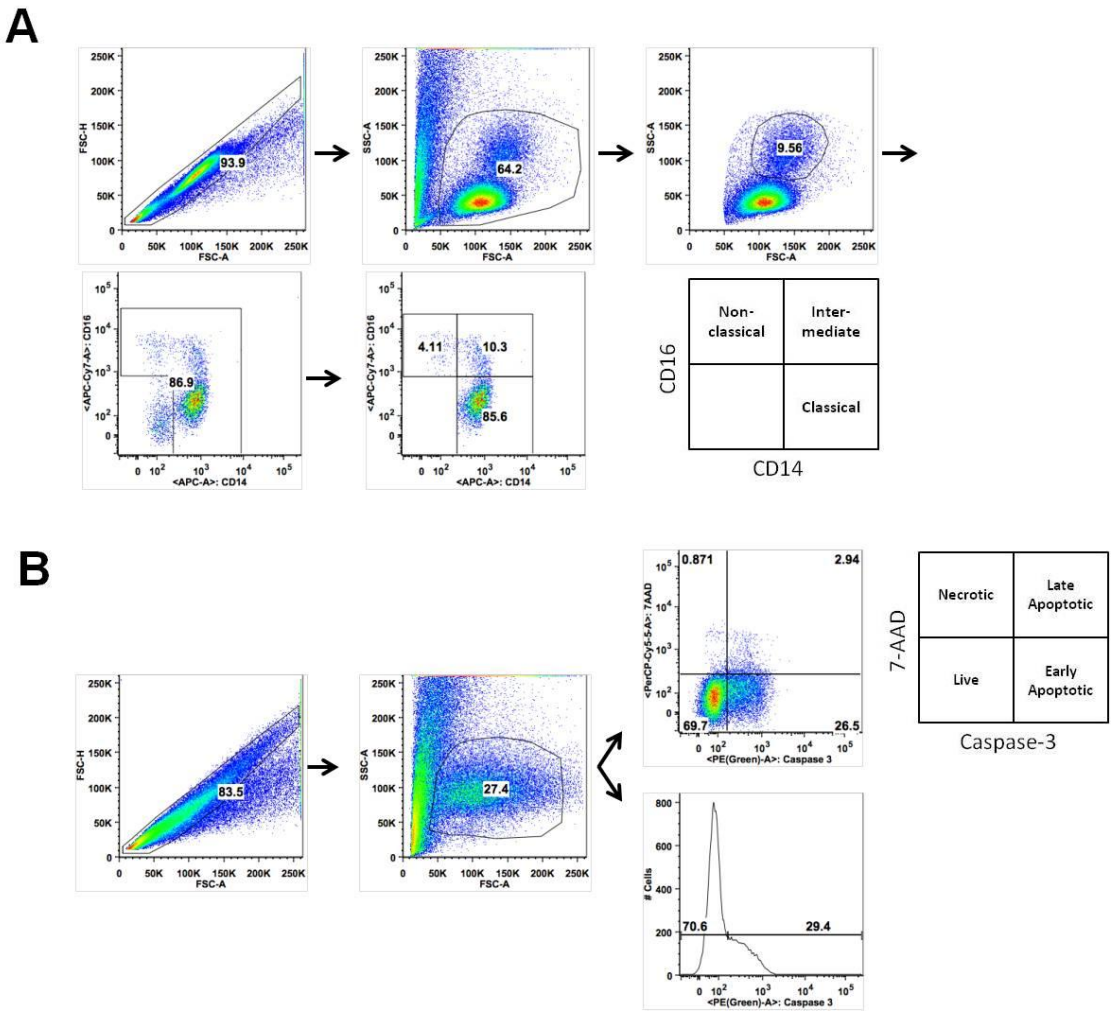

Figure 2.8: Monocyte subsets and apoptosis gating.
(A) PBMC gated on singlets, intact cells, monocyte scatter profile, and CD14/CD16 into non-classical ($CD14^{+}/CD16^{++}$), intermediate ($CD14^{++}/CD16^{+}$), and classical ($CD14^{++}/CD16^{-}$) monocyte subsets. (B) Negatively purified monocytes gated on singlets and intact cells and quantified for apoptosis by 7-AAD and active caspase-3 staining. Percent apoptotic cells counted as total caspase-3 positive cells (top right and bottom right quadrants).

Both constitutive and oxidative stress-induced apoptosis (20 μM $CdCl_2$) (197-200) (measured by active caspase-3) were elevated in monocytes from patients above 40,000 ($Log_{10}4.60$) copies/mL (constitutive $P = 0.0034$, induced $P = 0.0002$) when compared to lower viremic patients (Figure 2.9, 2.10A). Based

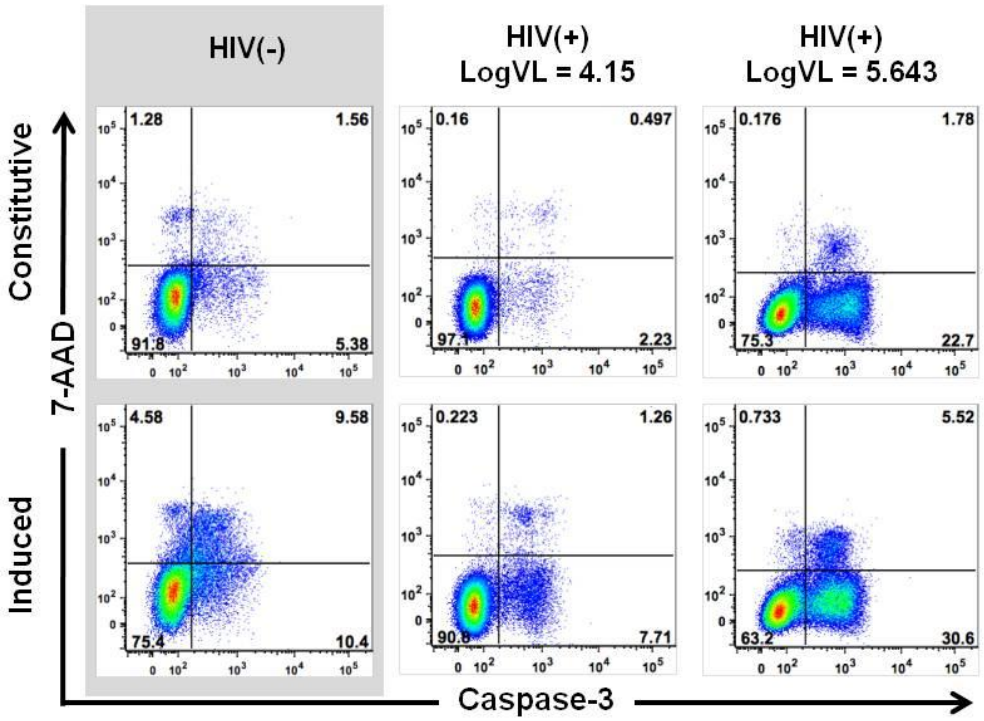

Figure 2.9: Monocyte apoptosis characterization.
Representative 7-AAD/caspase-3 dot plots of monocytes from uninfected and HIV(+) (14,000 and 439,508 copies/mL) individuals. Plots represent overnight constitutive apoptosis (first row) and oxidative stress induced apoptosis (20 μM $CdCl_2$) (second row).

on the analysis of the primary variable, monocyte apoptosis, HIV (+) patient variables are presented below and above a viral load cutoff of 40,000 HIV-1 copies/mL ($Log_{10}4.60$). Irrespective of viral load, increased T-cell apoptosis was observed in all HIV (+) patients as compared to uninfected donors (data not shown). Across all HIV (+) patients, constitutive and induced apoptosis were positively associated with viral load (P = 0.0256, R = 0.3883 and P = 0.0002, R = 0.5974, respectively) and inversely associated with CD4 count (P = 0.0128, R = –0.4288 and P = 0.0464, R = –0.3491, respectively) (Figure 2.10B, 2C). Supporting a threshold effect of viral load, the correlation of viral load with

apoptosis was not present if restricting to only patients above or below 40,000 copies/mL (all *P* values > 0.05, data not shown). Our data show higher HIV-1 viral load is associated with increased constitutive and induced apoptosis in circulating monocytes.

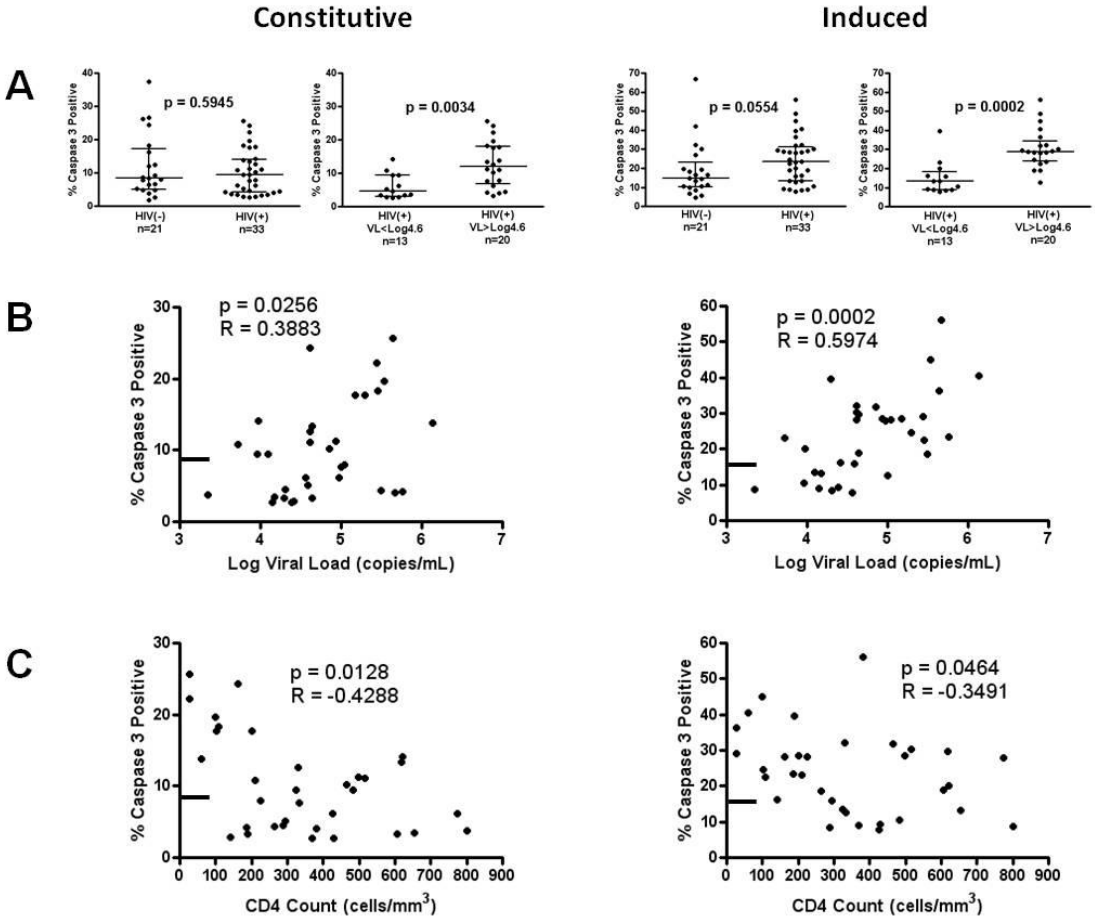

Figure 2.10: Monocyte apoptosis is elevated in patients above 40,000 copies/mL and associated with viral load and CD4 T-cell count.
(A) Group-wise comparison of constitutive (left) and induced (right) apoptosis in HIV(-) versus HIV(+) individuals and HIV(+) patients below versus above 40,000 ($Log_{10}4.6$) copies/mL. (B-C) Spearman ranked correlation of viral load (B) and CD4 count (C) versus monocyte apoptosis levels in HIV(+) patients. The line on the y-axis represents the median constitutive (8.48%) and induced (14.82%) apoptosis levels of the HIV(-) group. Group-wise comparison displays median and interquartile range using Mann-Whitney test (two-tailed) with $P < 0.05$ considered significant. Spearman (two-tailed) Rho and *P* values displayed with $P < 0.05$ considered significant.

2.3.2 Markers of innate immune activation are increased with HIV infection but do not associate with change in monocyte apoptosis

We wanted to test if observed differences in apoptosis were associated with monocyte/macrophage markers of activation in our cohort. Studies have described $CD14^{++}CD16^{+}$ intermediate monocytes (30, 32, 34, 35, 73), plasma sCD14 (86, 91, 151, 185), and plasma sCD163 (71, 176, 177, 201) as biomarkers of monocyte/macrophage activation and pathogenesis during SIV/HIV-1 infection. We found the $CD14^{++}/CD16^{+}$ intermediate subset and plasma sCD163 were elevated in the HIV (+) group compared to controls (Figure 2.11A, columns 1, 3), but did not detect differences within the HIV (+) groups (Figure 2.11B) or an association between these variables with viral load (Figure 2.11C), monocyte apoptosis (Figure 2.11D), or CD4 count (Figure 2.12A). Conversely, plasma sCD14 concentration was associated with viral load (Figure 2.11C) and CD4 count (Figure 2.12A), but not monocyte apoptosis (Figure 2.11D, $P = 0.1070$). Below a CD4 count of 500 cells/mm^3 (Figure 2.12B), CD4 count demonstrated a strong negative correlation with sCD14 ($P < 0.0001$) and negatively trended with sCD163 ($P = 0.0657$). Taken together, these data support the presence of monocyte/macrophage activation demonstrated by elevated sCD163 and $CD14^{++}CD16^{+}$ monocytes and an association of sCD14 with viremia and CD4 count that is independent of changes in monocyte apoptosis with viral load.

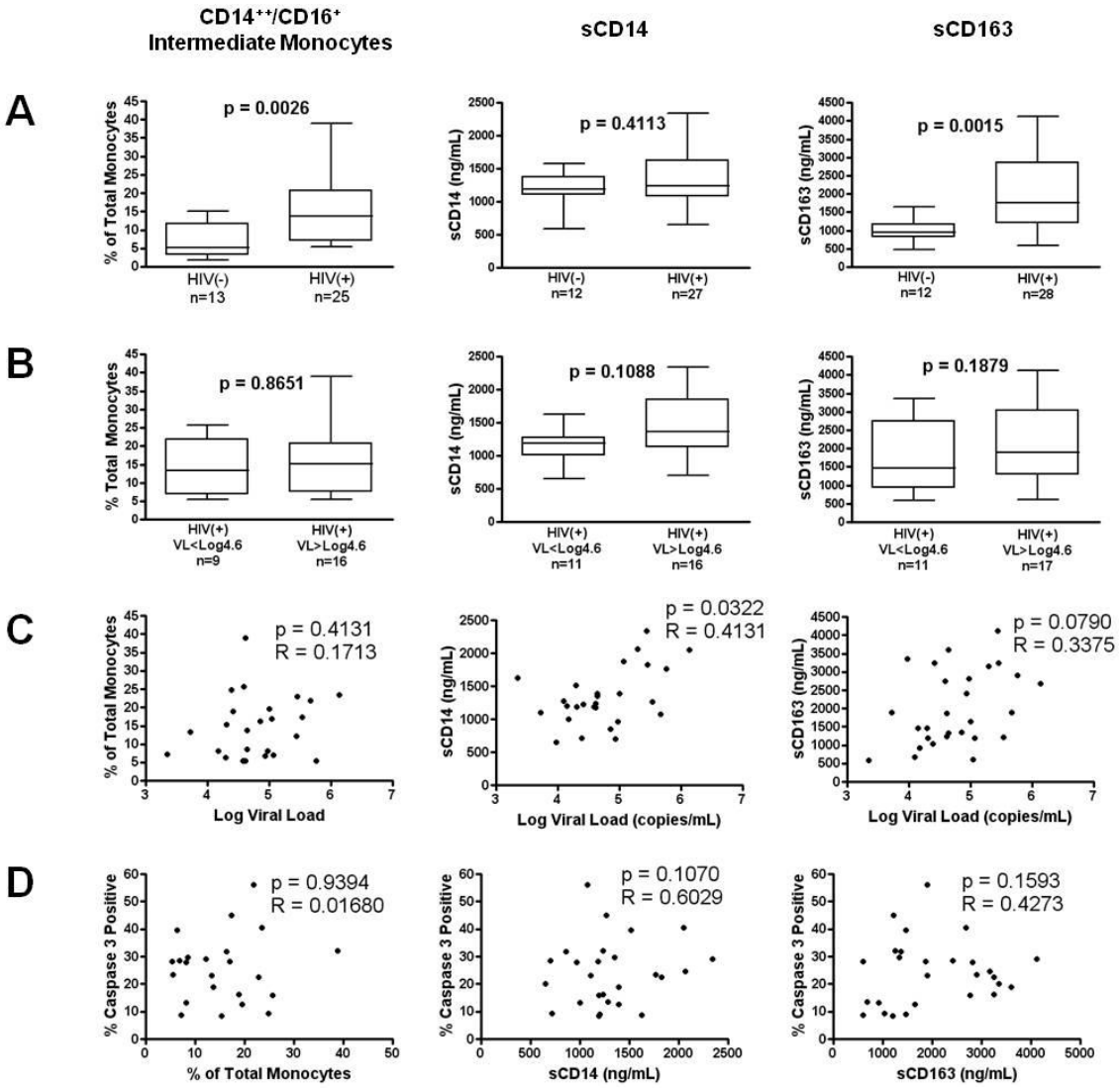

Figure 2.11: Monocyte/macrophage activation in HIV (+) patient cohort. (A-B) Group-wise comparison of percentage of intermediate $CD14^{++}/CD16^{+}$ monocytes (left), plasma sCD14 (middle), and plasma sCD163 (right) in HIV(-) versus HIV(+) individuals (A) and HIV(+) patients below versus above 40,000 ($Log_{10}4.6$) copies/mL (B). (C-D) Spearman ranked correlation of viral load (C) and induced apoptosis (D) versus monocyte/macrophage activation metrics. Group-wise comparison displays median, interquartile range (box), and range (whiskers) using Mann-Whitney test (two-tailed) with $P < 0.05$ considered significant. Spearman (two-tailed) Rho and P values displayed with $P < 0.05$ considered significant.

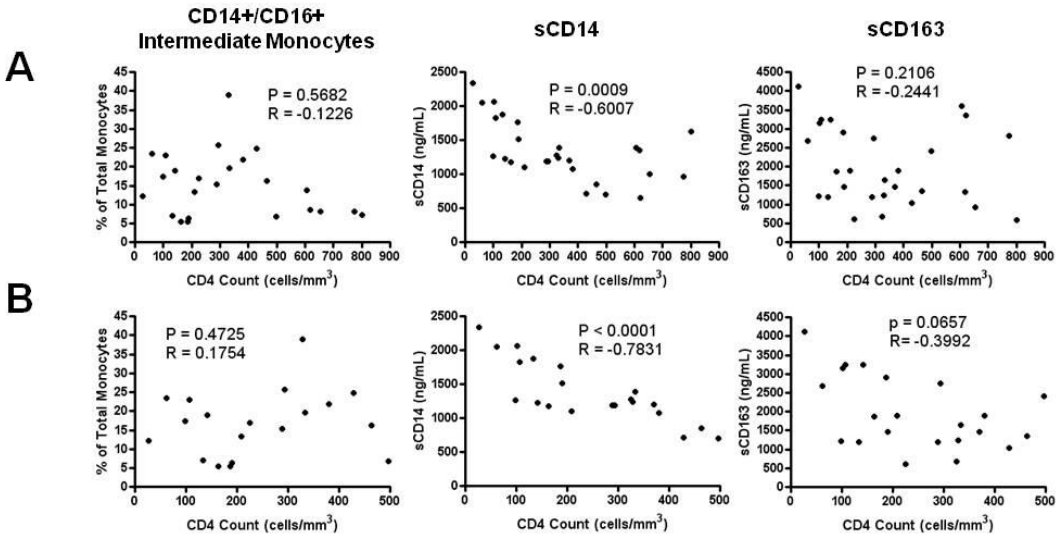

Figure 2.12: Monocyte/macrophage activation and CD4 count in HIV (+) patient cohort.
(A-B) Spearman ranked correlation of CD4 count with percentage of intermediate $CD14^{++}CD16^{+}$ monocytes (left), plasma sCD14 (middle), and plasma sCD163 (right) in total HIV(+) cohort (A) and HIV(+) patients below CD4 count of 500 cells/mm^3 (B). Spearman (two-tailed) Rho and *P* values displayed with $P < 0.05$ considered significant.

2.3.3 Apoptosis-related ISG family gene expression is altered in association with viral load

Pilot and *in vitro* experiments (**Section 2.2**) highlighted candidate apoptosis-regulatory gene families for follow-up in an expanded HIV (+) patient study. We chose to investigate monocyte expression of candidate p53 (105, 202, 203), Bcl2/cytochrome C (204-208), and ISG (170, 189-194, 196) family genes in viremic HIV (+) individuals (Table 2.4). RT-PCR analysis at time of isolation showed significantly higher Rb1 expression in the total HIV (+) group versus the HIV (-) group ($P = 0.0100$) but no association with viral load, consistent with reports of Rb1 contributions to apoptosis resistance (105) in circulating

Gene Symbol	Apoptotic Impact	Forward Primer 5' -3'	Reverse Primer 5' -3'	HIV(-), n=19 Median (IQR) (Expression units)	HIV (+), n=30 Median (IQR) (Expression units)	p-value HIV(-) versus HIV(+)
Rb1	**Anti -Apoptotic** [105, 202, 203]	GCC TCT CGT CAG GCT TGA G	TCA TCT AGG TCA ACT CGT GCA A	2.559 (1.729-8.421)	7.563 (5.633 -9.302)	0.0100
MDM2		GAA TCA TCG GAC TCA GGT ACA TC	TCT GTC TCA CTA ATT GCT CTC CT	1.359 (0.7060-3.316)	1.634 (1.192 -2.660)	n.s.
Bcl2	**Anti -Apoptotic** [205, 207, 208]	TTG CCA GCC GGA ACC TAT G	CGA AGG CGA CCA GCA ATG ATA	0.1108 (0.08957-0.3244)	0.3394 (0.09620-0.7771)	n.s.
Bcl-w	**Anti -Apoptotic** [205, 207, 208]	GCG GAG TTC ACA GCT CTA TAC	AAA AGG CCC CTA CAG TTA CCA	1.052 (0.6412-1.314)	0.6553 (0.4295-0.9256)	0.0169
Mcl-1	**Anti -Apoptotic** [205, 207, 208]	TGC TTC GGA AAC TGG ACA TCA	TAG CCA CAA AGG CAC CAA AAG	0.8846 (0.5637-1.242)	0.8340 (0.5756-1.101)	n.s.
Bax	**Pro-Apoptotic** [205, 207, 208]	CCC GAG AGG TCT TTT TCC GAG	CCA GCC CAT GAT GGT TCT GAT	0.6709 (0.4939-1.030)	0.8039 (0.6534-0.9233)	n.s.
Bak1	**Pro-Apoptotic** [205, 207, 208]	GTT TTC CGC AGC TAC GTT TTT	GCA GAG GTA AGG TGA CCA TCT C	1.868 (1.338-3.304)	2.201 (1.759 -2.906)	n.s.
Bik	**Pro-Apoptotic** [205, 207, 208]	GAC CTG GAC CCT ATG GAG GAC	CCT CAG TCT GGT CGT AGA TGA	0.6191 (0.3536-1.256)	0.6983 (0.4991-1.149)	n.s.
CycS	**Pro-Apoptotic** [204, 206]	CTT TGG GCG GAA GAC AGG TC	TTA TTG GCG GCT GTG TAA GAG	0.8745 (0.4069-1.406)	1.313 (0.9209 -1.627)	0.0392
Mx1		GTT TCC GAA GTG GAC ATC GCA	CCA TTC AGT AAT AGA GGG TGG GA	0.1703 (0.1163 -0.3839)	1.140 (0.4724 -2.399)	<0.0001
IFI6	**Anti -Apoptotic** [191, 192]	GGT CTG CGA TCC TGA ATG GG	TCA CTA TCG AGA TAC TTG TGG GT	0.8497 (0.4130-1.969)	5.150 (2.086 -12.72)	0.0002
IFI27	**Pro-Apoptotic** [193]	TGG CTC TGC CGT AGT TTT G	TCC TCC AAT CAC AAC TGT AGC A	0.3359 (0.1101 -0.8334)	158.7 (10.34 -533.5)	<0.0001
IFITM2	**Pro-Apoptotic** [194]	ATG AAC CAC ATT GTG CAA ACC T	CCC AGC ATA GCC ACT TCC T	1.798 (1.167-2.780)	3.128 (2.105 -4.960)	0.0015

Table 2.4: Apoptosis related p53, Bcl2/cytochrome C, and ISG family genes measured by absolute quantification RT-PCR.
Gene symbol, apoptotic impact, primers, expression in HIV (-) and HIV (+) groups, and *P* for HIV (-) versus total HIV (+) group comparison.

monocytes during chronic HIV-1 infection. Within the Bcl2/cytochrome C genes analyzed, the HIV (+) group was characterized by lower Bcl-w ($P = 0.0169$) and higher cytochrome C gene expression ($P = 0.0392$); however, neither gene was associated with viral load. In contrast, Mx1 and the apoptosis-regulatory ISG12 members (IFI6, IFI27, IFITM2) showed higher expression in the HIV (+) group, and IFI27 and IFITM2 expression was elevated in the HIV (+) group above 40,000 copies/mL relative to the HIV (+) group below 40,000 copies/mL (Figure 2.13A). The apoptosis-related ISGs (IFI6, IFI27, IFITM2) were also positively associated with viral load (Figure 2.13B). Taken together, our data demonstrate a

shift in monocyte gene expression with HIV-1 infection and increasing viral load that may support modulation of apoptosis outcome.

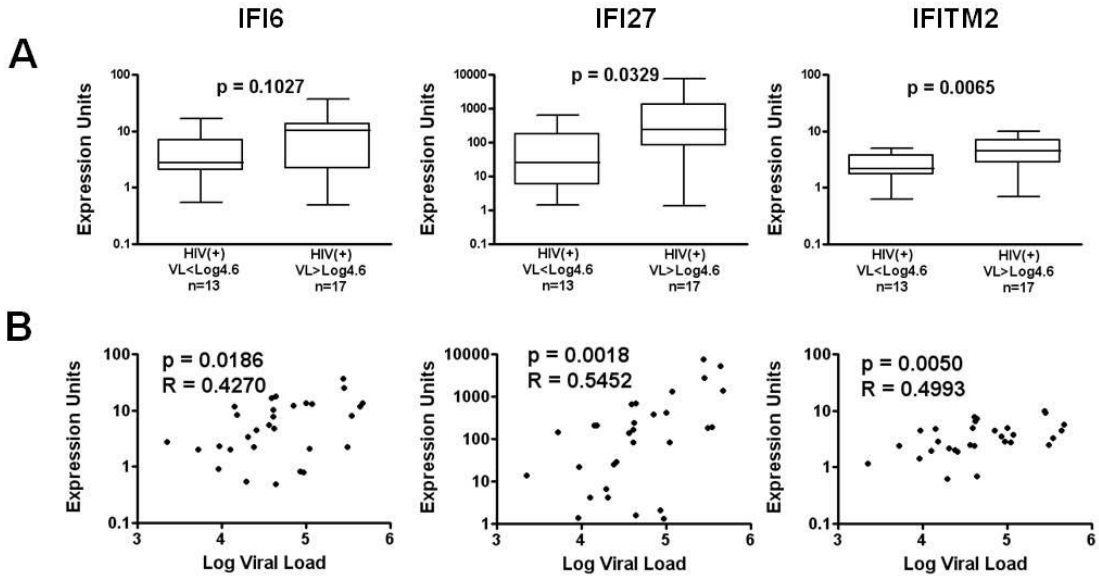

Figure 2.13: Monocyte ISG12 family expression is elevated in patients above 40,000 copies/mL and associated with viral load.
(A) Group-wise comparison IFI6, IFI27, and IFITM2 gene expression in HIV(+) patients below versus above 40,000 ($Log_{10}4.6$) copies/mL. (B) Spearman ranked correlation of viral load versus monocyte gene expression. Group-wise comparison displays median, interquartile range (box), and range (whiskers) using Mann-Whitney test (two-tailed) with $P < 0.05$ considered significant. Spearman (two-tailed) Rho and P values displayed with $P < 0.05$ considered significant.

2.3.4 Multivariate analysis identifies genes associated with changes in constitutive and induced apoptosis in HIV infection

Although gene expression within target gene families was correlated (p53, pro-apoptotic Bcl2-genes, and ISGs) (Figure 2.14), only IFITM2 was associated with constitutive apoptosis, indicating that single gene analysis could not a reflect change in both constitutive and induced apoptosis outcome. Multivariable stepwise regression modeling was applied to evaluate if the combination of viral

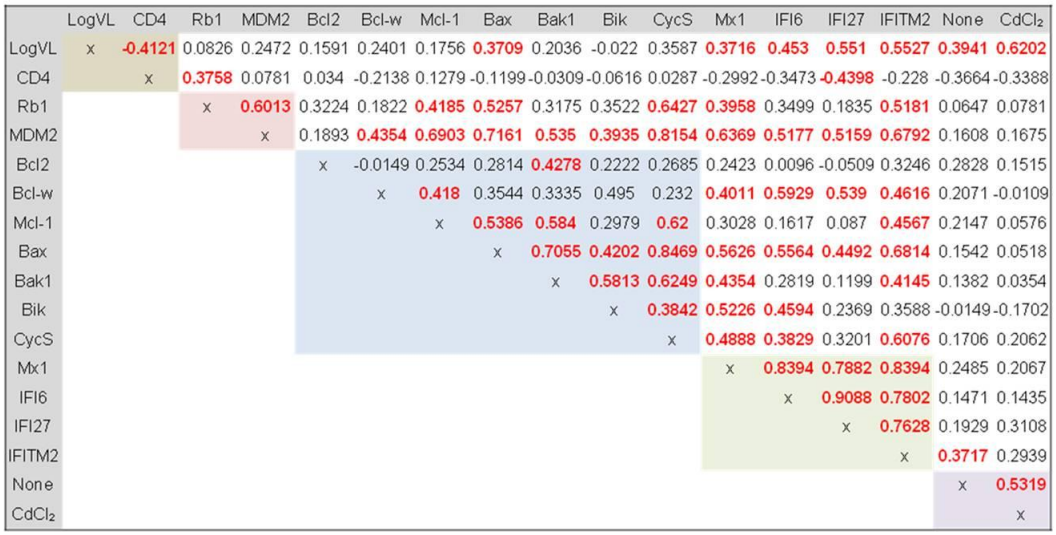

	LogVL	CD4	Rb1	MDM2	Bcl2	Bcl-w	Mcl-1	Bax	Bak1	Bik	CycS	Mx1	IFI6	IFI27	IFITM2	None	$CdCl_2$
LogVL	x	**-0.4121**	0.0826	0.2472	0.1591	0.2401	0.1756	**0.3709**	0.2036	-0.022	0.3587	**0.3716**	**0.453**	**0.551**	**0.5527**	**0.3941**	**0.6202**
CD4		x	**0.3758**	0.0781	0.034	-0.2138	0.1279	-0.1199	-0.0309	-0.0616	0.0287	-0.2992	-0.3473	**-0.4398**	-0.228	-0.3664	-0.3388
Rb1			x	**0.6013**	0.3224	0.1822	**0.4185**	**0.5257**	0.3175	0.3522	**0.6427**	**0.3958**	0.3499	0.1835	**0.5181**	0.0647	0.0781
MDM2				x	0.1893	**0.4354**	**0.6903**	**0.7161**	**0.535**	**0.3935**	**0.8154**	**0.6369**	**0.5177**	**0.5159**	**0.6792**	0.1608	0.1675
Bcl2					x	-0.0149	0.2534	0.2814	**0.4278**	0.2222	0.2685	0.2423	0.0096	-0.0509	0.3246	0.2828	0.1515
Bcl-w						x	**0.418**	0.3544	0.3335	0.495	0.232	**0.4011**	**0.5929**	**0.539**	**0.4616**	0.2071	-0.0109
Mcl-1							x	**0.5386**	**0.584**	0.2979	**0.62**	0.3028	0.1617	0.087	**0.4567**	0.2147	0.0576
Bax								x	**0.7055**	**0.4202**	**0.8469**	**0.5626**	**0.5564**	**0.4492**	**0.6814**	0.1542	0.0518
Bak1									x	**0.5813**	**0.6249**	**0.4354**	0.2819	0.1199	**0.4145**	0.1382	0.0354
Bik										x	**0.3842**	**0.5226**	**0.4594**	0.2369	0.3588	-0.0149	-0.1702
CycS											x	**0.4888**	**0.3829**	0.3201	**0.6076**	0.1706	0.2062
Mx1												x	**0.8394**	**0.7882**	**0.8394**	0.2485	0.2067
IFI6													x	**0.9088**	**0.7802**	0.1471	0.1435
IFI27														x	**0.7628**	0.1929	0.3108
IFITM2															x	**0.3717**	0.2939
None																x	**0.5319**
$CdCl_2$																	x

Figure 2.14: Gene expression correlation of p53, Bcl2, and ISG family genes in monocytes of HIV (+) donors.
Spearman ranked correlation matrix of clinical parameters (brown), p53 (pink), Bcl2 (blue), and ISG (green) family genes, and constitutive/induced apoptosis (purple). Spearman test (two-tailed, unadjusted) with $P < 0.05$ considered significant (bolded/red) and Spearman Rho is displayed. (n = 30).

load, CD4 count, and gene expression variables could generate a model for the distribution of constitutive and induced apoptosis responses observed in HIV-infected patients. The adjusted R-squared rank method identified IFI27, IFITM2, Rb1, and Bcl2 expression as the best model to describe variance in constitutive apoptosis ($P = 3.77\times10^{-5}$, adjusted-$R^2 = 0.5983$) (Table 2.5, Figure 2.15A). A reduction of this model showed the key variables were IFI27 and Bcl2, accounting for 96.4% of the adjusted R-squared. For oxidative stress-induced apoptosis, the model system identified log viral load, IFITM2, Rb1, and Bax expression ($P = 5.59\times10^{-5}$, adjusted-$R^2 = 0.5996$) (Table 2.5, Figure 2.15B), with log viral load and Rb1 expression representing 83.1% of the adjusted R-squared. Taken together, the shift in functional monocyte apoptosis observed with

increasing viral load was associated with a multi-gene association including changes in Rb1, ISG, and Bcl-2 expression.

Constitutive					
Coefficient	**Estimate**	**Std. Error**	**95% CI**	**t value**	**Pr(>|t|)**
(Intercept)	6.445281	2.2119471	1.8695—11.0210	2.914	7.82E-03
IFI27	0.003723	0.0008659	0.001932—0.005514	4.299	2.67E-04
IFITM2	-1.24797	0.6839378	-2.6628—0.16686	-1.825	0.081066
Rb1	0.393577	0.3363558	-0.3022—1.0894	1.17	2.54E-01
Bcl2	1.811856	0.4172257	0.9488—2.6750	4.343	2.40E-04
Multiple R-squared	0.6578				
Adjusted R-squared	0.5983				
F-statistic	11.05 on 4 and 23 DF				
p-value	3.77E-05				
Induced					
Coefficient	**Estimate**	**Std. Error**	**95% CI**	**t value**	**Pr(>|t|)**
(Intercept)	-98.354	21.986	-143.9495—-52.7577	-4.473	1.90E-04
Log Viral Load	19.890	3.532	12.5647—27.2153	5.631	1.16E-05
IFITM2	-5.899	4.277	-14.7694—2.9718	-1.379	0.18173
Rb1	15.037	5.332	3.978022—26.0957065	2.820	0.00997
Bax	-16.529	8.200	-33.534222—0.4762045	-2.016	0.0562
Multiple R-squared	0.6612				
Adjusted R-squared	0.5996				
F-statistic	10.73 on 4 and 22 DF				
p-value	5.59E-05				

Table 2.5: Multivariate analysis of monocyte apoptosis in HIV-1 viremic patients.
Constitutive and induced multivariate monocyte apoptosis models with R-squared, *P* value, and model gene/viral load components shown.

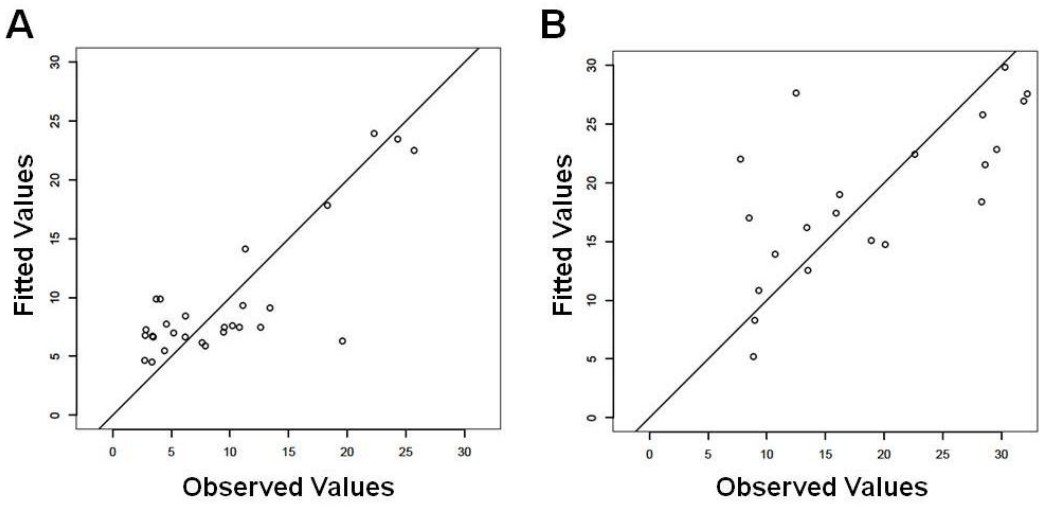

Figure 2.15: Multivariate analysis of monocyte apoptosis in HIV-1 viremic patients.
Top models generated showing (fitted) versus observed constitutive (A) and induced (B) apoptosis by multivariate stepwise regression of clinical parameters and apoptosis-gene expression.

2.4 Discussion, limitations, and future directions

Here we show for the first time that monocyte apoptosis is elevated in patients with greater than 40,000 HIV-1 copies/mL and negatively associated with CD4 count (Figure 2.10). Our data suggest that infection can modulate monocyte/macrophage activation, indicated by changes in $CD14^{++}CD16^{+}$ monocytes and sCD163, yet does not result in a rise in apoptosis until higher viral loads, clarifying conflicting reports of monocyte apoptosis in HIV and SIV infection (70, 96, 99, 103-105, 131).

Although elevated monocyte type 1 ISG expression (140, 144, 147) and monocyte/macrophage activation markers (30, 32, 40, 71, 73, 86, 91, 150, 151, 176, 177, 184, 185) have been described during HIV-1/SIV infection, the present

study extends these findings to include elevated monocyte apoptosis at high viral load in spite of active mechanisms of apoptosis resistance (i.e. Rb1 expression) (105). Change in ISG expression and increasing sCD14 with viral load may evidence increasing microbial translocation, as plasma LPS was associated with plasma IFN-α in HIV-1 viremic patients (86) and may contribute to the shift in monocyte ISG expression and apoptosis induction (209, 210).

Previous studies have demonstrated elevated sCD14 in multiple HIV (+) cohorts (relative to HIV (-) controls) (86, 151, 177, 178, 211), and while we demonstrate an association with viral load and CD4 count (Figure 2.11C and 2.12), we do not detect a significant difference between our HIV (-) and HIV (+) group (Figure 2.11A), which may reflect differences in sample size and the clinical characteristic of our HIV (+) cohort. Interestingly, others have observed biphasic CD163 expression on $CD14^{++}CD16^{+}$ monocyte subset relative to CD4 count (negative correlation below, positive correlation above 500 cells/mm^3) (31). Although we did not measure cell-associated CD163 expression, we observed a negative trend of CD4 count with sCD163, as well as a strong negative correlation of CD4 count and sCD14 in patients below 500 cells/ mm^3, supporting these observations (Figure 2.12B). Based on these findings, we would expect that the reversal of monocyte/macrophage activation markers upon ART-mediated suppression may vary qualitatively and temporally. This is supported by ART-mediated resolution of Rb1 protein expression (105), decreases in the $CD14^{++}CD16^{+}$ subset with treatment in early infection (177), persistence of

plasma sCD14 (177-179), and partial, but incomplete resolution of plasma sCD163 (150, 176, 177, 179). Longitudinal studies will be needed to establish the relationship between monocyte/macrophage activation, infection stage, and ART-mediated viral suppression (**Chapter 3**).

In addition to the primary findings per impact of viral load, multivariable analysis highlighted candidate ISG and Bcl2 genes as potential contributors to the functional apoptosis shift when added to rising viral load (Table 2.5, Figure 2.15). Members of the ISG12 family (189, 190) examined here, including IFI6 (191, 192), IFI27 (193), and IFITM2 (194), have described apoptosis-regulation functions. Of interest, IFITM2 was the only gene associated with apoptosis outcome at the single gene level (Figure 2.14) and IFITM2 and Rb1 were present in both models (Table 2.5, Figure 2.15), supporting specific candidate roles of these genes as determinant of monocyte apoptosis in HIV-infected patients. The impact of HIV-1 on Bcl2 family-mediated apoptosis in the CD4 compartment is also well described (Reviewed in (22)), and the effect on non-CD4 cell types, namely CD8 T-cells (212), dendritic cells (100), and now monocytes, suggests a global impact of HIV-1 viremia and immune activation on Bcl2-mediated apoptosis regulation. In addition, while Rb1 can override p53-mediated apoptosis induction *in vitro* (203), it remains to be determined whether Bax and ISG12 family expression can override anti-apoptotic Rb1 expression as suggested by our data. The multiple genes measured *ex vivo* as contributing to apoptosis regulation makes it highly unlikely the functional phenotype can be accounted by

any one gene. However, future work should determine how the described pro-apoptotic (IFI27, IFITM2, Bax) and anti-apoptotic (IFI6, Rb1, Bcl2) proteins exert regulation of apoptosis when co-expressed/knocked down to defining overall dominance or additive effects.

Our data do not address the potential impact of age and gender on monocyte apoptosis (150, 151, 213). Both HIV (-) and HIV (+) groups represent similar gender (no more than 25% female) and age distributions, but our cohort is limited in the representation of females and elderly individuals (Table 2.3). Future studies will need to address the impact of age and gender on monocyte apoptosis and apoptosis-gene expression.

Although we interpret a direct role of target genes in apoptosis outcome, a limitation of this study is the lack of single- and multi-gene over-expression/knockdown in monocytes to establish a role of target genes. Mechanism and the impact of target gene over-expression on apoptosis outcome are the primary objectives addressed in **chapter 4**. Also, while we focused on the relationship between apoptosis and the expression of apoptosis-regulatory gene families within monocytes (p53, ISG, Bcl2), our data do not exclude contributions by external mechanisms *in vivo* affecting total monocyte numbers such as *de novo* production/turnover described in SIV NHP models (70, 71) or external pressures such as elevated soluble-TRAIL (99, 112) and increased TRAIL-mediated apoptosis (96, 107, 109, 113).

In summary, we establish a shift in monocyte apoptosis and gene expression in association with high HIV-1 viral load and low CD4 count, which may bear on mechanisms for immunodeficiency, HIV replication, and/or HIV reservoir retention during HIV-1 infection *in vivo*.

2.5 Materials

2.5.1 Pilot RNA sequencing and analysis

Aphaeresis material was obtained from HIV-seronegative (n=2) and HIV-seropositive donors (n=4), and monocytes and CD4 T-cells were isolated by the University of Pennsylvania Human Immunology Core (HIC) using the RosettaSep kits from Stem Cell Technologies. RNA from purified CD4 T-cells and monocytes from pilot cohort (Table 2.1) was obtained by trizol isolation (Sigma) and pooled per group for analysis. Samples were Poly-A purified for mRNA and fragmented, cDNA was synthesized, and 175-225 base pair cDNAs were purified from agarose gel and sequenced in 36 base pair reads using the Illumina Genome Analyzer II platform. Analysis included read filtering (removing rRNA and mitochondrial reads) and alignment to genome and a custom-built transcription. The CD4 T-cell expression profile was not available in the HVL group due to low CD4 T-cell recovery.

2.5.2 Donor population

HIV-1 seropositive donors (n = 35, 11.4% female, median age = 43.0 years) were recruited from the Hospital of the University of Philadelphia (HUP) and Philadelphia Field Initiating Group for HIV-1 Trials (FIGHT) and were not on therapy at the time of the single draw. Viremic patients showed a broad spectrum of viremia (viral load range: 2,243-1,359,041 copies/mL; CD4 range 7-801 cells/mm^3) (Table 2.7). Viral load and CD4 count are reported from the most recent clinical visit (at most 3 months). HIV-1 seronegative donors (n = 33, 24.2% female, median age = 43.5 years) were recruited from the University of Pennsylvania Human Immunology Core and the Wistar Donors Program (Table 2.8). Assays data showing less than the total recruited HIV (-) or HIV (+) population reflect limited patient material. All participants provided informed consent prior to blood draw, and all protocols were approved by the institutional review boards of the National Institutes of Health and The Wistar Institute.

2.5.3 Monocyte and CD4 T-cell isolation and characterization

Heparinized blood (70-200 mL) was processed within 1-3 hours of draw. PBMC and plasma samples were obtained using Ficoll-Paque (Amersham Pharmacia Biotech) gradient separation. HIV (-) and HIV (+) donor CD4 T-cells were obtained from the University of Pennsylvania's Center for AIDS Research Human Immunology Core obtained by Rosette Sep (Stemcell Technologies) isolation from leukapheresis-PBMC. Monocytes were isolated by negative selection using the Monocyte Isolation Kit II (Miltenyi Biotec, 139-091-153) with a

mean biological purity greater than 85%. PBMC and isolated monocytes from each sample were stained with CD4-V450, CD14-APC, CD16-APCH7, CD3-PerCPCy5.5, and CD8-FITC for determination of purity, T-cell subsets, and monocyte subsets. All flow cytometry antibodies were purchased from BD Biosciences and used per the manufacturer's instructions.

2.5.4 Plasma monocyte/macrophage activation markers

HIV (-) and HIV (+) plasma samples were assayed by ELISA (enzyme-linked immunosorbent assay) for sCD14 (R&D Systems) and sCD163 (Trillium Diagnostics), using 1:500 dilutions, according to the manufacturers' instructions. Plates were read on a BioTek Synergy HT microplate reader at 450 nm with the appropriate wavelength corrections.

2.5.5 Quantitative real-time PCR

Total RNA was isolated from 2-5 million cells using the RNeasy Plus II Kit (Qiagen) per the manufacturer's protocol. Up to 250 ng of RNA was used with the iScript cDNA synthesis kit (BioRad) as instructed. Quantitative real-time PCR was performed in a 20 µL reaction using Power SYBR Green PCR Master Mix (Life Technologies) and custom designed primers (Inegrated DNA Technologies) (Table 2.9) using the AB 7000 Sequence Detection System. The QuantumRNA Universal 18s Internal Standard (Ambion) was used due to its robust and consistent expression across all samples. All primer sets were assayed by serial dilution PCR across multiple donors to allow for absolute RNA quantification by

the standard curve method. The mean of three replicates of each primer-sample pair was input in the standard curve method and normalized to the sample's 18s value to generate an absolute RNA expression units value. (Expression units defined as relative expression value to 18s after standardization.)

2.5.6 Apoptosis induction assay

Purified monocytes and CD4 T-cells were incubated overnight (18-22 hours) in non-adherent conditions (monocytes in Teflon pots to prevent attachment) in the presence of RPMI 1680 media with 1% Penicillin/Streptomycin (Corning), 1% L-Glutamine (Corning), and 10% Human Serum (Gemini Bio-Products) with or without the addition of 20 μM $CdCl_2$ (Sigma). All staining was performed at room temperature (22°C). Between 500,000 and 1 million cells were washed and incubated with FACS wash (DPBS (Life Technologies) containing 3 mM NaN_3 (Fisher), 1% Bovine Serum Albumin (Sigma), 5%Human Serum (Gemini Bio-Products)) as an Fc-receptor block. Cells were stained with CD3-Pacific Blue, CD14-APC and 7-aminoactinomycin D for 15 minutes. Cell fixation/permeabilization was performed using the BD Cytofix/Cytoperm kit per the manufacturer's instructions and washed in 1× PermWash buffer. Cells were then stained with anti-active caspase 3-PE (BD Biosciences), washed, and resuspended in 300 μL 1× PermWash buffer. Apoptosis was also assayed at baseline isolation in select samples. Up to 100,000 events were analyzed on a 14-color LSR II (BD Biosciences).

2.5.7 Flow cytometry gating and analysis

Flow cytometry data analysis was performed with FlowJo software (TreeStar) (Figure 2.9). Singlets were gated using forward scatter height and area. Live cells were gated, excluding debris and aggregates, with forward and side scatter. To characterize monocyte subsets in PBMC, monocytes were gated based on distinct forward and side scatter parameters and then $CD14^{+}$ or $CD16^{+}$ cells within this population. Monocytes were then divided into classical ($CD14^{++}CD16^{-}$), intermediate ($CD14^{++}CD16^{+}$), and non-classical ($CD14^{+}CD16^{++}$) subsets. In the apoptosis analysis, all events were gated on singlets, intact cells, and either lymphocyte or monocyte forward/side scatter parameters. Cells were analyzed using 7-AAD and caspase-3, and all cells in the early apoptotic and late apoptotic quadrants were counted when determining the percent of apoptotic cells within the population.

2.5.8 Statistical analysis

All dot, box and whisker, and scatter plots were constructed and statistically tested using Prism 4 (GraphPad, La Jolla, CA). All group-wise comparisons were performed using Mann-Whitney test with p-value displayed. Correlations between two variables were performed using Spearman's Correlation (Rho) test with *P* and Rho (noted as R) values displayed. All tests were two-sided and $P < 0.05$ was considered significant. The Spearman correlation matrix was created with JMP10 software. Based on the analysis of the

primary variable (monocyte apoptosis), HIV (+) patient measured variables are presented below and above a viral load cutoff of 40,000 copies/mL ($Log_{10}4.60$).

2.5.9 Multivariate linear regression modeling

A stepwise multiple linear regression analysis was performed to model constitutive and induced apoptosis using the combination of clinical and gene expression variables. We conducted log transformation on the independent variables and confirmed lack of multi-co-linearity in the final models within independent variables by means of the variance inflation factor (VIF). The Cook's distance was used in outlier detection and removal of each independent model. The model selection package "leaps" (Lumley and Miller 2009) in R was utilized to identify the best subset of clinical/gene expression parameters that predicted constitutive and induced apoptosis in the linear regression. The regsubsets function within "leaps" was used to find the best subset of predictive parameters. The adjusted R-squared statistic was used as the criterion for selecting the best model with four or less variables per total input variable size. Various diagnostic plots were used to check the assumptions for the multiple linear regressions (data not shown). Q-Q plot was used to examine normality. Residuals plot was used to examine the equal variance assumption.

CHAPTER 3: Antiretroviral therapy in HIV-1 infected individuals with CD4 count below 100 cells/mm^3 results in differential reversal of monocyte/macrophage activation

3.1 Introduction

Persistent immune activation during HIV-1 infection is associated with disease progression and sub-optimal immune recovery after ART (16, 23-25). Ongoing viremia has been noted to promote a state of innate immune activation inclusive of changes in natural killer cells (179) and monocytes/macrophages. Activation of monocytes and macrophages has been noted as a potentially major source of inflammation due to mechanisms of activation that may not be fully reversed during ART (80, 86, 91, 150, 174, 176-179) (Reviewed in **Section 1.5**).

During viremia, the $CD14^{++}CD16^{+}$ intermediate monocyte subset is expanded in both HIV-1 (32, 34-36) and SIV infection (30) and associated with HIV pathogenesis (32, 47, 150, 180). The significance of this subset as a potential indicator of long-term inflammation is supported by similar elevations described in patients with cardiovascular disease (35, 180). Soluble biomarkers of monocyte/macrophage activation are also well-characterized in HIV disease, including sCD14 and sCD163. Elevated sCD14 has been described as a marker of HIV-associated microbial translocation and increases in plasma LPS (86, 152, 185). Cell-associated CD163 expression and shedding (as sCD163) from monocytes and macrophages is also elevated during HIV/SIV infection (31, 69, 71, 177) and associated with both cardiac and CNS pathology (36, 71, 80, 176, 184). The relationship between innate and adaptive activation during viremia and the expected decrease of both on ART raises the hypothesis that reduction in T-

cell activation would be associated with reduction in monocyte and macrophage activation.

ART-mediated resolution of monocyte/macrophage activation has become a growing area of focus due the relationship with metabolic disease and retention of immune activation during HIV infection (36, 47, 150, 176, 184) (Table 3.1). The $CD14^{++}CD16^{+}$ intermediate monocyte subset is decreased in patients treated during early infection, but not chronic infection (177); cross-sectional comparison has demonstrated that suppressed patients reach comparable levels to HIV (-) donors (35). Interestingly, a reduction of the intermediate monocyte subset was

Manuscript (first, last)	Study Type	sCD14	sCD163	Other Finding
Brenchley Douek Nat Med 2006	Longitudinal	**Persistent** at48 weeks ART		
Wallet Goodenow AIDS 2010	Longitudinal (Pediatric)	**Persistent** at 24 weeks **Partial** at 96 weeks		
Rajasuriar Lewin JID 2010	Longitudinal	**Partial** resolution at 12 months		
Sandler Douek JID 2011	Cross sectional	Slightly higher in ART with VL<400 over untreated		
Burdo Williams JID 2011	Longitudinal	**Persistent** at 3 months	**Partial** resolution (early treatment)	Decreased $CD14^{++}16^{+}$ subset (early treatment)
Burdo Grinspoon JID 2011	Cross sectional		**Partial**: ART does not reduce to HIV(-) levels	
Lederman Rodriguez JID 2011	Cross sectional	Immune failure higher than success higher than HIV (-)		$CD14^{++}CD16^{+}$ subset resolution
Lichtfuss Jaworowski JImm2012	Cross sectional	No difference From viremic	**Partial**: ART does not reduce to HIV(-) levels	
Hearps Crowe AIDS 2012	Cross sectional		**Partial**: ART does not reduce to HIV(-) levels	$CD14^{++}CD16^{+}$ subset resolution **Partial**: CXCL10 resolution
Noel Lambotte AIDS 2014	Cross sectional	No difference From viremic	**Partial**: ART does not reduce to HIV(-) levels	**Partial**: CXCL10 resolution
Somsouk Hunt AIDS 2015	Cross sectional	No difference From viremic		**Partial**: resolution colorectal mucosal apoptosis

Table 3.1: Monocyte/macrophage activation during ART.
Study type, sCD14 impact, sCD163 impact, and other findings shown for reports on monocyte/macrophage activation during ART.

noted in patients with CD4 counts below 350 cells/mm^3, but this study did not examine other markers of T-cell or monocyte/macrophage activation (34). Plasma sCD163 was reduced to normal levels in patients treated during early infection, but not those treated at later stages (177). Additionally, cross-sectional studies suggest sCD163 does not reach normal levels with viremic suppression (150, 176, 177, 179). Plasma sCD14 is even less plastic. Longitudinal studies have found elevated sCD14 levels persist despite viral suppression (86, 174, 177) and are only partially resolved after extended ART (174, 175). Cross-sectional comparisons have demonstrated that sCD14 levels are not resolved to normal levels in ART-treated patients (91, 152, 174, 178, 179).

A major component of monocyte/macrophage activation during viremia is the upregulation of ISG expression (Reviewed in **Section 1.4**). Among these, CD169 (Sialoadhesin, SN, SIGLEC1) is a surface-expressed ISG (IFN-α, IFN-γ inducible) on monocytes, macrophages, and dendritic cells that is highly expressed during HIV-1 infection (143, 154, 156) and other inflammatory diseases (155, 157). CD169 can also facilitate trans-infection of target cells by both monocytes and dendritic cells (156, 158, 159). Its expression can be reversed with viral suppression after ART in SIV infection (160).

Studies have suggested that CCR5 antagonism may improve resolution of T-cell activation during ART initiation (temporary advantage) (214, 215) yet data is not uniform across intensification studies to date (215-218). Regarding

monocyte/macrophage activation, Maraviroc-inclusive ART has yielded mixed results regarding sCD14 resolution (216, 217, 219, 220) (Table 3.2). Some

Manuscript (first, last)	Study Type	sCD14	sCD163	Other Finding
Funderburg Lederman PLoSOne 2010	Longitudinal **Maraviroc** (Intensification) Two arm			Temporary advantage in $CD38^+$ decrease on CD4 T-cells
Gutierrez Moreno PLoSOne 2011	Longitudinal **Maraviroc** (Intensification) Single arm	Increased		
Wilkin Tenorio JID 2012	Longitudinal **Maraviroc** (Intensification) Single arm			Decreased $CD38^+$ on CD4, CD8 during MVC, increased after discontinuation (INR, immunological non-responder, cohort)
Romero-Sanchez Leal AAC 2012	Longitudinal **Maraviroc** (Initiation) Two arm	Decreased in virological responders		
Hunt Deeks Blood 2013	Longitudinal **Maraviroc** (Intensification) Two arm	Trending increase (not significant)	No benefit	(INR cohort)
Rusconi Marchetti PLoSOne 2013	Longitudinal **Maraviroc** (Intensification) Two arm			No improved CD4 reconstitution (INR cohort)
Puertas Martinez-Picado AIDS 2014	Longitudinal **Maraviroc** (Intensification) Two arm	No difference		Temporal advantage in decrease in **viral DNA**
Hileman McComsey JID 2015	Longitudinal **Elvitegravir** (Initiation)	Greater sCD14 resolution		
Funderburg McComsey AIDS 2015	Longitudinal **Rosuvastatin** (Intensification)	Greater sCD14 resolution		Greater **$CD14^+CD16^{++}$** subset decrease Greater **CXCL10** decrease Lower **$CD38^+HLA\text{-}DR^+$** on CD4 and CD8

Table 3.2: Monocyte/macrophage activation during non-standard ART. Study type, sCD14 impact, sCD163 impact, and other findings shown for reports on monocyte/macrophage activation during non-standard ART (Maraviroc, Elvitegravir, Rosuvastatin).

variability may be attributed to cohort and therapy differences, as intensification studies often target immunological non-responders (215, 217, 218). Taken together, the immunological impact of a Maraviroc-inclusive regimen in patients initiating ART from advanced infection has not been described. Although addition of CCR5 antagonism (Maraviroc) did not impact the degree of CD4 recovery in patients starting with nadir CD4 counts in the parent study (221), we hypothesize

it may reduce monocyte/macrophage activation by inhibiting monocyte/macrophage recruitment and viral-CCR5 interactions (222, 223).

In this chapter, we describe the changes in biomarkers of monocyte and macrophage activation and the impact of CCR5 antagonism in patients initiating ART in advanced disease (CD4 count below 100 cells/mm^3). Our primary analysis aimed at determining the degree and kinetics of reversal of monocyte/macrophage activation with respect to T-cell activation, while secondary analysis addressed the impact of CCR5 antagonism on monocyte/macrophage activation. With 24 weeks of suppressive ART, we observed a differential reversal of biomarkers of monocyte/macrophage activation. Apart from increases in the percentage of peripheral blood monocytes expressing CCR5, no Maraviroc-mediated effects on monocyte/macrophage activation markers with ART were noted.

3.2 Antiretroviral therapy in HIV-1 infected individuals with CD4 count below 100 cells/mm^3 results in differential reversal of monocyte/macrophage activation

3.2.1 Study cohort and baseline characteristics

Patients were recruited in the CADIRIS (CCR5 antagonism to decrease the incidence of immune reconstitution inflammatory syndrome) study examining the impact of Maraviroc-inclusive ART on IRIS incidence in low CD4 count HIV-1

patients initiating ART between five study sites in Mexico and one in South Africa (221). Patients received placebo or Maraviroc (600 mg) in addition to a background of Efavirenz (EFV, 600 mg), Tenofovir, (TDF, 300 mg), and Emtricitabine, (FTC, 200 mg), and plasma and PBMC were isolated from whole blood at 0 (pre-ART), 12, and 24 weeks. Archived plasma and PBMC were analyzed from 65 patients from the South Africa site that were virologically suppressed at week 24 (defined as viral load less than 400 HIV-1 RNA copies/mL). Inclusion criteria of the parent study required a baseline CD4 count of less than or equal to 100 CD4 T-cells/mm^3, allowing us to investigate the impact of ART-mediated suppression on monocyte/macrophage activation biomarkers in advanced HIV-1 infection. Consistent with the parent study, no difference in gender, age, and baseline clinical metrics (viral load, CD4 count, CD8 count) was observed between the placebo and Maraviroc groups in the sub-study (Table 4.3). Baseline T-cell and monocyte/macrophage activation markers were also not different between groups.

	ART + Placebo	ART + Maraviroc	Total	p
n	31	34	65	
Age (years)	38 (34-45)	37.5 (33.75-44)	38 (34-44)	0.712
Gender, no. female (%)	18 (58.1%)	19 (55.9%)	37 (56.9%)	1.0000
Log Viral Load (RNA copies/mL)	5.201 (4.934-5.604)	5.467 (5.000-5.728)	5.407 (5.000-5.679)	0.3703
CD4 count (cells/mm^3)	46 (25-72)	41 (23-53.5)	41 (25-66.5)	0.2483
CD8 count (cells/mm^3)	585 (426-796)	431 (339-706.5)	531 (375.8-730.3)	0.1544
%HLA-DR+, CD38+ CD4 T-cells	14.5 (10.17-24.1)	14.65 (8.990-21.10)	14.5 (9.223-22.30)	0.7561
%HLA-DR+, CD38+ CD8 T-cells	23.65 (14.40-29.90)	19.55 (12.73-24.95)	20.55 (13.80-28.38)	0.2112
%CD14++CD16+ Monocytes	17.95 (11.53-23.50)	15.70 (10.90-21.45)	15.90 (11.00-21.90)	0.4415
%CD163 Monocytes	4.430 (0.735-11.40)	3.870 (1.117-11.90)	4.010 (0.8360-10.80)	0.9102
%CD169 Monocytes	81.95 (76.63-87.43)	81.50 (68.70-88.95)	81.50 (72.80-87.90)	0.6544
Tetherin (MFI)	2195 (957.5-3407)	1276 (943.0-2832)	1688 (972.0-3298)	0.6372
sCD14 (ng/mL)	2861 (2143-3712)	2398 (1905-3223)	2774 (2069-3464)	0.1437
sCD163 (ng/mL)	1496 (1123-2408)	1449 (1086-1712)	1449 (1087-1926)	0.4715

Table 3.3: Cohort baseline characteristics.
Demographic, clinical, and T-cell and monocyte/macrophage activation baseline metrics are shown for ART + Placebo group, ART + Maraviroc group, and total ART cohort. *P* values were calculated by Mann-Whitney test for all comparisons, excluding gender which was calculated by Fisher's exact test.

3.2.2 Change in T-cell count and biomarkers of T-cell activation

Median CD4 count increased from 46 and 41 (placebo and Maraviroc group) to 149 and 177 cells/mm^3 during 24 weeks ART ($P < 0.0001$ for both groups, $P = 0.5710$ between groups at week 24) (Figure 3.1A). The parent study and others have observed higher CD8 counts in Maraviroc groups during ART (217, 221), and the sub-study observed a similar trend ($P = 0.0579$, week 24) (Figure 3.1B). As these patients initiated therapy from advanced infection, we did

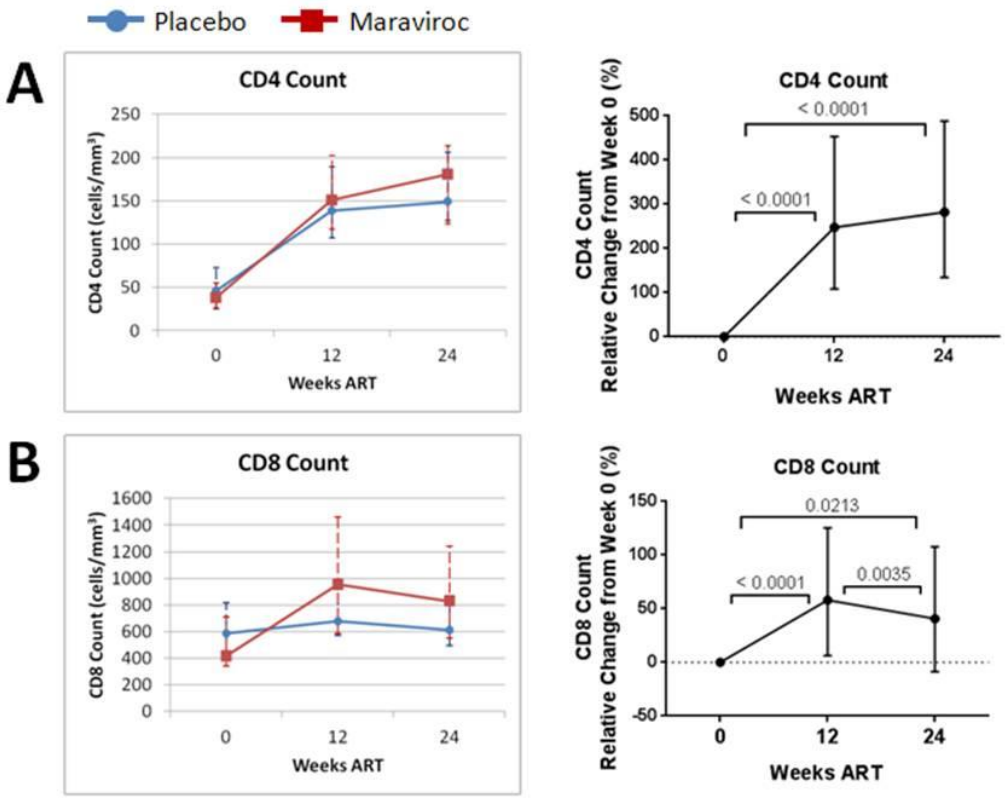

Figure 3.1: CD4 and CD8 T-cell count during ART.
Shown are placebo (blue) versus Maraviroc (red) group CD4 count (A) and CD8 count (B) absolute and relative to baseline change. Median and interquartile range (IQR) are displayed, and only patients with all time points are shown. Mann Whitney comparison between groups was performed at each time point with $P < 0.05$ considered significant and displayed. Longitudinally, Friedman test and post hoc Dunn test were performed with $P < 0.05$ considered significant and displayed.

not expect uniform decreases in T-cell activation markers by week 24 (24, 25). However, T-cell activation, measured by $CD38^+$, $HLA\text{-}DR^+$ T-cells, was uniformly reduced in both CD4 and CD8 T-cells in both groups by week 24 ($P < 0.0001$ for CD4 and CD8) (Figure 3.2, 3.3A, B). At week 24, we detected a small but significant difference in $CD38^+$, $HLA\text{-}DR^+$ CD4 T-cells (3.555% in placebo versus 2.620% in Maraviroc, $P = 0.0072$, Figure 3.3A). The percent of CD4 and CD8 T-cells expressing CD38 was also significantly reduced in both arms ($P < 0.001$ for CD4 and CD8) (Figure 3.3C, D). Independent of group, the percent of CD4 or CD8 T-cells expressing CD38 or CD38 and HLA-DR was reduced by 49-70% from baseline (Figure 3.3).

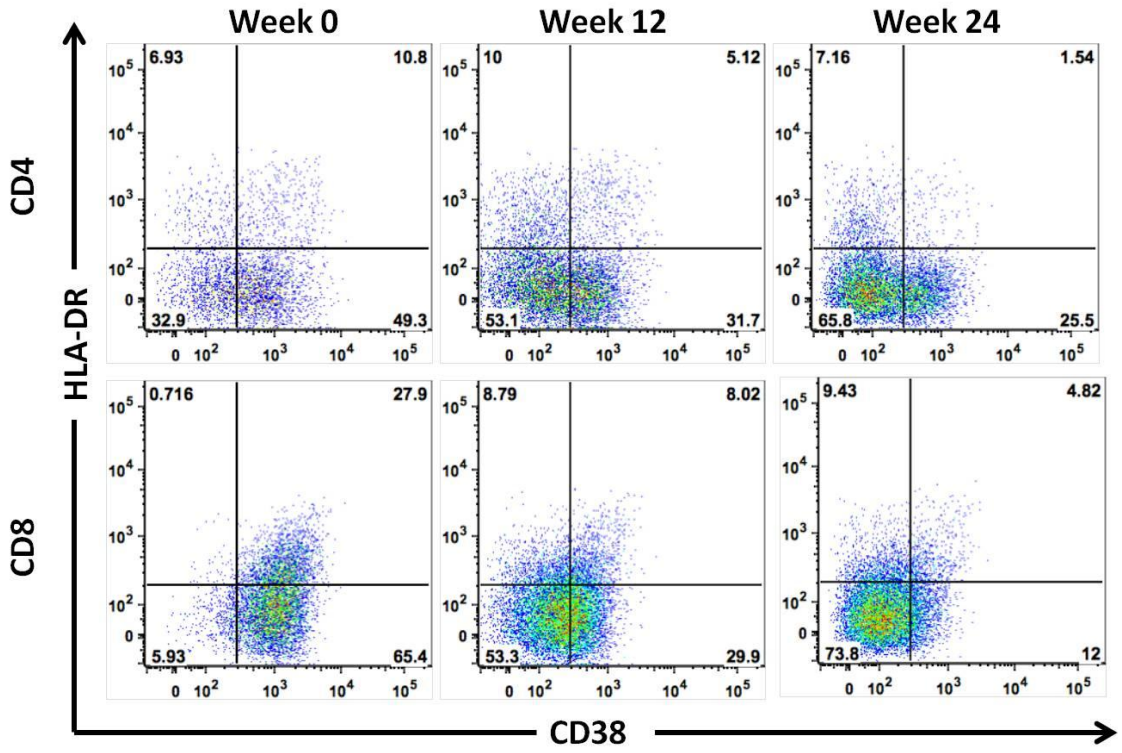

Figure 3.2: Representative T-cell activation biomarkers during ART. Representative donor CD4 (top) and CD8 (bottom) T-cell expression of CD38 (x-axis) and HLA-DR (y-axis) during ART are shown.

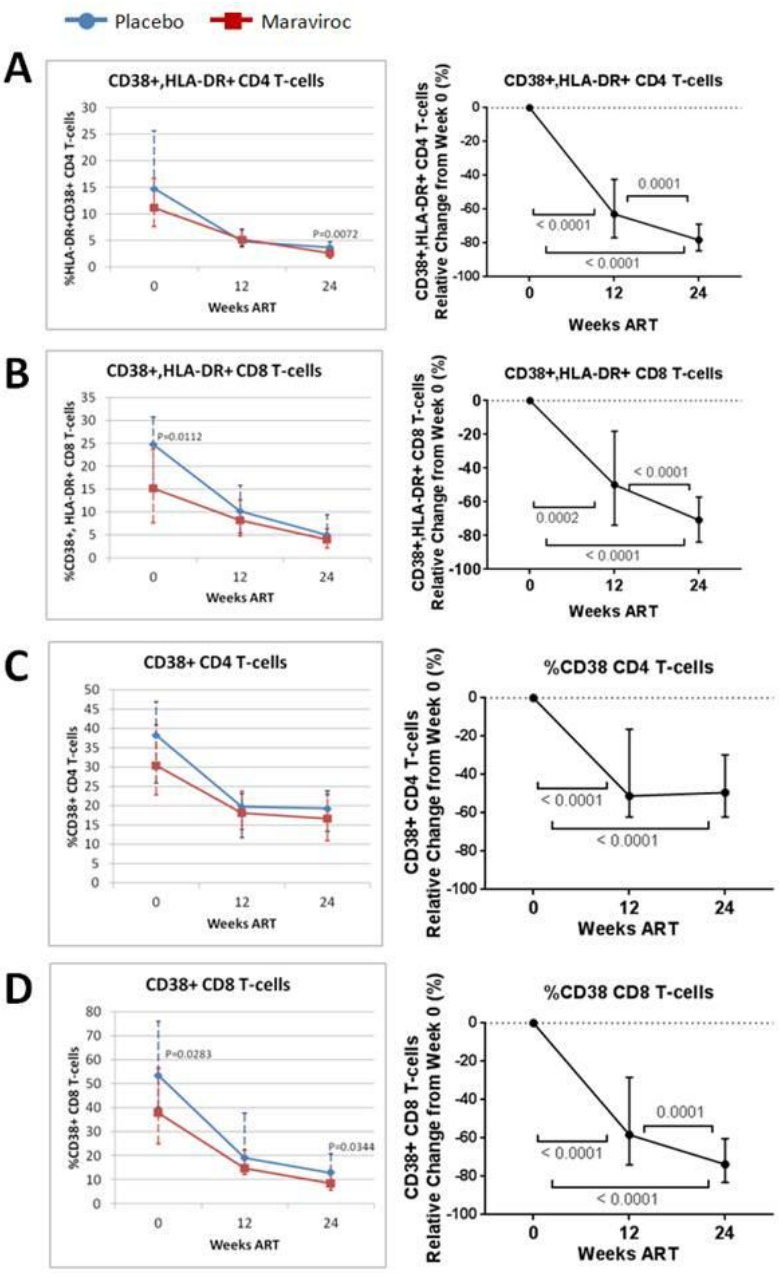

Figure 3.3: T-cell activation markers during ART.
Shown are placebo (blue) versus Maraviroc (red) group percent of $CD38^+$, HLA-DR^+ CD4 T-cells (A), $CD38^+$, HLA-DR^+ CD8 T-cells (B), $CD38^+$ CD4 T-cells (C), and $CD38^+$ CD8 T-cells (D) during ART absolute and relative to baseline change. Median and interquartile range (IQR) are displayed, and only patients with all time points are shown. Mann Whitney comparison between groups was performed at each time point with $P < 0.05$ considered significant and displayed. Longitudinally, Friedman test and post hoc Dunn test were performed with $P < 0.05$ considered significant and displayed.

3.2.3 *In vivo* impact of Maraviroc on monocyte/macrophage activation markers and T-cell and monocyte CCR5 expression

Markers of monocyte/macrophage activation were not significantly different between groups (data not shown). We observed a higher percentage of CCR5 expressing CD4 T-cells, CD8 T-cells, and monocytes in PBMC of the Maraviroc group during ART (Figure 3.4), as evidence of therapy exposure and as reported by others (217). We interpret this to reflect a lack of ligand-mediated receptor internalization and/or lack of tissue migration of $CCR5^{+}$ cells in the Maraviroc group. As we did not detect an impact of Maraviroc on monocyte/macrophage biomarkers of activation, from this point onwards, we opted to analyze ART-mediated changes independent of study group.

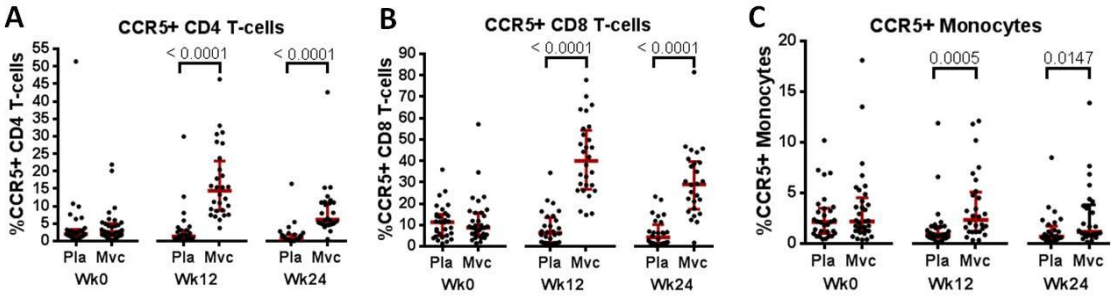

Figure 3.4: Maraviroc-inclusive ART results in a greater percent of CCR5-positive T-cells and monocytes in PBMC.
Shown are percent of CCR5-positive CD4 T-cells (A), CD8 T-cells (B), and total monocytes (C) during ART in placebo (Pla) versus Maraviroc (Mvc) groups. Mann Whitney comparison between groups was performed at each time point with $P < 0.05$ considered significant and displayed.

3.2.4 ART reduces cell-associated and soluble markers of monocyte/macrophage activation

The reversal of cell-associated and soluble markers of monocyte/macrophage activation is not well-described during ART in advanced infection, and their potential reversal may inform prognosis of such cohorts, as markers of monocyte/macrophage activation are associated with pathogenesis/predict outcome (78, 80, 91, 92, 176, 180). Based on previous ART studies (Reviewed in **Section 1.5**, Table 3.1), we predicted ART and viral suppression will reduce the percent of the $CD14^{++}CD16^{+}$ intermediate monocytes, the percent of $CD163^{+}$ monocytes, and the level of plasma sCD163, while plasma sCD14 will not change. Within total monocytes, the percent of $CD14^{++}CD16^{+}$ intermediate monocytes (Figure 3.5) and $CD163^{+}$ monocytes were

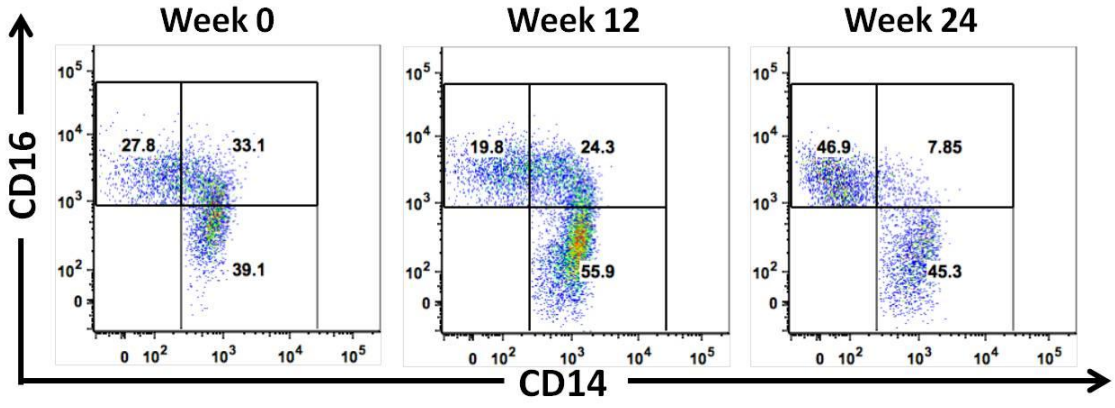

Figure 3.5: Representative change in monocyte subsets during ART. Representative donor monocyte subsets during ART determined by CD14 (x-axis) and CD16 (y-axis). Subsets are defined as classical ($CD14^{++}CD16^{-}$), intermediate ($CD14^{++}CD16^{+}$), and non-classical ($CD14^{+}CD16^{++}$) subsets.

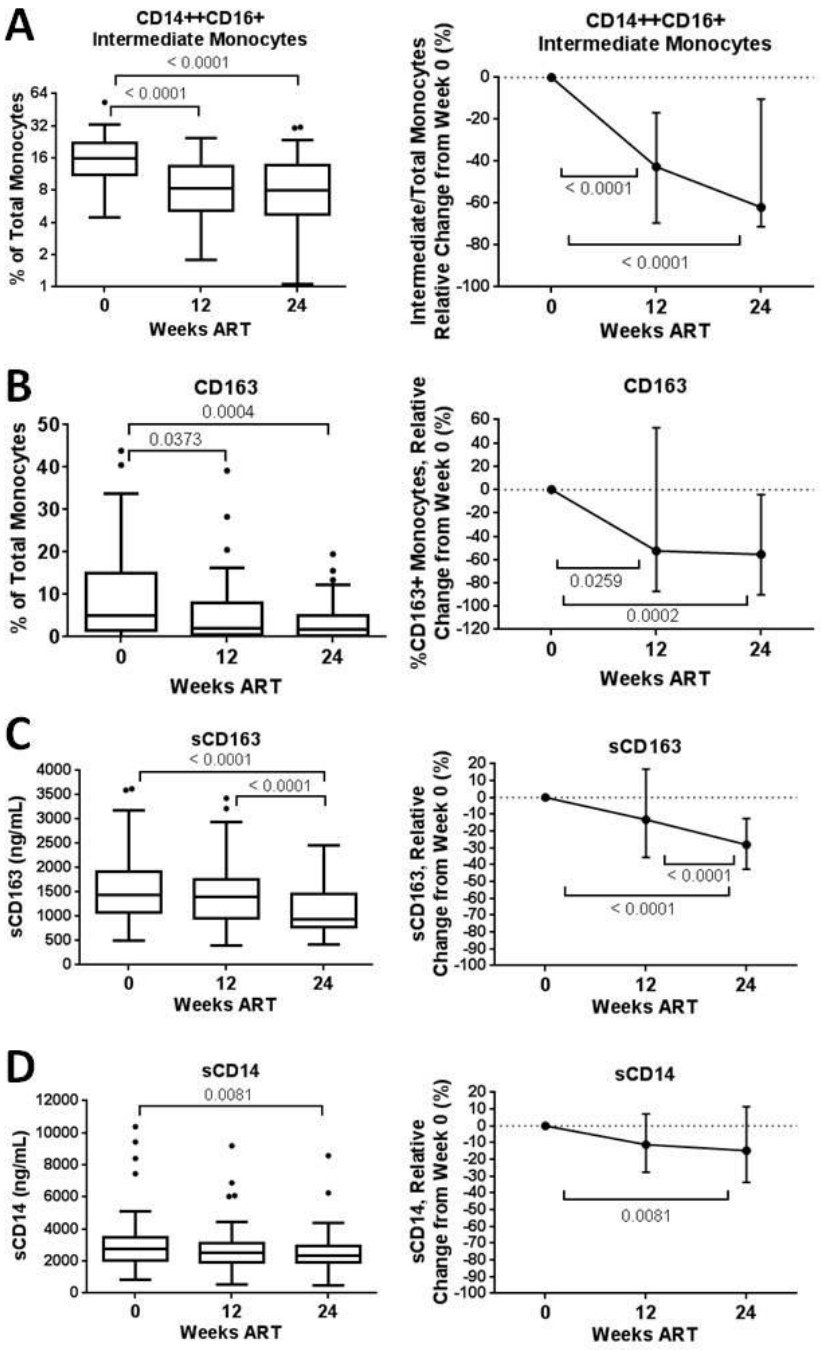

Figure 3.6: Monocyte/macrophage activation biomarkers during ART. Shown are percent of intermediate monocytes (A), CD163-positive monocytes (B), plasma sCD163 (C), and plasma sCD14 (D) absolute and relative to baseline change. Longitudinal comparisons display median and interquartile range with Tukey's method using the Friedman test and Dunn post hoc test with $P < 0.05$ considered significant and displayed.

significantly reduced by week 24 ($P < 0.0001$ and $P = 0.0004$) with a relative reduction of 61.96% and 55.54% from baseline (Figure 3.6A, B, Table 3.4). Complete subset and subset activation markers are provided in Table 3.5. In plasma, sCD163 was also significantly reduced at week 24 with a relative reduction of 28.04% from baseline ($P < 0.0001$) (Figure 3.6C). Plasma sCD14 was significantly reduced by week 24 but with only a 14.70% reduction from baseline ($P = 0.0081$) (Figure 3.6D). We show a reduction in both cell-associated and soluble markers of monocyte/macrophage activation.

Target	Week 0	Week 12	Week 24
%CD163+	4.950 (1.478-15.08)	2.050 (0.4300-8.073)	1.820 (0.3108-5.068)
%CD169+	80.15 (70.15-86.33)	1.330 (0.4003-9.893)	0.8925 (0.4905-2.250)
Tetherin (MFI)	1438 (850.3-3407)	1340 (687.5-1968)	1196 (772.3-1787)
Zinc content (Fold-control)	1.358 (1.085-1.935)	1.017 (0.8051-1.545)	1.026 (0.7379-1.567)

Table 3.4: Total monocyte activation markers.
Median and interquartile range are displayed. Values for week 12 and 24 are displayed in red if decreased ($P < 0.05$) from Week 0. Friedman test and Dunn post hoc test.

Target	Subset	Week 0	Week 12	Week 24
% of Total Monocytes	Classical	59.85 (48.03-68.05)	63.70 (53.28-73.35)	60.10 (51.05-68.43)
	Intermediate	15.80 (11.23-21.23)	8.295 (5.148-13.53)	8.330 (4.850-15.05)
	Non-classical	24.40 (14.28-34.40)	25.75 (18.33-34.20)	29.45 (21.40-36.95)
%CD163+	Classical	5.240 (1.360-16.90)	1.380 (0.2515-8.303)	1.550 (0.2805-6.178)
	Intermediate	11.05 (2.535-23.98)	5.230 (1.006-15.20)	4.590 (1.190-11.43)
	Non-classical	1.505 (0.3335-4.570)	0.7680 (0.2093-1.845)	0.3170 (0.1500-1.240)
%CD169+	Classical	98.65 (95.25-99.80)	2.035 (0.5093-11.88)	1.225 (0.6768-3.375)
	Intermediate	92.40 (84.93-97.18)	2.365 (0.4068-11.50)	1.190 (0.5428-3.253)
	Non-classical	19.50 (14.30-37.23)	0.0846 (0-0.5605)	0.02285 (0-0.3018)
Tetherin (MFI)	Classical	2852 (1268-4251)	2040 (952.0-3120)	1875 (1127-2653)
	Intermediate	2138 (1277-4042)	1753 (940.5-2405)	1473 (941.8-2397)
	Non-classical	552.0 (362.0-883.8)	404.0 (304.8-648.8)	390.5 (275.8-594.3)
Zinc content (Fold-control)	Classical	1.123 (0.8660-1.633)	0.8596 (0.6631-1.249)	0.8997 (0.6567-1.250)
	Intermediate	2.288 (1.725-2.812)	1.942 (1.403-2.744)	2.079 (1.438-3.0139)
	Non-classical	1.480 (1.281-2.196)	1.104 (0.9253-1.838)	1.352 (0.8605-1.914)

Table 3.5: Monocyte subsets and subset activation markers.
Median and interquartile range are displayed. Values for week 12 and 24 are displayed in red if decreased ($P < 0.05$) from Week 0. Friedman test and Dunn post hoc test.

3.2.5 Reduction of markers of monocyte ISG expression

We also investigated the reversal of markers of ISG expression (CD169, tetherin) as ISG expression in monocytes/macrophages may contribute to HIV-1 associated immune dysfunction (Reviewed in **Section 1.4**). CD169 was highly expressed on total monocytes pre-ART and was reduced to marginal expression after 12 weeks ART ($P < 0.0001$) (Figure 3.7A, Table 3.4). Tetherin expression was also reduced by 24 weeks ($P = 0.0153$, 38.94% reduction) (Figure 3.7B, Table 3.4). Both CD169 and tetherin expression were significantly reduced in all monocyte subsets at weeks 12 and 24 (Table 3.5). The rapid and near complete reduction of monocyte CD169 expression stands out as a very early and reversible marker of HIV-1 viremia, suggesting that control of viral replication removes a major stimulus for monocyte ISG induction.

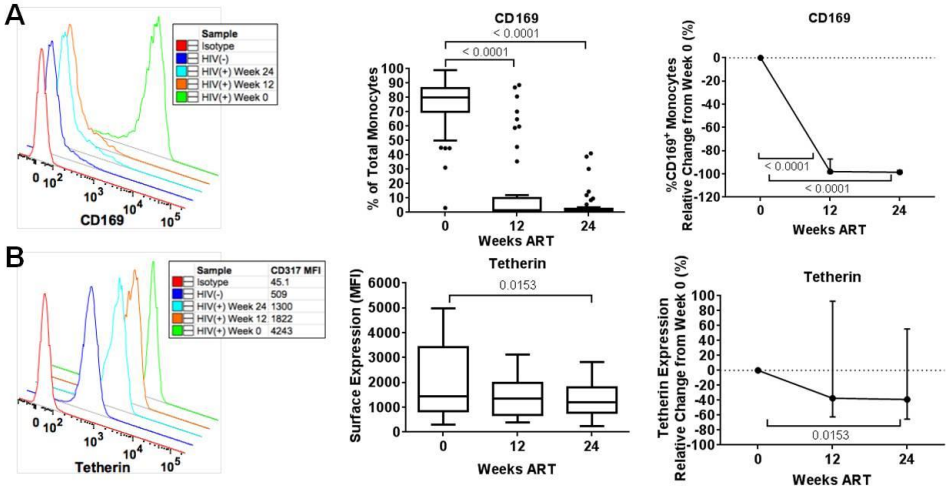

Figure 3.7: ART reduction of monocyte ISG markers.
Shown are the percent of $CD169^+$ monocytes (A) and tetherin expression (B) with representative donors (left), absolute values (middle), and change relative to baseline (right) during 24 weeks ART. Longitudinal comparisons display median and interquartile range with Tukey's method using the Friedman test and Dunn post hoc test with $P < 0.05$ considered significant and displayed.

3.2.6 Correlates of monocyte apoptosis resistance during ART

Previous findings have demonstrated that signaling through CCR5 (103, 105) and elevated intracellular monocyte zinc content (104) are mechanisms associated with apoptosis resistance in monocytes from viremic HIV-1 patients. To address the potential reversal of these mechanisms, we investigated monocyte CCR5 expression and zinc content (Figure 3.8). As noted earlier, the percent of monocytes expressing CCR5 was higher in the Maraviroc group during therapy (Figure 3.8B); however, no difference in zinc content was noted

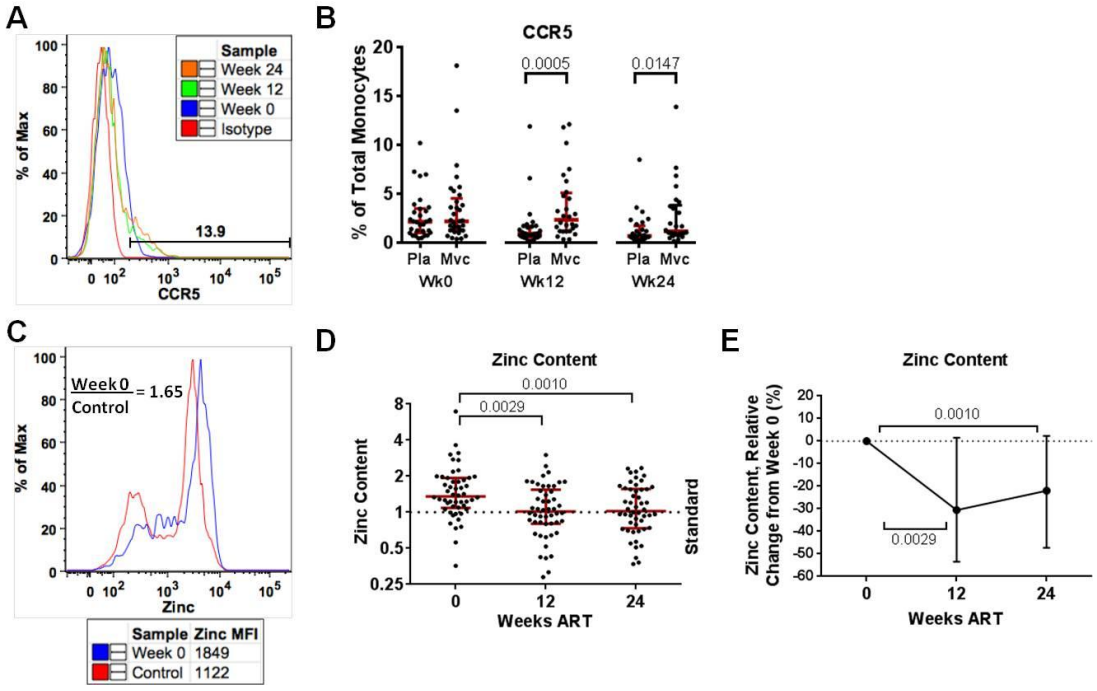

Figure 3.8: Correlates of monocyte apoptosis resistance during ART. Representative (Maraviroc patient) (A) and cohort (B) CCR5 expression during 24 weeks ART in placebo (Pla) and Maraviroc (Mvc) groups. Group comparisons display median and interquartile range using the Mann Whitney test. Monocyte zinc content (representative (C), relative value (D), relative change (E)) during 24 weeks ART. The dotted line (D, E) represents the MFI of the HIV (-) standard repeated during each experiment. Longitudinal comparisons display median and interquartile range using the Friedman test and Dunn post hoc test with $P < 0.05$ considered significant and displayed.

between therapy groups (data not shown). Zinc content was decreased by 12 weeks in total monocytes (Figure 3.8D) and the classical subset, but was unchanged in the intermediate and non-classical subset (Table 3.5). We interpret ART may reduce the anti-apoptotic impact of monocyte zinc content, by reduction within classical monocytes or reduction of the size of the intermediate subset.

3.2.7 Correlates in the change of T-cell and monocyte/macrophage activation biomarkers

We last examined the association of change within the activation markers examined and CD4 count to determine which monocyte/macrophage markers would inform the resolution of T-cell activation and CD4 reconstitution (Figure 3.9, total monocytes; Figure 3.10, monocyte subsets). Interestingly, the change

	T-Cell Activation				Monocyte and Macrophage Activation						
Cell Type	CD4		CD8		Total Monocytes				Plasma		Clinical
Marker	CD38	CD38, HLA-DR	CD38	CD38, HLA-DR	% Intermediate	CD163	CD169	Tetherin	sCD14	sCD163	CD4 Count
CD38/CD4 (-16.90%)	x	**0.7296**	**0.5721**	**0.4975**	0.0129	0.0703	0.1755	**0.4299**	0.2246	-0.0493	-0.0703
CD38, HLA-DR/CD4 (-9.66%)		x	**0.4657**	**0.5194**	-0.1036	-0.0872	0.0871	**0.3834**	0.2083	-0.0104	-0.0971
CD38/CD8 (-36.73%)			x	**0.7158**	0.1226	**0.3155**	**0.3962**	**0.5263**	**0.3443**	0.2073	**-0.4692**
CD38, HLA-DR/CD8 (-12.80%)				x	0	0.1291	**0.3815**	**0.5315**	0.2464	**0.2886**	-0.0587
Intermediate monocytes (-8.20%)					x	-0.0633	0.1400	-0.2373	-0.0020	-0.0450	0.0397
CD163 (-1.91%)						x	0.2140	0.2239	**0.3315**	0.1151	**-0.4593**
CD169 (-78.02%)							x	**0.4333**	**0.2968**	0.2191	-0.1662
Tetherin (-546.0 MFI units)								x	0.2027	0.0623	-0.1458
sCD14 (-313.3 ng/mL)									x	0.1484	**-0.2973**
sCD163 (-394.5 ng/mL)										x	-0.1095
CD4 Count (+116.0 cells/mm^3)											x

Figure 3.9: Correlation of change in T-cell and total monocyte/macrophage activation biomarkers.
Spearman rho is displayed with $P < 0.05$ considered significant and displayed in green, $P < 0.01$ in blue, and $P < 0.001$ in red. Median 24 week change is shown in column one parentheses.

in CD4 count was negatively associated with the change in CD163^{+} total monocytes, suggesting the reversal of CD163 expression may be useful as a monocyte benchmark of immune reconstitution. Data show that the change in CD8 activation (CD38^{+}, HLA-DR^{+}) was associated with change in CD169 and tetherin expression on total monocytes. Interestingly, CD4 or CD8 T-cell activation (CD38^{+}, HLA-DR^{+}) change was not associated with changes in the CD14^{++}CD16^{+} intermediate subset, CD163 expression, or plasma sCD14. These data suggest decreases in markers of T-cell activation, observed after viremic suppression, are mirrored by monocyte markers of ISG expression (CD169, tetherin) as opposed to those associated with inflammatory cascades.

	T-Cell Activation				Monocyte and Macrophage Activation																	
Marker	CD38		CD38, HLA-DR		Monocyte Subsets			CD163				CD169				Tetherin				Plasma		Clinical
Cell Type	CD4	CD8	CD4	CD8	Classical	Intermediate	Non-class	Total	Classical	Inter	Non-class	Total	Classical	Inter	Non-class	Total	Classical	Inter	Non-class	sCD14	sCD163	CD4 Count
CD38/CD4 (-16.90%)	x	0.5721	0.7296	0.4975	0.0485	0.0129	-0.1270	0.0703	0.0092	0.0782	0.0198	0.1755	0.2281	0.3324	0.1660	0.4299	0.4748	0.4872	0.5387	0.2246	-0.0493	-0.0703
CD38/CD8 (-36.73%)		x	0.4657	0.7158	0.0752	0.1226	-0.2102	0.3155	0.3608	0.2769	0.1913	0.3962	0.4849	0.4995	0.2084	0.5263	0.5425	0.5116	0.3771	0.3443	0.2073	-0.4692
CD38, HLA-DR/CD4 (-9.66%)			x	0.5194	0.0383	-0.1036	0.0136	-0.0872	-0.0412	-0.0618	-0.1127	0.0871	0.1598	0.1945	0.0638	0.3834	0.4381	0.4464	0.4791	0.2083	-0.0104	-0.0971
CD38, HLA-DR/CD8 (-12.80%)				x	0.1483	0.0000	-0.2238	0.1291	0.1621	0.0896	0.0794	0.3815	0.3079	0.4142	0.2210	0.5315	0.4878	0.4476	0.5456	0.2464	0.2886	-0.0587
Classical monocytes (+2.60%)					x	-0.6201	-0.8283	0.1010	0.0183	0.1101	0.0945	0.4114	0.0099	0.0998	0.0165	0.4311	0.2856	0.1743	0.1103	0.0982	0.0858	-0.0949
Intermediate monocytes (-8.20%)						x	0.1412	-0.0633	-0.1270	-0.0985	0.2871	0.1400	0.0609	0.1295	0.3946	-0.2373	-0.3022	-0.2267	0.0049	-0.0020	-0.0450	0.0397
Non-classical monocytes (+6.90%)							x	-0.0785	0.1012	-0.0594	-0.3802	-0.6288	-0.0163	-0.2188	-0.2517	-0.3887	-0.1591	-0.0494	-0.1566	-0.1855	-0.0779	0.0507
CD163/Total (-1.91%)								x	0.8896	0.9201	0.4492	0.2140	0.3670	0.1560	-0.1215	0.2239	0.2965	0.2063	-0.0474	0.3315	0.1151	-0.4593
CD163/Class (-1.622%)									x	0.8434	0.1650	0.0806	0.3615	0.1312	-0.2486	0.2238	0.3200	0.2216	-0.0180	0.1937	0.1372	-0.4423
CD163/Inter (-4.440%)										x	0.3757	0.1649	0.2709	0.2056	-0.1674	0.2544	0.3438	0.2820	0.0442	0.2835	0.0474	-0.3601
CD163/Non (-0.487%)											x	0.3400	0.1084	0.0716	0.2096	-0.0709	-0.1566	-0.1968	-0.1977	0.1645	0.1166	-0.2919
CD169/Total (-78.02%)												x	0.4478	0.5858	0.6311	0.4333	0.3137	0.2383	0.2446	0.2968	0.2191	-0.1662
CD169/Class (-95.94%)													x	0.5792	0.2703	0.2656	0.3671	0.3219	0.1103	0.1434	-0.0116	-0.3235
CD169/Inter (-88.41%)														x	0.3951	0.3819	0.4135	0.3484	0.2658	0.3185	0.1299	-0.2593
CD169/Non (-25.10%)															x	0.1164	0.0409	0.0969	0.1982	0.2093	0.0140	-0.1109
Tetherin/Total (-546.0 MFI units)																x	0.9123	0.8453	0.7320	0.2027	0.0623	-0.1458
Tetherin/Class (-842.0 MFI units)																	x	0.9105	0.6603	0.2590	0.0651	-0.1761
Tetherin/Inter (-616.0 MFI units)																		x	0.7257	0.1672	-0.0164	-0.1524
Tetherin/Non (-132.5 MFI units)																			x	0.1681	0.0645	0.1621
sCD14 (-313.3 ng/mL)																				x	0.1484	-0.2973
sCD163 (-394.5 ng/mL)																					x	-0.1095
CD4 Count (+116.0 cells/mm^3)																						x

Figure 3.10: Correlation of change in T-cell and monocyte subset/macrophage activation biomarkers.
Spearman rho is displayed with $P < 0.05$ considered significant and displayed in green, $P < 0.01$ in blue, and $P < 0.001$ in red. Median 24 week change is shown in column one parentheses.

3.3 Discussion, limitations, and future directions

Our data indicate that ART-mediated viral suppression in advanced HIV-1 infection results in differential reduction of monocyte/macrophage activation markers relative to T-cell activation markers. Additionally, CCR5 antagonism (Maraviroc) did not impact markers of monocyte and macrophage activation beyond use of ART alone. The latter indicates suppression of viral replication is dominant over CCR5 antagonism in determining change in innate immune activation. However, as we did not examine activation in tissue, as done by other studies (217), we cannot exclude a long-term impact of CCR5 antagonism on tissue damage, repair, and reconstitution, as should be a focus of future studies. Although other studies have addressed retention of activation in monocyte subsets after viral suppression, our study reports for the first time the differential changes observed when ART is initiated in advanced infection.

While we generally observed decreases across biomarkers of monocyte and macrophage activation with viral suppression, different degrees of change were observed between markers. At one end, monocyte CD169 expression was greatly reduced by 12 weeks (median 97.94% relative reduction), representing the marker with the closest alignment to control of viral replication. Others have described a correlation of CD169 expression and viral load (156); however, we did not detect this association, possibly due to the narrow viral load distribution of our cohort (Log viral load (copies/mL): 4.378–6.383). CD169 expression is reversed with ART in the SIV macaque model (160). Our data support this finding

in HIV-1 patients initiating ART during advanced infection. The level of $CD14^{++}CD16^{+}$ (intermediate) monocytes was significantly reduced by greater than 50% by week 24 (Figure 3.6), aligning with similar ART-mediated decreases (34, 35).

Unexpectedly, CD163 monocyte expression was not correlated with sCD163. As follows, monocyte CD163 expression may represent independent immunological pressures from those driving receptor shedding. Interestingly, our measurement of CD163 expression may under-represent *in vivo* expression levels as others have described lower values on PBMC as compared to whole blood staining (CD163 antibody clone GHI/61 used both here and referenced studies) (31, 224). Our prior work has described the impact of viremia on monocyte ISG expression and apoptotic regulation (103-105, 225). Our data support the relationship between viral suppression and an immediate reduction in ISG expression in contrast to the change in markers of TLR-mediated activation. Plasma sCD14 was the least plastic biomarker over 24 weeks ART, supporting previous studies (86, 174, 175, 177, 179). Our data suggest sCD14 is stable in the majority of patients during ART treatment in advanced HIV-1 infection.

The absence of age, gender, and geographically-matched HIV-seronegative donors limits our ability to interpret resolution to normal levels. However, this does not affect our ability to interpret what variables best reflect changes in T-cell activation, viral suppression, and immune reconstitution.

Second, the absence of functional responses limits assessment regarding retention of plasma sCD14 and altered TLR responses. Third, data analysis on patients with viral suppression by week 24 and complete datasets (week 0, 12, 24) may introduce selection bias limiting our interpretation to patients with favorable clinical outcomes. Finally, due to the use of cryopreserved PBMC and the absence of gene expression data, we are unable to directly measure monocyte apoptosis and are therefore limited to describing changes in variables that are expect to reflect apoptosis resistance mechanisms (Figure 3.8) (103-105).

In summary, we describe a spectrum of reduction of indicators of monocyte/macrophage activation in advanced HIV-1 infection during 24 weeks ART. We also differentiate activation variables closely associated with control of viral replication (CD169), CD4 reconstitution (CD163), and those showing a strong relationship with decreased CD8 T-cell activation (CD169 and tetherin). The lack of greater change in both sCD14 and sCD163 after ART suggests that microbial translocation and associated activation may be of greater concern in advanced infection despite viral suppression.

3.4 Materials

3.4.1 Donor population

HIV-1 seropositive patients (n = 65; 56.9% female; median age = 38 years) were recruited as part of sub-study B (South Africa study site) within the CADIRIS parent study (221). Inclusion criteria targeted ART-naïve individuals with a CD4 count less than 100 cells/mm^3 (Table 3.3). Patient data with failure to suppress viral load below 400 RNA copies/mL by week 24 were excluded from analysis. Patients received placebo or Maraviroc (600 mg) in addition to a background of Efavirenz (EFV, 600 mg), Tenofovir, (TDF, 300 mg), and Emtricitabine, (FTC, 200 mg), and plasma and PBMC were isolated from whole blood at 0 (pre-ART), 12, and 24 weeks. Data showing less than the total cohort reflect unavailable patient material or limited assay capacity. Figures expressing paired, longitudinal data (Figure 3.1, 3.3, 3.6, 3.7, 3.8) include patients with only complete data (0, 12, and 24 weeks). All participants produced informed consent in accordance with clinical trial NCT 00988780.

3.4.2 T-cell and monocyte flow cytometry

T-cell activation and monocyte activation were characterized by flow cytometry analysis of PBMC samples (Table 3.6). T-cell activation markers were measured in PBMC were thawed and stained with CD3-V450, CD38-APC, HLA-DR-APCH7, CD4-PerCPCy5.5, CCR5-PE, and CD8-FITC. Monocyte activation and ISG expression markers were measured in PBMC with CD3-V450

	V450 /Pacific Blue	APC	APC-H7	PerCPCy5.5	PE	FITC	BV510
T Cell	CD3	CD38	HLA-DR	CD4	CCR5	CD8	AquaLiveDead
Mono-A	CD3	CD14	CD16		CD169	CD163	AquaLiveDead
Mono-B	CD14	CD253 TRAIL	CD16	CD3	CD317 Tetherin	CCR5	AquaLiveDead
Zinc	CD11b	CD14	CD16	CD3		Zinc 5uM, 10 uL In 100 uL	AquaLiveDead
Isotype	CD14	IGG_1K	CD16	IGG_1K	IGG_1K	IGG_1K	CD3

Table 3.6: PBMC Flow cytometry panel.

(exclusion), CD14-APC, CD16-APCH7, CCR5-PerCPCy5.5, CD169-PE, and CD163-FITC as well as CD14-V450, CD16-APCH7, CD3-PerCPCy5.5 (exclusion), CD317-PE (Tetherin), and CCR5-FITC. Cell type-matched gates ($CD3^+$ for T-cells, CD14, CD16 combined gate for monocytes) isotypes were used for negative/positive gating. Aqua Live/Dead (Life Technologies) was used for dead cell exclusion. All flow cytometry antibodies were purchased from BD Biosciences (with the exception of CD169-PE from eBioscience and CD317-PE from BioLegend) and used per the manufacturers' instructions. T-cells were gated on singlets using forward scatter height and area, lymphoid scatter profile, $CD3^+$ cells, followed by $CD4^+$ and $CD8^+$ T-cells (Figure 3.11A). Monocytes were gated on singlets, monocyte scatter profile, CD3 exclusion, total monocytes (CD14, CD16 combined gate), and the monocyte subsets, classical monocytes ($CD14^{++}CD16^-$), intermediate monocytes ($CD14^{++}CD16^+$), and non-classical monocytes ($CD14^+CD16^{++}$) (Figure 3.11B, C). All figures depicting monocyte activation markers represent the total monocyte population. Flow cytometry data

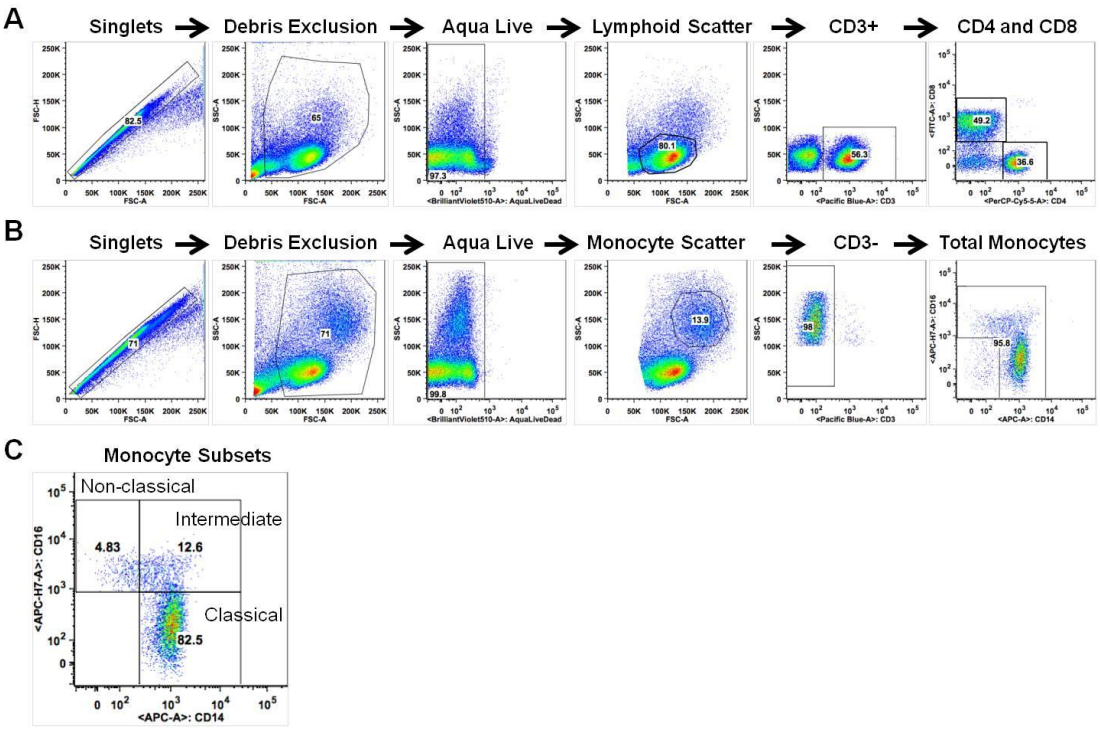

Figure 3.11: Flow cytometry gating.
Representative T-cell (A) and monocyte (B) flow cytometry gating strategy. Target molecule expression was evaluated on CD4 and CD8 subsets for T-cells (A) and total monocytes and classic, intermediate, and non-classical subsets for monocytes (B-C).

analysis and images was generated with FlowJo software (TreeStar). All flow cytometry data reported display percent of positive cells relative to the parent population with the exception of tetherin (MFI) (Figure 3.7B) and zinc content (Figure 3.8C-E).

3.4.3 Monocyte zinc content

Monocyte zinc content was determined in PBMC using CD11b-V450, CD14-APC, CD16-APCH7, CD3-PerCPCy5.5 (exclusion), and 5 μM Newport Green DCF Diacetate cell permeate zinc indicator (Life Technologies). Control

PBMC from the same HIV-seronegative donor was thawed each time the assay was performed and stained in parallel as a standard to which each sample was normalized. The MFI (mean fluorescence intensity) of each sample was divided by the MFI of the control donor in order to calculate the relative zinc content (Figure 3.8C).

3.4.4 Plasma activation markers

Plasma samples were assayed by ELISA for sCD14 (R&D Systems) and sCD163 (Trillium Diagnostics), using 1:500 dilutions, according to the manufacturers' instructions. Plates were read on a BioTek Synergy HT microplate reader at 450 nm with the appropriate wavelength corrections.

3.4.5 Statistical analysis

All dot and box-and-whisker plots were generated and statistically tested using Prism 6 (GraphPad, La Jolla, CA) and two-group longitudinal graphs (Figure 3.1, 3.3) were generated using Microsoft Excel. All graphical plots show median and interquartile range and box-and-whisker plots are displayed using Tukey's method. Relative change was calculated as percent change relative to week 0 (Pre-ART). Group comparisons at the same time point were performed using the Mann-Whitney test (two-tailed). Longitudinal comparisons were performed using the Friedman test with the Dunn post hoc test between time points. *P* values less than 0.05 were considered significant and are displayed. Correlation of T-cell and monocyte/macrophage biomarker change (Week 24-

Week 0) (Figure 3.9, 3.10) was calculated with Spearman's test (two-tailed) with rho displayed and $P < 0.05$ in green, $P < 0.01$ in blue, and $P < 0.001$ in red. Correlation matrices (Figure 3.9, 3.10) were not adjusted for multiple testing.

CHAPTER 4: Mechanistic investigation of HIV-1 induced monocyte apoptosis resistance: Impact of ISG12 family gene expression

4.1 Introduction

- 4.1.1 Background
- 4.1.2 Rationale

4.2 IFI6 and IFI27 ectopic expression system and induction *in vitro*

4.3 Impact of IFI27 over-expression on apoptosis in Monomac1 cell line

4.4 Discussion, limitations, and future directions

4.5 Materials

- 4.5.1 Generation of inducible expression Monomac1 cell lines
- 4.5.2 Apoptosis induction in transduced Monomac1 cell lines

4.1 Introduction

4.1.1 Background

Pilot RNA sequencing and RT-PCR follow-up highlighted members of the ISG12 gene family as candidate genes that may contribute to the regulation of monocyte apoptosis during HIV-1 infection (Reviewed in (189, 190)). Within this family, expression of IFI6, IFI27, and IFITM2 was elevated in HIV (+) individuals (compared to HIV (-) individuals) and associated with viral load (Table 2.4, Figure 2.13).

The ISG12/FAM14 family consists of low molecular weight hydrophobic (often membrane-associated) proteins highly induced by interferons and during viral infection (189, 190, 193, 195, 226, 227). IFI6/G1P3 is a 13 kDa protein with known anti-apoptotic properties (190). Specifically, IFI6 is upregulated in myeloma and gastric cancer cell lines and facilitates apoptosis resistance to intrinsic, mitochondrial-mediated apoptosis (191, 192). Upregulation of IFI6 during Dengue virus infection of endothelial cells is associated with protection from infection-induced apoptosis (228).

IFI27 is a 12 kDa hydrophobic protein (encoded by ISG12a/FAM14D) that localizes to the mitochondrial membrane and facilities mitochondrial-mediated pro-apoptotic impact (190, 193), similar to mouse ISG12b2 (195). IFI27 expression is upregulated during various viral infections (VSV, CMV, HCV, RSV,

HIV) (140, 193, 195, 226, 227), and may predict treatment outcome during HCV infection (229, 230). Similar to IFI27, IFITM2 has also be described as a pro-apoptotic ISG12 member (194). Also members of the ISG12/FAM14 family, the IFITM proteins (IFITM1-3) and the ubiquitin-like ISG15 protein have demonstrated anti-viral and anti-HIV properties, but are beyond the focus of these studies (170, 196, 231-233).

4.1.2 Rationale

An increase in monocyte apoptosis with increasing viral load paired was paired with elevated ISG expression (**Chapter 2**). The latter prompted an investigation of underlying mechanistic pathways that may account for this effect. This chapter will investigate the independent role of ISG12 family gene expression on monocyte apoptosis sensitivity. Based on the observation that ISG12 family expression was elevated in HIV (+) patients with elevated monocyte apoptosis *ex vivo* (**Chapter 2**), we tested the hypothesis that elevated pro-apoptotic ISG12 family gene expression would be sufficient to increase apoptosis sensitivity in a monocytic cell line. Specifically, we tested if induced expression of IFI6 or IFI27 could modulate monocyte apoptosis outcomes. Work described in this chapter includes the design and implementation of an inducible gene expression system to gauge the impact of pro- and anti-apoptotic ISG12 members on monocyte apoptosis.

4.2 IFI6 and IFI27 ectopic expression system and induction *in vitro*

We tested the hypothesis that ectopic expression of IFI6 or IFI27 would impact apoptosis outcome in a monocytic cell line. Based on the described apoptotic functions of these proteins (**Section 4.1**), our hypothesis predicts expression of IFI6 would protect cells from apoptosis and expression of IFI27 would sensitize cells to apoptosis.

To investigate our hypothesis, we generated stably transduced cell lines expressing each of the genes of interest under an inducible promoter. Three splice variants of IFI6 have been described (189): the 130 amino acid IFI6a, IFI6b with four additional amino acids at position 24, and IFI6 with 8 additional amino acids at position 24; however, to our knowledge, no functional impact of these variants has been described. IFI6a (130aa) was chosen based on template availability. IFI27/ISG12 exists in four isoforms, the full length ISG12, a splice variant lacking exon 2 designated ISG12-S, a three amino acid deleted variant designated ISG12Δ, and the combined ISG12-SΔ (189, 234). We chose the full length ISG12 based on template availability and because it retains both transmembrane domains (189).

The Monomac1 (MM1) cell line, established from an acute monocytic leukemia, was chosen for its ease of culture for flow cytometry applications, functional capacity (produces TNF-α after LPS stimulation, data not shown), and permissiveness to HIV-1 infection (235, 236). Cloning primers were engineered

with 5' BamHI and 3' Nhe1 restriction sites and IFI6 and IFI27 gene fragments were generated from commercial templates (Figure 4.1). A dual-transduction

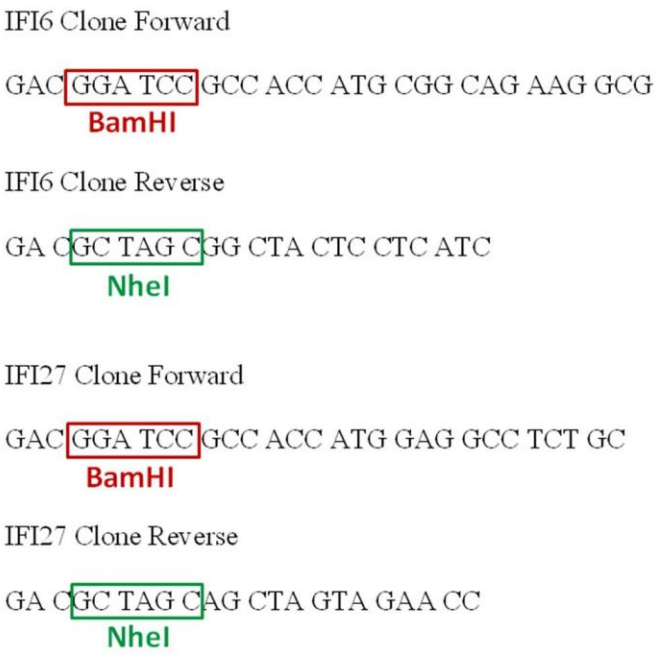

Figure 4.1: IFI6 and IFI27 cloning primers.
Shown are BamHI (red) and NheI (green) restriction site-engineered primers for the cloning of IFI6 and IFI27 gene fragments into delivery plasmid.

system was set up using the pLU-EF1aL-rtTA3-iCherry ("helper plasmid") and pLU-TREmin-MCS-pGFP ("transducing plasmid") constructs in a VSV-delivery system (Figure 4.2). The mCherry (under the IRES promoter) and eGFP (under the hPGK promoter) provide fluorescent markers to sort and purify dual-transduced cells. The gene of interest is cloned into the transducing plasmid downstream of the Tet-response element (TREmin) and requires both rtTA3, constitutively produced from the helper plasmid, and exogenous Doxycycline treatment to induce gene expression. Three transducing plasmids/viruses were generated: TREmin-MCS-pGFP (no gene of interest control), TREmin-IFI6-

pGFP, and TREmin-IFI27-pGFP, each to be co-transduced with the mCherry helper virus.

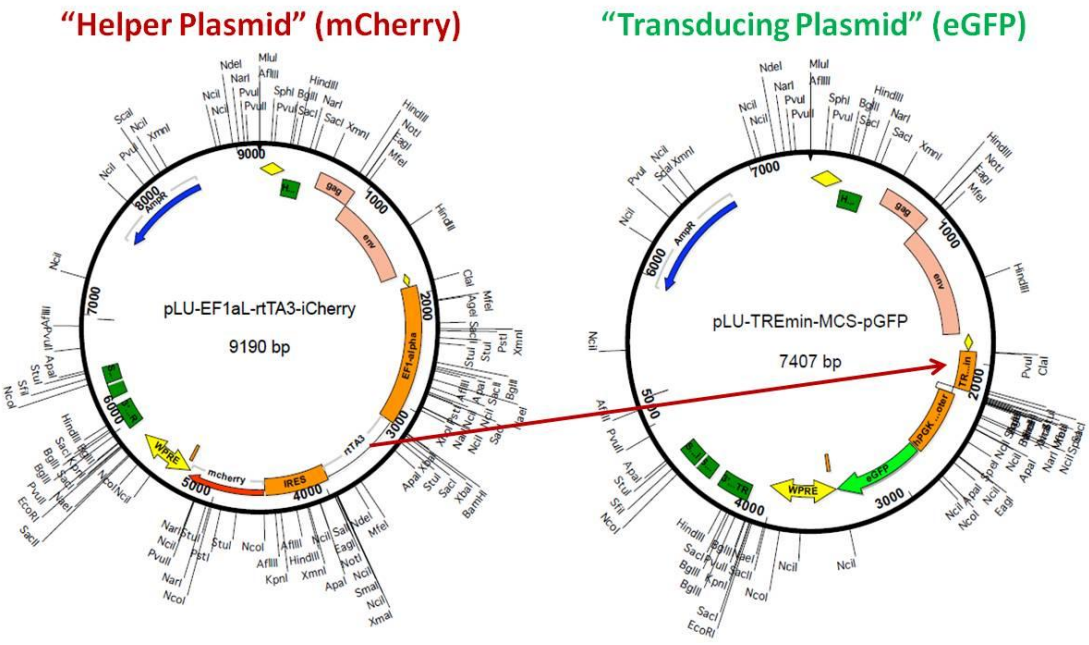

Figure 4.2: Gene delivery plasmids.
Shown are plasmid maps for "helper plasmid" (red) and "transducing plasmid" (green). rtTA3 gene product from "helper plasmid" and exogenous doxycyline treatment are both required for gene expression from inducible promoter on "transducing plasmid."

We titrated the 3-day transduction capacity of each virus and found greater than 90% transduction at 2.5 µL of each eGFP virus (MCS, IFI6, IFI27). The mCherry helper virus had less separation and up to 23.7% transduction at 5 µL of virus (Figure 4.3A-B) (Virus treatment given at µL virus stock per 2 million cells). We then examined the co-transduction efficiency of these viruses and found 38.8-44.5% co-transduction (2.5 µL each GFP virus plus 5 µL rtTA3-mCherry) (Figure 3.3C). We proceeded to sort two single transduced populations (MCS-GFP alone and rtTA3-mCherry alone) as controls (i.e. compensation) and

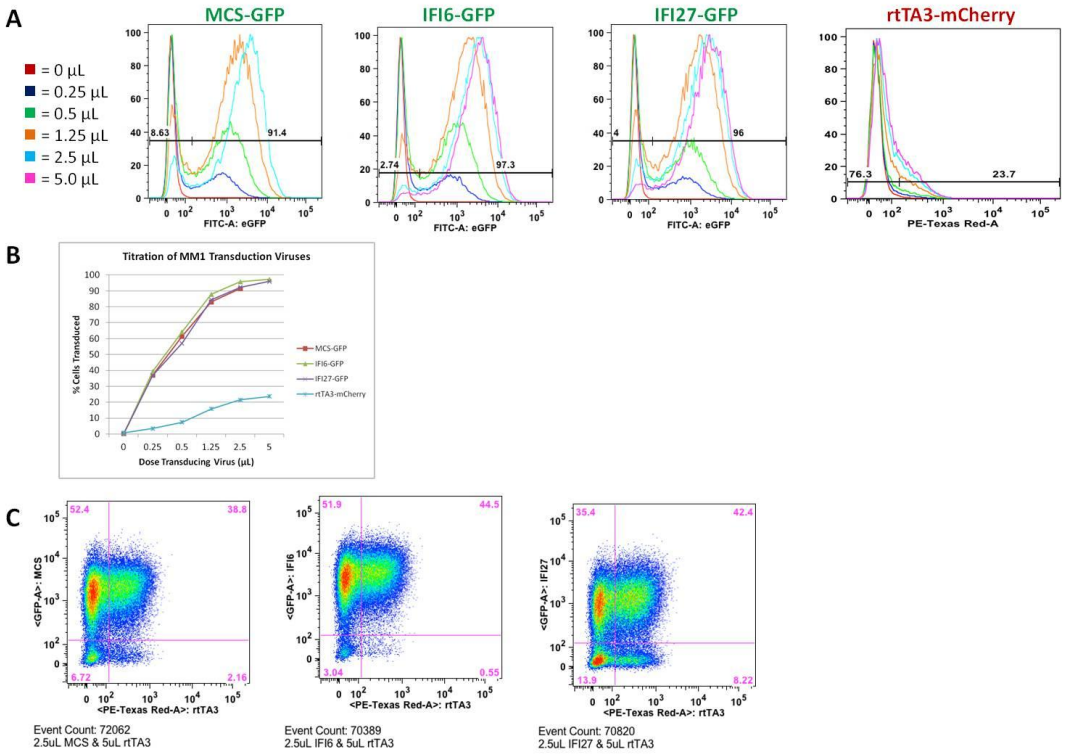

Figure 4.3: Single and co-transduction titrations.
(A-B) Single transduction titration (0-5 µL transducing virus) of control (MCS-GFP), IFI6-GFP, IFI27-GFP, and rtTA3 transducing viruses. (C) Dual-transduction of rtTA3-mCherry (2.5 µL) and MCS-GFP (left), IFI6-GFP (center), and IFI27-GFP (right). Plots show mCherry (x-axis) and GFP (y-axis) fluorescence.

the three target co-transduced lines (Figure 4.4A-B). Although the co-transduction efficiency was much lower (5-7%) compared to the previous titration (38-44%), we successfully purified all target cell lines. Sorted cells were expanded by subsequent culture and archived as stock cultures. Cultures were periodically restarted from stored stocks as we also noted that time in culture resulted in eventual dilution of the transduced population (Figure 4.4C). This may be the result of loss of reporter expression or outgrowth of a small population of un-transduced contaminants.

A

#	Name	Virus 1	Vol per 2M cells	Virus 2	Vol per 2M cells	Cells Transduced	Transduced Cells Recovered
1	Untransduced	None				4 M	
2	GFP	Empty-eGFP-MCS	2.5 uL			4 M	250,000
3	mCherry	rtTA3-mCherry	5 uL			4 M	79,000
4	MCS	Empty-eGFP-MCS	2.5 uL	rRTA3-mCherry	5 uL	20 M	140,000
5	IFI6	IFI6-eGFP	2.5 uL	rRTA3-mCherry	5 uL	20 M	177,000
6	IFI27	IFI27-eGFP	2.5 uL	rRTA3-mCherry	5 uL	20 M	102,000

B

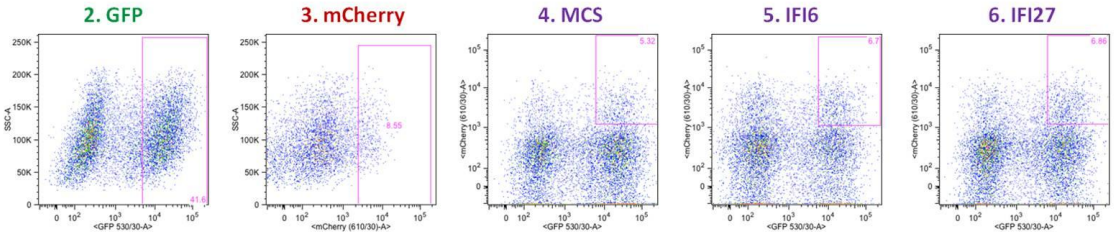

C

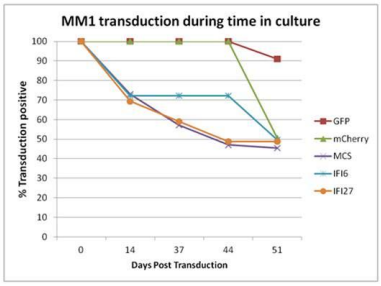

Figure 4.4: Dual-transduction and sorting.
(A) Single and dual-transduced cell line set up showing viruses used and cells transduced/sorted. (B) Transduction efficiency and populations sorted. Dual transduction (4, 5, 6) show GFP (x-axis) and mCherry (y-axis) fluorescence. (C) Transduced stocks were periodically examined for reporter expression. Graph shows the remained single or dual-transduced (by indicator) cells in active culture.

We then tested for an apoptosis response in the Monomac1 cell line by titrating apoptosis-inducing agents (independent of target gene induction). Cadmium chloride ($CdCl_2$), used as an oxidative stress inducer in primary monocytes (103-105, 225), was titrated on the cell line. A target of 15% caspase-positive cells at 35 μM $CdCl_2$ was chosen (Figure 4.5A) (n=3). The topoisomerase II inhibitor, etoposide (237), was also evaluated and induced apoptosis on this cell line (Figure 4.5B).

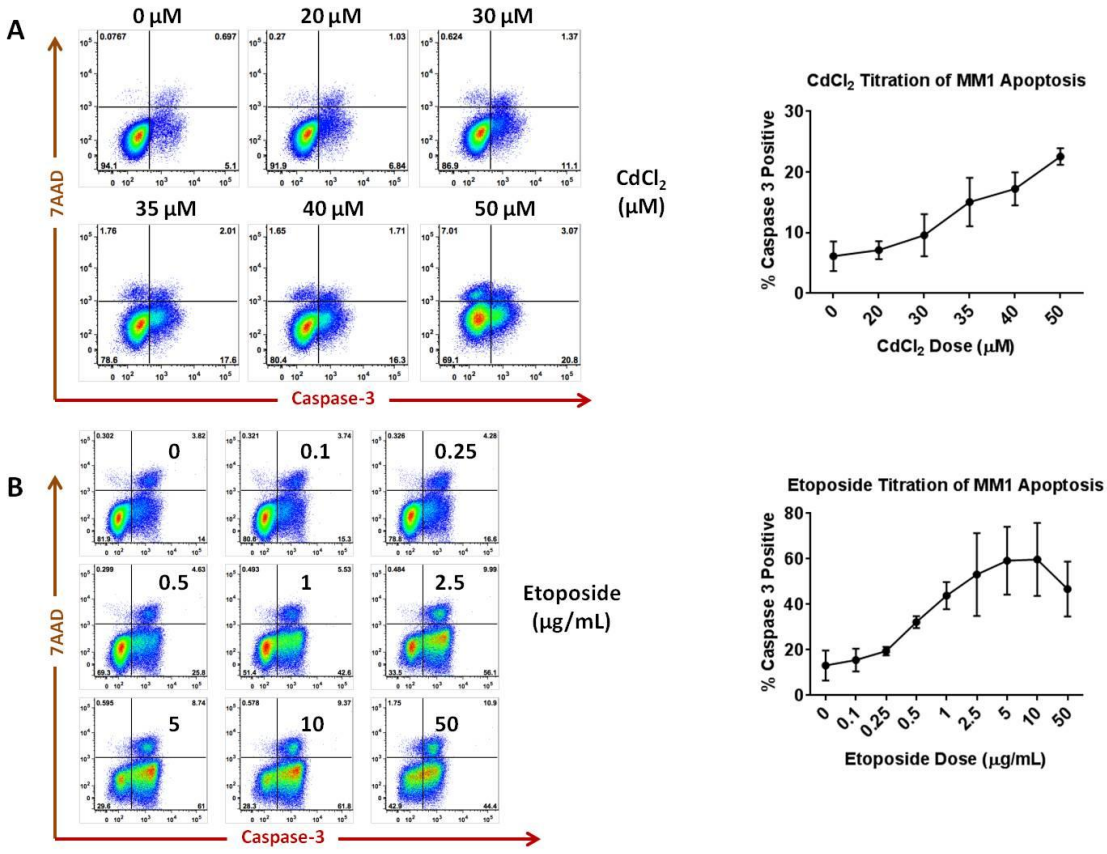

Figure 4.5: Monomac1 apoptosis induction titration.
(A) Dose-response titration of $CdCl_2$ treatment (µM) versus apoptosis induction (measured by active caspase-3) (representative of n=3 replicates). (B) Dose-response titration of etoposide treatment (µg/mL) versus apoptosis induction (measured by active caspase-3) (representative of n=2 replicates).

4.3 Impact ofIFI6 and IFI27 over-expression on apoptosis in Monomac1 cell line

We first confirmed specific gene induction by RT-PCR using a 24 hour, 0-1000 ng/mL doxycycline dose-response (Figure 4.6). Doxycycline did not induce expression of off-target genes in any cell line, such as the Rb1 or the prototypic ISG, Mx1, in any cell line (Figure 4.6A-B). IFI6 RNA expression peaked at 4.5 expression units in the IFI6 cell line (Figure 4.6C), comparable to HIV (+) RNA

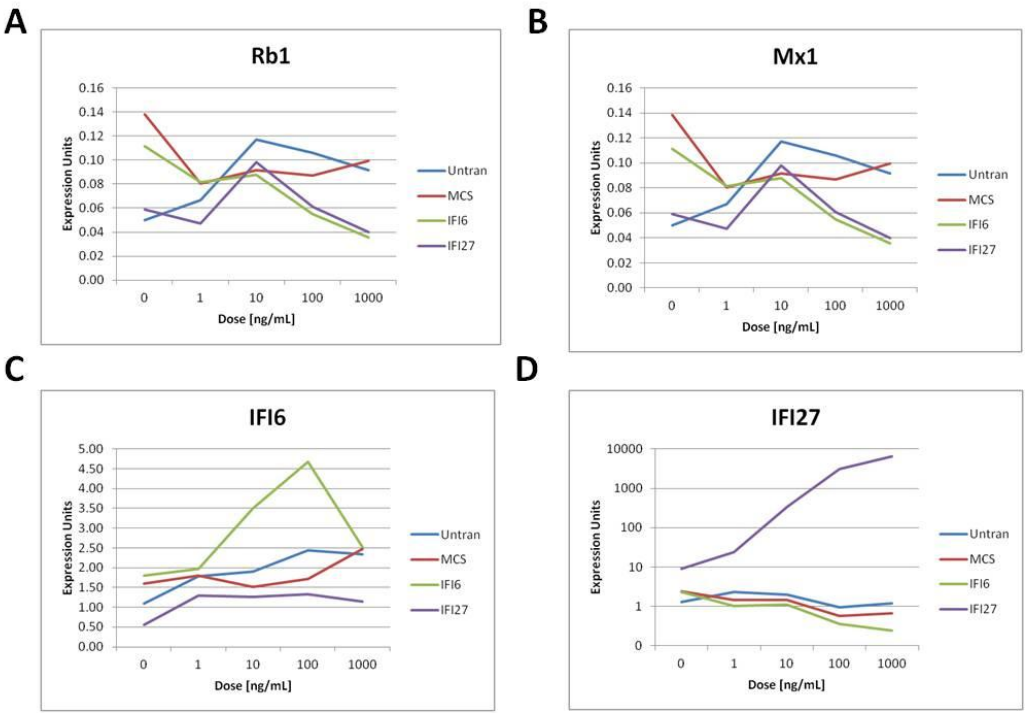

Figure 4.6: Monomac1 gene induction dose response.
Shown is Rb1 (A), Mx1 (B), IFI6 (C), and IFI27 (D) gene expression measured by RT-PCR in transduced cell-lines treated with 0-1000 ng/mL doxycycline for 24 hours. Show are untransduced MM1 (blue), MCS-no gene control (red), IFI6-transduced (green), and IFI27-transduced (purple) cell lines.

expression *ex vivo* (Table 2.4, Figure 2.13). IFI27 was robustly induced in its specific cell line (Figure 4.6D), above 6000 units at 1000 ng/mL doxycycline, again, comparable to *ex vivo* HIV (+) patient monocytes (Table 2.4, Figure 2.13) and IFN-α treated HIV (-) monocytes *in vitro* (Figure 2.5). These data demonstrate induction of specific genes of interest in the target cell lines. Based on the ISG12 induction kinetics observed with IFN-α treatment (Figure 2.6) we also conducted a time course of gene expression in our inducible cell lines (at 1000 ng/mL doxycycline) (Figure 4.7). Similar to IFN-α treatment in primary monocytes, IFI6 expression peaked at 4 hours post induction in the inducible

system and declined thereafter (Figure 4.7A). IFI27 expression exceeded 1000 expression units by 8 hours and remained elevated beyond 24 hours (Figure 4.7B). Based on induction optimization experiments, functional experiments were carried out with 1 ng/mL doxycycline and 4-8 hours of post-induction gene expression.

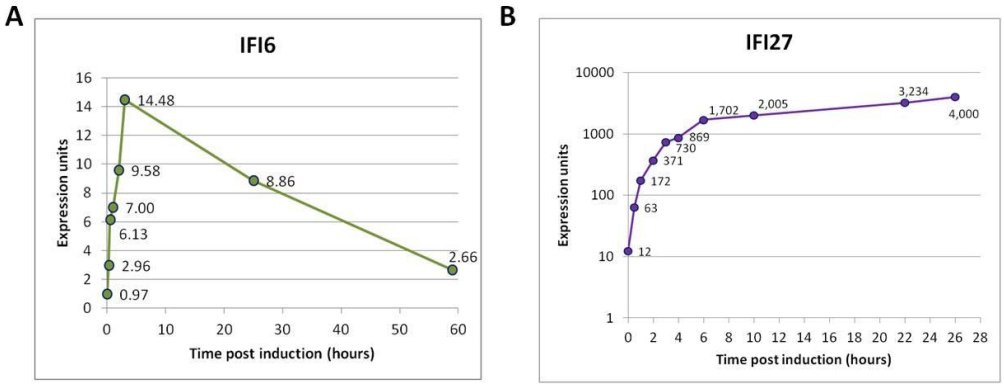

Figure 4.7: Monomac1 gene induction time course.
IFI6 (A) and IFI27 (B) cell lines were treated with 1000 ng/mL doxycycline and RNA was isolated over time. Show is gene expression of the target gene measured by RT-PCR.

We tested the impact of IFI27 expression on Monomac1 apoptosis outcome (constitutive and etoposide-induced) (Figure 4.8). IFI27 and MCS cell lines were treated with doxycycline (1000 ng/mL, 8 hours), inducing expression in the IFI27 line (data not shown), followed by etoposide apoptosis challenge (18 hour, 0, 1, and 5 µg/mL) (Figure 4.8A-B). Data show similar constitutive and etoposide-challenged apoptosis response in the presence (IFI27-Doxy) or absence (MCS-Doxy) of IFI27 expression (Figure 4.8A-B) and in un-induced conditions (IFI27-None) (Figure 4.8B). We also monitored apoptosis in the IFI27 cell line (relative to untransduced Monomac1) over a 14 hour gene induction

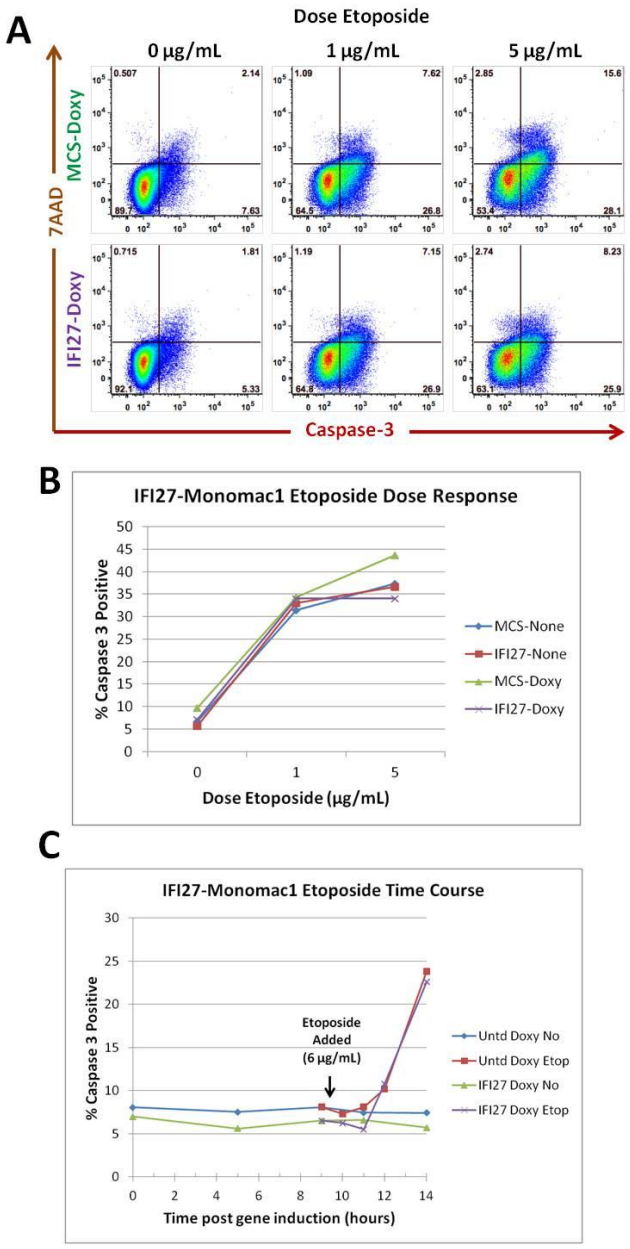

Figure 4.8: IFI27 transgene expression and apoptosis outcome in Monomac1 cells.

(A) Shown are apoptosis plots (active caspase-3 versus 7-AAD) of the MCS-control (top row) and IFI27 (bottom row) cell lines treated with 1000 ng/mL doxycycline for 8 hours, washed, and challenged overnight (18 hr) with 0, 1, or 5 µg/mL etoposide. (B) Quantification of induction-challenge experiment in (A) with doxy-induced MCS (green), doxy-induced IFI27 (purple), un-induced-MCS (blue), and un-induced IFI27 (red). (C) Time-course of untransduced and IFI27 cell line. Gene-expression was induced in all conditions (1000 ng/mL doxycycline) and cells were untreated or etoposide-challenge (6 µg/mL) at 9 hours.

(1000 ng/mL doxycycline) with etoposide apoptotic challenge (6 µg/mL) beginning at 9 hours and, again, did not detect augmentation of apoptosis in the presence of IFI27 gene expression (Figure 4.8C).

Based on the described function of IFI27, we sought to determine if IFI27 expression had any upstream effect on mitochondrial membrane potential (195). IFI27 and MCS cell lines were treated with doxycycline (250 ng/mL, 4 hours). Cells were challenged with etoposide (600 ng/mL) and mitochondrial membrane potential (MitoProbe DilC1) and apoptosis (Annexin V) were monitored for 24 hours (Figure 4.9). Disruption of membrane potential, measured as the percent of MitoTracker-negative cells of the transduced population ($mCherry^+$, GFP^+), was observed in both MCS and IFI27 cell lines at 24 hours at 41.7% and 41.1% (etoposide challenged) and 9.7%, 9.3% (no challenge), respectively. No differences were detected at any time point (n=3 internal replicates). These data show expression of the IFI27 transgene did not have a detectable impact on mitochondrial membrane potential or augment apoptosis outcome in the Monomac1 cell line.

Multiple IFI6 expression-apoptosis experiments were conducted in parallel ($CdCl_2$/etoposide induction, caspase-3/MitoProbe detection) and yielded a similar lack of relationship between gene expression and function outcome (data not shown).

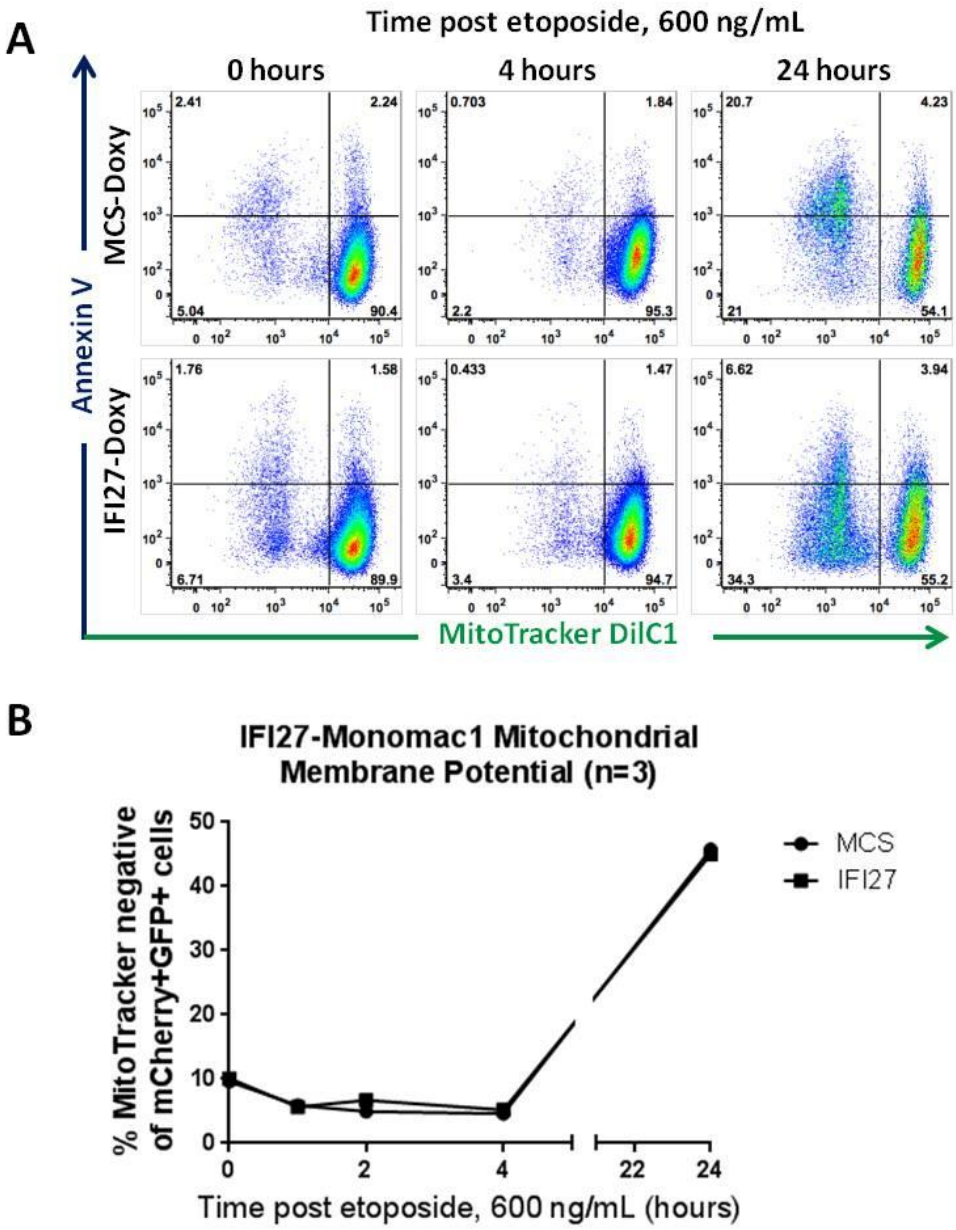

Figure 4.9: IFI27 transgene expression and mitochondrial membrane potential measurement.
(A) MCS-control (top row) and IFI27 (bottom row) cell lines treated with 250 ng/mL doxycycline for 4 hours, washed, etoposide-challenged (600 ng/mL), and assayed for apoptosis at 0, 1, 2, 4, and 24 hours post etoposide. MitoTrackerDilC1 (x-axis) shows cells with ($Mito^+$) and without ($Mito^-$) mitochondrial membrane potential. Annexin-V is shown on the y-axis. (B) The amount of $Mito^-$ cells as a percentage of the dual-fluorescent population is shown in MCS (circle) and IFI27 (square) cell lines after etoposide treatment over 24 hours (n=3 internal replicates).

4.4 Discussion, limitations, and future directions

Expression of pro-apoptotic ISG12 genes (IFI27), which was observed in viremic patients in relation to elevated apoptosis (**Chapter 2**), did directly affect apoptosis regulation in the monocyte Monomac1 cell line *in vitro*. Thus, our data do not support the hypothesis that IFI27 over-expression would augment apoptosis outcome *in vitro*. The finding that single gene over-expression was not sufficient to impact apoptosis reinforces the interpretation that multiple genes (i.e. ISG12, Bcl2) induced with immune and viral pressure may account for regulation of apoptosis outcome *in vivo* (**Chapter 2**).

While our data do not support reports of functional links between expression IFI6 and IFI27 and mitochondrial membrane potential and apoptosis outcome (191-193, 228), experimental limitations and considerations may qualify our interpretation. First, while we demonstrated the induction of IFI27 RNA expression, we did not have suitable tools to confirm IFI27 protein expression. Second, our over-expression system does not preclude that gene knockdown in primary cells would not yield an apoptosis phenotype, as was demonstrated for Rb1 in primary HIV (-) monocytes (105). Third, the Monomac1 system, while chosen for control and reproducibility, introduces its own limitations in interpretation as a cancer cell line as oncogenic and pro-survival mutations and gene expression in a cell line may maintain viability to a point that cannot be overcome by over-expression of IFI27.

This suggests follow-up work in primary monocytes and macrophages, while presenting challenges in gene delivery/expression and/or gene knockdown, may still be required to support or refute a positive impact of the genes described here. The association of monocyte ISG expression and apoptosis with HIV-1 clinical metrics (established in **chapter 2**) would allow future studies to test the impact of IFI27 gene knockdown *ex vivo*. With optimized reagents and sufficient material, the impact of multiple candidate genes, highlighted in **chapter 2**, could be tested simultaneously.

In summary, we established Monomac1 cells lines for the doxycycline-inducible expression of the apoptosis regulatory ISG12 genes, IFI6 and IFI27. Despite robust gene expression, we did not detect an impact on mitochondrial membrane potential or apoptosis outcome in this system. Our data suggest gene knockdown in primary monocytes may be a superior approach to address the mechanistic roles of IFI6 and IFI27 in the regulation of monocyte apoptosis.

4.5 Materials

4.5.1 Generation of inducible expression Monomac1 cell lines

IFI6 and IFI27 gene fragments were engineered with 5’ BamHI and 3’ Nhe1 restriction sites by PCR amplification from commercially obtained templates (Open Biosystems, clone ID 4654295 and 6495362 for IFI6 and IFI27) (Figure 4.1). The expression vectors pLU-EF1aL-rtTA3-iCherry (“helper plasmid”)

and pLU-TREmin-MCS-pGFP (“transducing plasmid”) were obtained from the Wistar Protein Expression Core. Gene fragments were ligated into the transducing plasmid and packaged in a VSV-delivery system for transduction (Wistar Protein Expression Core). We validated hPGK promoter activity (transducing plasmid) in the Monomac1 cell line (data not shown). The transduced cell lines (GFP, mCherry, MCS, IFI6, and IFI27) were sorted using the University of Pennsylvania Flow Cytometry Core (Figure 4.4A-B). Transduction for sort was scaled up to 4 million cells per single transduction and 20 million cells per co-transduction. Gene expression was quantified by RT-PCR as done in **Section 2.5.5**. The primers used to detect Rb1, Mx1, IFI6, and IFI27 (Figure 4.6) are detailed in Table 2.4.

4.5.2 Apoptosis induction in transduced Monomac1 cell lines

Gene expression induction (doxycycline) and apoptosis challenge ($CdCl_2$, etoposide) were optimized over multiple experiments. Experiments shown (Figure 4.8, 4.9) were conducted at 250-1000 ng/mL doxycycline and 0.6 to 6 ug/mL etoposide. Caspase-3 and Annexin-V apoptosis detection antibodies (BD Biosciences) and MitoProbe DilC1 (ThermoFischer) were used per the manufacturers’ instructions. Samples were prepared for flow cytometry as in **Section 2.5.6**. Up to 100,000 events were analyzed on a 14-color LSR II (BD Biosciences). Flow cytometry data analysis was performed with FlowJo software (TreeStar).

Chapter 5: Conclusions and future directions

5.1 Summary of main findings

5.2 Context

5.2.1 “High viremia” monocytes apoptosis: ISG expression and innate activation, common denominators

5.2.2 Reversal of monocyte/macrophage activation during advanced infection: Filling in the picture

5.3 Future Directions

5.3.1 Elucidating immune and viral pressures driving monocyte apoptosis

5.3.2 Macrophages: Targeting tissue activation and apoptosis

5.4 The role of HIV-1 disease state and viral/immunological pressures on monocyte apoptosis and monocyte/macrophage activation

5.1 Summary of main findings

In this dissertation, we focused on changes in apoptosis and activation in circulating monocytes during HIV-1 infection between low and high viremic patients and from pre-ART to ART suppressed conditions. The role of monocytes and macrophages in pathogenesis has been a focal point of the HIV research field for decades. However, investigations of the impact of HIV/SIV infection and virus-cell interactions on monocyte apoptotic outcome generated seemingly conflicting findings between *in vitro* studies, NHP models, and *ex vivo* patient cohort studies. Additionally, the description of HIV-1-associated microbial translocation has highlighted the presence and clinical significance of innate immune activation during HIV-1 infection. ART-mediated reversal of monocyte/macrophage activation during advanced infection has been understudied. To address the degree of monocyte apoptosis during high viremia, reversal of monocyte/macrophage activation during ART, and underlying mechanisms, we performed the following sets of experiments:

1. We investigated *ex vivo* monocyte apoptosis from low and high viral load HIV (+) patients and performed hypothesis-generating RNA sequencing.
2. We validated a shift in *ex vivo* monocyte apoptosis observed in high viral load conditions and investigated target gene expression in a broader HIV (+) cohort.

3. We examined the ART-mediated reversal of monocyte/macrophage activation during advanced HIV-1 infection in the presence and absence of CCR5 antagonism (Maraviroc).
4. We tested the impact of the ISG12 genes IFI6 and IFI27 as a possible underlying mechanism regulating monocyte apoptosis in the context of HIV-1 infection.

We show, for the first time, that monocyte apoptosis is elevated in HIV (+) patients with viral loads above 40,000 HIV-1 copies/mL. The impetus to investigate apoptosis at high HIV-1 viral loads arose from the seemingly incongruous reports of anti-apoptotic impacts of HIV-1 infection on monocytes *in vivo/ex vivo* (103-105) and increased monocyte turnover and pro-apoptotic outcomes in SIV-NHP and *in vitro* HIV-1 studies (70, 71, 96). Furthermore, decreased monocyte viability may represent a source of monocyte dysfunction during advanced infection (97). Consequently, we initiated a pilot study to investigate CD4 T-cell and monocyte apoptosis and examine gene expression by RNA sequencing in HIV (+) patients with elevated viremia, and collected preliminary data suggesting apoptosis resistance observed during low, steady-state viral load may shift to heightened apoptosis sensitivity at high viral loads. RNA sequencing analysis highlighted multiple gene families and genes, such as IFI6 and IFI27, for follow-up analysis that may regulate monocyte apoptosis during HIV-1 infection.

It remained to be determined if a shift in monocyte apoptosis could be confirmed in a HIV (+) cohort spanning a broad spectrum of viral load and CD4 count, and if detected, how a potential distribution of monocyte apoptosis sensitivity would be related to better-described monocyte/macrophage phenotypes during HIV-1 infection, including ISG expression (**Section 1.4**) and cell-associated and soluble markers of activation (**Section 1.5**). In a cross-sectional cohort of HIV (+) individuals (n=35), we confirmed elevated constitutive and induced monocyte apoptosis in patients above 40,000 HIV-1 copies/mL and modeled the distribution of apoptosis outcome using observed changes in viral load and p53, ISG, and Bcl2 family gene expression (**Chapter 2**). Future studies in acute infection, elite controllers, and longitudinal ART cohorts (**Chapter 3**) may help determine the contributions of viremia, monocyte ISG expression, and innate immune activation in driving monocyte apoptosis outcome during HIV-1 disease.

Next, we demonstrated differential reversal of cell-associated and soluble monocyte and macrophage activation biomarkers during ART in advanced HIV-1 infection (**Chapter 3**). We monitored biomarkers of T-cell activation, monocyte/macrophage activation (cell-associated and soluble), monocyte ISG expression, and correlates of monocyte apoptosis outcome in an advanced HIV-1 infection cohort (n=65) characterized by baseline CD4 count below 100 cells/mm^3 and viral suppression after 24 weeks ART. We also determined the

impact of CCR5 antagonism (ART versus ART + Maraviroc) on markers of T-cell and monocyte/macrophage activation and CCR5 expression in PBMC.

We did not detect an impact of Maraviroc on markers of T-cell activation or monocyte/macrophage activation, excluding a minor effect on CD4 T-cell activation, above ART alone. We did observe a higher percentage of CCR5 expressing CD4 T-cells, CD8 T-cells, and monocytes in PBMC of the Maraviroc group during ART. As we did not examine tissue activation, as done elsewhere (217), we do not exclude a long-term impact of CCR5 antagonism on tissue damage, repair, and reconstitution, as should be a focus of future studies.

We show decreasing monocyte ISG expression is closely associated with decreased CD8 T-cell activation and greater relative reductions in cell-associated biomarkers of monocyte activation ($CD14^{++}CD16^{+}$ monocytes, CD163) compared to plasma soluble markers of monocyte/macrophage activation (sCD14, sCD163). The lack of greater change in both sCD14 and sCD163 after ART in advanced infection supports that microbial translocation and associated activation may be of greater concern in advanced infection independent of viral suppression. Our data highlight the benefits of viral suppression in advanced infection despite sub 200-CD4 reconstitution at 24 weeks and may provide monocyte immune reconstitution benchmarks, such as monocyte CD163 expression, that can be monitored to inform CD4 recovery (**Chapter 3**).

Lastly, we show over-expression of IFI6 or IFI27, candidate ISGs regulating apoptosis outcome and expressed in monocytes of patients with viral loads above 40,000 HIV-1 copies/mL, is insufficient to augment apoptosis outcome in a monocyte cell line *in vitro* (**Chapter 4**). This suggests single-gene over-expression fails to recapitulate the multi-family gene expression changes (Bcl2, p53, ISG) that may be required to affect apoptosis deregulation *in vivo* or simply cannot overcome the intrinsic transforming/survival pressures of the Monomac1 cell line used. An alternative hypothesis is the in the *in vitro* system used does not deliver a secondary stress or inflammatory signal required to observe an effect on apoptotic outcome. This is supported by the observation that monocyte-derived macrophages matured in the presence of HIV-1, GM-CSF, and IL-6 are sensitized to LPS/IFN-γ induced apoptosis (96).

Findings presented in **chapter 2** suggest the presence of at least two distinct phases of monocyte/macrophage apoptosis and activation during untreated infection (Figure 5.1): (1) below 40,000 HIV-1 copies/mL, characterized by increases in plasma sCD163 and the $CD14^{++}16^{+}$ monocyte subset, Rb1 expression, and maintained viability (as described in (103-105)), and (2) above 40,000 HIV-1 copies/mL, described here, characterized by increasing plasma sCD14 with viral load, high ISG expression, and elevated apoptosis.

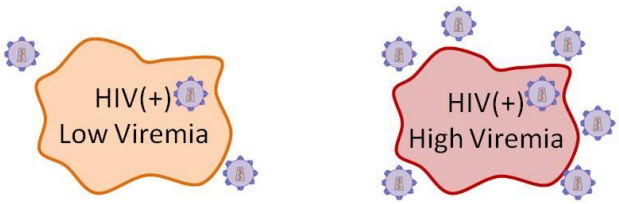

Viral Load (copies/mL)	2,000 – 40,000	> 40,000
CD4 Count (cells/mm^3)	> 200	< 200
Apoptosis	Resistant	Sensitive
ISG Expression	+	+++
CD14^{++}/16^{+} Subset	++	+++
sCD163	++	+++
sCD14	+	+++

Figure 5.1: Model of monocyte apoptosis and activation during chronic, untreated HIV-1 infection.
Shown are clinical and monocyte apoptosis, ISG, and activation profiles with low (left) and high viremia (right) during chronic, untreated HIV-1 infection.

Our ART study indicates that monocyte/macrophage biomarkers of activation, often interpreted jointly, exhibit a differential reversal and may reflect distinct mechanisms of activation. These findings support a working model with a spectrum of reversal of monocyte/macrophage activation biomarkers (Figure 5.2, **Chapter 3**). At one end, we interpret categorical resolution of monocyte CD169 expression by 12 weeks closely mirrors suppression of plasma viremia, followed by decreases in the remaining monocyte cell-associated markers and T-cell activation markers. On the other end of the spectrum, sCD14 and sCD163 may represent more clinically significant biomarkers of residual immune cross-talk and microbial translocation associated ligands (such as LPS) that may or may not be

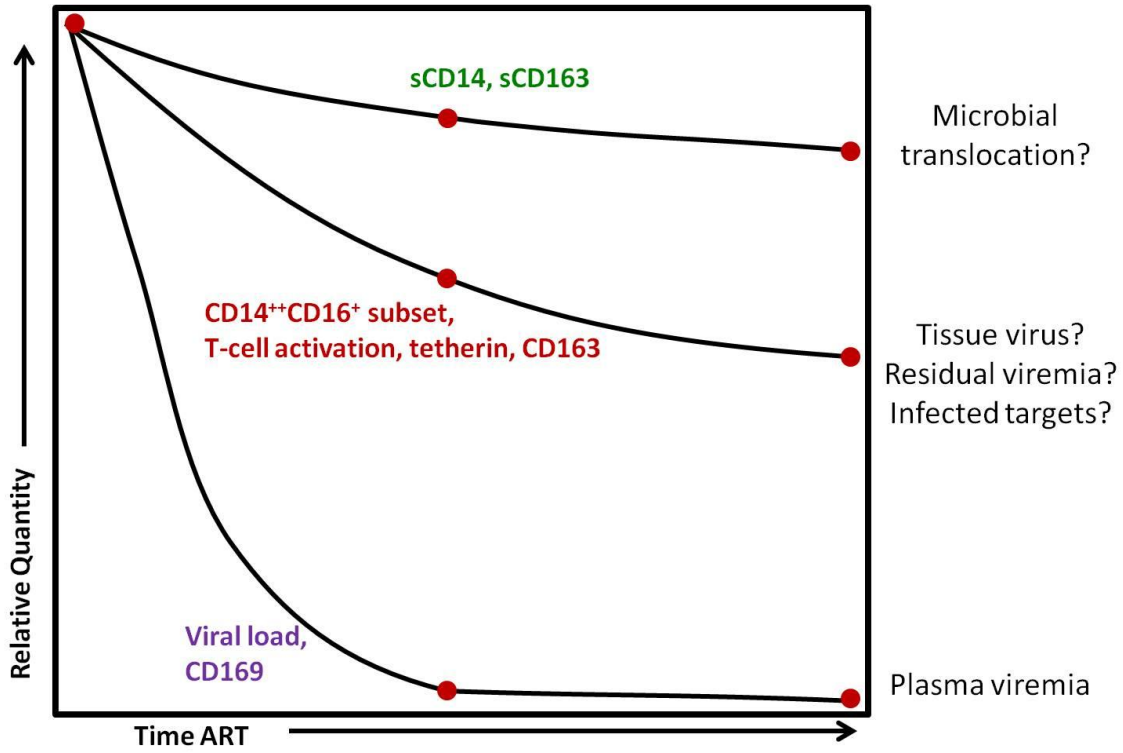

Figure 5.2: Spectrum model of monocyte/macrophage activation biomarkers during ART in advanced HIV-1 infection.
Shown is a simplified model of reversal of monocyte/macrophage activation markers during ART and potential viral and immunological drivers.

efficiently reversed with ART in advanced infection. Finally, although these findings represent independent cross-sectional and longitudinal studies, we can supplement our initial model to generate a simplified representation of the plasticity of monocyte apoptosis and activation with HIV-1 infection state (Figure 5.3).

Taken together, our work demonstrates monocyte/macrophage apoptosis outcomes and activation markers are a complex reflection of infection state and the associated collection of underlying host and pathogen pressures.

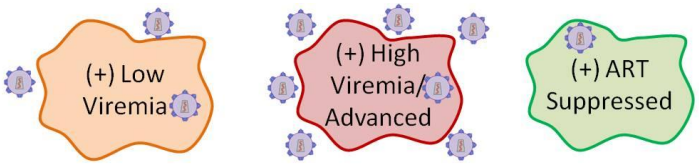

Viral Load (copies/mL)	2,000 – 40,000	> 40,000	< 50
CD4 Count (cells/mm^3)	> 200	< 200	150 – 200+
Apoptosis	Resistant	Sensitive	Sensitive? (Zinc?)
ISG Expression	+	+++	+/-
CD14^{++}/16^{+} Subset	++	+++	+
sCD163	++	+++	++
sCD14	+	+++	++
T-Cell Activation		+++	+

Figure 5.3: Model of monocyte/macrophage apoptosis and activation relative to HIV-1 infection state.
Shown is an extension of Figure 5.1 to include impact of ART-mediated viral suppression (right) in addition to low viremia (left) and high viremia (center) during untreated, chronic HIV-1 infection.

5.2 Context

5.2.1 "High viremia" monocytes apoptosis: ISG expression and innate activation, common denominators

Our description of elevated apoptosis in monocytes from HIV (+) patients with viral loads above 40,000 HIV-1 copies/mL highlights underlying themes in previous monocyte apoptosis studies in NHP-SIV, HIV, and *in vitro* systems (70, 71, 96, 99). Elevated "off-ART" constitutive apoptosis (compared to HIV (-)

individuals) was observed in a small but broad viral load cohort (n=10, mean viral load = 94,000 HIV-1 copies/mL, range = 6,000-300,000 HIV-1 copies/mL) (99). Elevated STAT1 protein expression in the “off-ART” group and the association of STAT1 expression with apoptosis outcome in this group align with our findings of elevated ISG expression and monocyte apoptosis in high viral load patients within our HIV (+) cohort.

A pro-apoptotic impact of HIV-1 *in vitro* has been demonstrated when monocytes are differentiated in the presence of HIV-1 (Bal), GM-CSF, and IL-6, sensitizing them to activation-induced (IFN-γ/LPS) apoptosis (compared to GM-CSF, IL-6 conditions alone) (96). Although we did not measure plasma IL-6 and LPS in our study, plasma sCD14 was associated with viral load (Figure 2.11C), and elevated plasma IL-6 in both viremic and ART-suppressed patients (compared to HIV (-) individuals) has been described elsewhere (35). We interpret this *in vitro* system may mimic inflammatory and activation pressures present during high HIV-1 viremia *in vivo*.

Our data join an increasing body of evidence suggesting that high HIV/SIV viral load and low CD4 count may be associated with changes in monocyte functional responses, including greater monocyte turnover (associated with plasma sCD163) (70, 71), tissue migration (70, 71, 94), and macrophage apoptosis in tissue (70). This study complements studies in SIV-infected macaques (using *in vivo* BrdU labeling) in which disease progression (i.e. high

viral load) was associated with increased monocyte turnover, associated with higher tissue apoptosis (70). Overall, our data suggest as viral load rises, added TLR-mediated activation and/or ISG induction may override existing anti-apoptotic mechanisms, resulting in higher monocyte turnover.

5.2.2 Reversal of monocyte/macrophage activation during advanced infection: Filling in the picture

First described almost a decade ago (86), microbial translocation and associated immune activation during HIV-1 infection have been established as a strong predictor of mortality (91, 92) and are associated with CNS pathogenesis (77) and immune dysfunction (211). Incomplete resolution of monocyte/macrophage activation after ART described here (advanced infection) and elsewhere (Table 3.1) supports persistence of innate activation despite viral suppression.

Here we show reversal of activated monocyte subsets and markers of ISG expression despite nadir CD4 counts below 100 cells/mm^3, highlighting early immunological benefits of ART in advanced infection. Nonetheless, the persistence of sCD14 during ART as an indicator of lasting microbial translocation supports the investigation of interventions targeting innate activation. Recently, two clinical trials targeting vascular inflammation in HIV (+) cohorts demonstrated clinical benefit regarding reversal of innate immune activation. First, the integrase inhibitor, Elvitegravir reduced sCD14 beyond

standard ART alone (238). Second, addition of Rosuvastatin to a standard ART regimen reduced sCD14, the non-classical ($CD14^{+}CD16^{++}$) monocyte subset, plasma CXCL10, and CD4 and CD8 T-cell activation over placebo (239, 240). Our data demonstrating elevated innate immune activation with increasing viral load (**Chapter 2**) and the persistence of innate activation despite suppressive ART in advanced infection (**Chapter 3**), reinforce the significance of the development of these next generation ART strategies.

5.3 Future Directions

5.3.1 Elucidating immune and viral pressures driving monocyte apoptosis

The HIV (+) cohort in this thesis with elevated monocyte apoptosis at high viral loads (**Chapter 2**) represents HIV-1 disease with high viremia, evidence of innate immune activation and microbial translocation (Figure 2.11, 2.12), and ISG expression (Table 2.4, Figure 2.13) (absent symptomatic opportunistic infection). The impact of ART initiated from high viral load on monocyte apoptosis remains to be described directly. Our data (**Chapter 3**) suggest ART-mediated viral suppression and ISG reversal proceed reversal of TLR-mediated activation, allowing one to investigate the impact of residual TLR-mediated activation on monocyte apoptosis in the absence of viremia and ISG expression. Interestingly, cross-sectional data from our lab show induced monocyte apoptosis is higher in ART-patients than a low level viremic cohort (median viral load = 13,468 HIV-1 copies/mL) (and evidence loss off anti-apoptotic Rb1 activity with ART) (105).

Conversely, characterization of monocyte apoptosis in patients during acute infection would evaluate the impact of peak viremia and ISG expression absent established microbial translocation (86).

5.3.2 Macrophages: Targeting tissue activation and apoptosis

Recently, attention has focuses on HIV-1 tissue reservoirs as a significant challenge to the cure initiative, within which macrophages play a major role (49, 241, 242). The degree to which monocyte apoptosis (**Chapter 2**) and activation phenotypes (**Chapter 2, Chapter 3**) extend to tissue macrophages have significant implications regarding pathogenesis and viral reservoirs.

While macrophage apoptosis has been described in CNS and lymph nodes during SIV NHP infection (70, 95), direct measurements during HIV-1 infection have been limited. Future studies should take advantages of lymph node and rectal biopsy techniques to determine the degree of macrophage apoptosis in tissue during viremic and ART-suppressed HIV-1 infection. Such studies would inform potential contributions of macrophage apoptosis/dysfunction to gut epithelial barrier damage (88, 93, 94) and the development of opportunistic infection.

On a related note, tissue characterization of macrophage activation may similarly inform on gut epithelial barrier damage and microbial translocation (88, 93, 94). Additionally, these studies could determine if retention of tissue

macrophage activation is associated with, and may contribute to, the size and persistence of the HIV-1 tissue reservoir in both CD4 T-cells and macrophages. This will inform the relationship between innate activation in tissue and viral persistence and may highlight mechanisms important in targeting the HIV-1 tissue reservoir.

5.4 The role of HIV-1 disease state and viral/immunological pressures on monocyte apoptosis and monocyte/macrophage activation

The work presented in this dissertation demonstrates the plasticity of monocyte/macrophage apoptosis and activation markers and their association with the stage of HIV-1 infection and infection-associated pressures (viremia, ISG expression, and microbial translocation). Previous studies and work presented here suggest the apoptotic fate of monocytes may represent a barometer of immune stress manifest during infection *in vivo*. Additionally, the spectrum of reversal of different biomarkers of monocyte/macrophage activation with ART may be useful in informing both immune reconstitution and the persistence of microbial translocation and associated activation.

Understanding the immunological and viral pressures driving functional changes in monocytes and macrophages will be vital in the targeting and reversing HIV-1 associated innate immune activation.

6. References

1. 1981. Kaposi's sarcoma and Pneumocystis pneumonia among homosexual men--New York City and California. MMWR Morb Mortal Wkly Rep **30:**305-308.
2. 1981. Pneumocystis pneumonia--Los Angeles. MMWR Morb Mortal Wkly Rep **30:**250-252.
3. **Gottlieb MS, Schroff R, Schanker HM, Weisman JD, Fan PT, Wolf RA, Saxon A.** 1981. Pneumocystis carinii pneumonia and mucosal candidiasis in previously healthy homosexual men: evidence of a new acquired cellular immunodeficiency. N Engl J Med **305:**1425-1431.
4. **Durack DT.** 1981. Opportunistic infections and Kaposi's sarcoma in homosexual men. N Engl J Med **305:**1465-1467.
5. **Masur H, Michelis MA, Greene JB, Onorato I, Stouwe RA, Holzman RS, Wormser G, Brettman L, Lange M, Murray HW, Cunningham-Rundles S.** 1981. An outbreak of community-acquired Pneumocystis carinii pneumonia: initial manifestation of cellular immune dysfunction. N Engl J Med **305:**1431-1438.
6. **Siegal FP, Lopez C, Hammer GS, Brown AE, Kornfeld SJ, Gold J, Hassett J, Hirschman SZ, Cunningham-Rundles C, Adelsberg BR, et al.** 1981. Severe acquired immunodeficiency in male homosexuals, manifested by chronic perianal ulcerative herpes simplex lesions. N Engl J Med **305:**1439-1444.
7. 1982. Update on acquired immune deficiency syndrome (AIDS)--United States. MMWR Morb Mortal Wkly Rep **31:**507-508, 513-504.
8. **Gallo RC, Sarin PS, Gelmann EP, Robert-Guroff M, Richardson E, Kalyanaraman VS, Mann D, Sidhu GD, Stahl RE, Zolla-Pazner S, Leibowitch J, Popovic M.** 1983. Isolation of human T-cell leukemia virus in acquired immune deficiency syndrome (AIDS). Science **220:**865-867.
9. **Barre-Sinoussi F, Chermann JC, Rey F, Nugeyre MT, Chamaret S, Gruest J, Dauguet C, Axler-Blin C, Vezinet-Brun F, Rouzioux C, Rozenbaum W, Montagnier L.** 1983. Isolation of a T-lymphotropic retrovirus from a patient at risk for acquired immune deficiency syndrome (AIDS). Science **220:**868-871.
10. **O'Brien SJ, Hendrickson SL.** 2013. Host genomic influences on HIV/AIDS. Genome Biol **14:**201.
11. **Fauci AS, Pantaleo G, Stanley S, Weissman D.** 1996. Immunopathogenic mechanisms of HIV infection. Ann Intern Med **124:**654-663.
12. **Guadalupe M, Reay E, Sankaran S, Prindiville T, Flamm J, McNeil A, Dandekar S.** 2003. Severe CD4+ T-Cell Depletion in Gut Lymphoid Tissue during Primary Human Immunodeficiency Virus Type 1 Infection

and Substantial Delay in Restoration following Highly Active Antiretroviral Therapy. Journal of Virology **77:**11708-11717.

13. **Koup RA, Safrit JT, Cao Y, Andrews CA, McLeod G, Borkowsky W, Farthing C, Ho DD.** 1994. Temporal association of cellular immune responses with the initial control of viremia in primary human immunodeficiency virus type 1 syndrome. J Virol **68:**4650-4655.
14. **Safrit JT, Koup RA.** 1995. The immunology of primary HIV infection: which immune responses control HIV replication? Curr Opin Immunol **7:**456-461.
15. **Mellors JW, Rinaldo CR, Jr., Gupta P, White RM, Todd JA, Kingsley LA.** 1996. Prognosis in HIV-1 infection predicted by the quantity of virus in plasma. Science **272:**1167-1170.
16. **Giorgi JV, Lyles RH, Matud JL, Yamashita TE, Mellors JW, Hultin LE, Jamieson BD, Margolick JB, Rinaldo CR, Jr., Phair JP, Detels R.** 2002. Predictive value of immunologic and virologic markers after long or short duration of HIV-1 infection. J Acquir Immune Defic Syndr **29:**346-355.
17. **Alkhatib G.** 2009. The biology of CCR5 and CXCR4. Current Opinion in HIV and AIDS **4:**96-103.
18. **Badley AD, Pilon AA, Landay A, Lynch DH.** 2000. Mechanisms of HIV-associated lymphocyte apoptosis. Blood **96:**2951-2964.
19. **Yue FY, Kovacs CM, Dimayuga RC, Gu XX, Parks P, Kaul R, Ostrowski MA.** 2005. Preferential apoptosis of HIV-1-specific CD4+ T cells. J Immunol **174:**2196-2204.
20. **Fauci AS, Mavilio D, Kottilil S.** 2005. NK cells in HIV infection: paradigm for protection or targets for ambush. Nat Rev Immunol **5:**835-843.
21. **Berger CT, Alter G.** 2011. Natural killer cells in spontaneous control of HIV infection. Curr Opin HIV AIDS **6:**208-213.
22. **Cummins NW, Badley AD.** 2010. Mechanisms of HIV-associated lymphocyte apoptosis: 2010. Cell Death Dis **1:**e99.
23. **Giorgi JV, Hultin LE, McKeating JA, Johnson TD, Owens B, Jacobson LP, Shih R, Lewis J, Wiley DJ, Phair JP, Wolinsky SM, Detels R.** 1999. Shorter survival in advanced human immunodeficiency virus type 1 infection is more closely associated with T lymphocyte activation than with plasma virus burden or virus chemokine coreceptor usage. J Infect Dis **179:**859-870.
24. **Hunt PW, Martin JN, Sinclair E, Bredt B, Hagos E, Lampiris H, Deeks SG.** 2003. T cell activation is associated with lower CD4+ T cell gains in human immunodeficiency virus-infected patients with sustained viral suppression during antiretroviral therapy. J Infect Dis **187:**1534-1543.
25. **Benito JM, Lopez M, Lozano S, Ballesteros C, Martinez P, Gonzalez-Lahoz J, Soriano V.** 2005. Differential upregulation of CD38 on different T-cell subsets may influence the ability to reconstitute CD4+ T cells under successful highly active antiretroviral therapy. J Acquir Immune Defic Syndr **38:**373-381.

26. **Day CL, Kaufmann DE, Kiepiela P, Brown JA, Moodley ES, Reddy S, Mackey EW, Miller JD, Leslie AJ, DePierres C, Mncube Z, Duraiswamy J, Zhu B, Eichbaum Q, Altfeld M, Wherry EJ, Coovadia HM, Goulder PJR, Klenerman P, Ahmed R, Freeman GJ, Walker BD.** 2006. PD-1 expression on HIV-specific T cells is associated with T-cell exhaustion and disease progression. Nature **443:**350-354.
27. **Said EA, Dupuy FP, Trautmann L, Zhang Y, Shi Y, El-Far M, Hill BJ, Noto A, Ancuta P, Peretz Y, Fonseca SG, Van Grevenynghe J, Boulassel MR, Bruneau J, Shoukry NH, Routy J-P, Douek DC, Haddad EK, Sekaly R-P.** 2010. Programmed death-1–induced interleukin-10 production by monocytes impairs CD4+ T cell activation during HIV infection. Nature Medicine **16:**452-459.
28. **Rodriguez-Garcia M, Porichis F, de Jong OG, Levi K, Diefenbach TJ, Lifson JD, Freeman GJ, Walker BD, Kaufmann DE, Kavanagh DG.** 2011. Expression of PD-L1 and PD-L2 on human macrophages is up-regulated by HIV-1 and differentially modulated by IL-10. J Leukoc Biol **89:**507-515.
29. **Sugimoto C, Hasegawa A, Saito Y, Fukuyo Y, Chiu KB, Cai Y, Breed MW, Mori K, Roy CJ, Lackner AA, Kim WK, Didier ES, Kuroda MJ.** 2015. Differentiation Kinetics of Blood Monocytes and Dendritic Cells in Macaques: Insights to Understanding Human Myeloid Cell Development. J Immunol **195:**1774-1781.
30. **Kim WK, Sun Y, Do H, Autissier P, Halpern EF, Piatak M, Jr., Lifson JD, Burdo TH, McGrath MS, Williams K.** 2010. Monocyte heterogeneity underlying phenotypic changes in monocytes according to SIV disease stage. J Leukoc Biol **87:**557-567.
31. **Tippett E, Cheng WJ, Westhorpe C, Cameron PU, Brew BJ, Lewin SR, Jaworowski A, Crowe SM.** 2011. Differential expression of CD163 on monocyte subsets in healthy and HIV-1 infected individuals. PLoS One **6:**e19968.
32. **Pulliam L, Gascon R, Stubblebine M, McGuire D, McGrath M.** 1997. Unique monocyte subset in patients with AIDS dementia. The Lancet **349:**692-695.
33. **Amirayan-Chevillard N, Tissot-Dupont H, Capo C, Brunet C, Dignat-George F, Obadia Y, Gallais H, Mege JL.** 2000. Impact of highly active anti-retroviral therapy (HAART) on cytokine production and monocyte subsets in HIV-infected patients. Clin Exp Immunol **120:**107-112.
34. **Han J, Wang B, Han N, Zhao Y, Song C, Feng X, Mao Y, Zhang F, Zhao H, Zeng H.** 2009. CD14(high)CD16(+) rather than CD14(low)CD16(+) monocytes correlate with disease progression in chronic HIV-infected patients. J Acquir Immune Defic Syndr **52:**553-559.
35. **Funderburg NT, Zidar DA, Shive C, Lioi A, Mudd J, Musselwhite LW, Simon DI, Costa MA, Rodriguez B, Sieg SF, Lederman MM.** 2012. Shared monocyte subset phenotypes in HIV-1 infection and in uninfected subjects with acute coronary syndrome. Blood **120:**4599-4608.

36. **Liang H, Duan Z, Li D, Wang Z, Ren L, Shen T, Shao Y.** 2015. Higher levels of circulating monocyte-platelet aggregates are correlated with viremia and increased sCD163 levels in HIV-1 infection. Cell Mol Immunol **12:**435-443.
37. **Ancuta P, Liu KY, Misra V, Wacleche VS, Gosselin A, Zhou X, Gabuzda D.** 2009. Transcriptional profiling reveals developmental relationship and distinct biological functions of CD16+ and CD16- monocyte subsets. BMC Genomics **10:**403.
38. **Zhu T, Muthui D, Holte S, Nickle D, Feng F, Brodie S, Hwangbo Y, Mullins JI, Corey L.** 2002. Evidence for Human Immunodeficiency Virus Type 1 Replication In Vivo in CD14+ Monocytes and Its Potential Role as a Source of Virus in Patients on Highly Active Antiretroviral Therapy. Journal of Virology **76:**707-716.
39. **Crowe S, Zhu T, Muller WA.** 2003. The contribution of monocyte infection and trafficking to viral persistence, and maintenance of the viral reservoir in HIV infection. J Leukoc Biol **74:**635-641.
40. **Ellery PJ, Tippett E, Chiu YL, Paukovics G, Cameron PU, Solomon A, Lewin SR, Gorry PR, Jaworowski A, Greene WC, Sonza S, Crowe SM.** 2007. The CD16+ monocyte subset is more permissive to infection and preferentially harbors HIV-1 in vivo. J Immunol **178:**6581-6589.
41. **Williams KC, Corey S, Westmoreland SV, Pauley D, Knight H, deBakker C, Alvarez X, Lackner AA.** 2001. Perivascular macrophages are the primary cell type productively infected by simian immunodeficiency virus in the brains of macaques: implications for the neuropathogenesis of AIDS. J Exp Med **193:**905-915.
42. **Burdo TH, Lackner A, Williams KC.** 2013. Monocyte/macrophages and their role in HIV neuropathogenesis. Immunol Rev **254:**102-113.
43. **Lewin SR, Kirihara J, Sonza S, Irving L, Mills J, Crowe SM.** 1998. HIV-1 DNA and mRNA concentrations are similar in peripheral blood monocytes and alveolar macrophages in HIV-1-infected individuals. Aids **12:**719-727.
44. **Sonza S, Mutimer HP, Oelrichs R, Jardine D, Harvey K, Dunne A, Purcell DF, Birch C, Crowe SM.** 2001. Monocytes harbour replication-competent, non-latent HIV-1 in patients on highly active antiretroviral therapy. Aids **15:**17-22.
45. **McElrath MJ, Pruett JE, Cohn ZA.** 1989. Mononuclear phagocytes of blood and bone marrow: comparative roles as viral reservoirs in human immunodeficiency virus type 1 infections. Proc Natl Acad Sci U S A **86:**675-679.
46. **Calantone N, Wu F, Klase Z, Deleage C, Perkins M, Matsuda K, Thompson EA, Ortiz AM, Vinton CL, Ourmanov I, Lore K, Douek DC, Estes JD, Hirsch VM, Brenchley JM.** 2014. Tissue myeloid cells in SIV-infected primates acquire viral DNA through phagocytosis of infected T cells. Immunity **41:**493-502.

47. **Fischer-Smith T, Croul S, Sverstiuk AE, Capini C, L'Heureux D, Regulier EG, Richardson MW, Amini S, Morgello S, Khalili K, Rappaport J.** 2001. CNS invasion by CD14+/CD16+ peripheral blood-derived monocytes in HIV dementia: perivascular accumulation and reservoir of HIV infection. J Neurovirol **7:**528-541.
48. **Bergamaschi A, Pancino G.** 2010. Host hindrance to HIV-1 replication in monocytes and macrophages. Retrovirology **7:**31.
49. **Campbell JH, Hearps AC, Martin GE, Williams KC, Crowe SM.** 2014. The importance of monocytes and macrophages in HIV pathogenesis, treatment, and cure. Aids **28:**2175-2187.
50. **Neil S, Martin F, Ikeda Y, Collins M.** 2001. Postentry restriction to human immunodeficiency virus-based vector transduction in human monocytes. J Virol **75:**5448-5456.
51. **Peng G, Greenwell-Wild T, Nares S, Jin W, Lei KJ, Rangel ZG, Munson PJ, Wahl SM.** 2007. Myeloid differentiation and susceptibility to HIV-1 are linked to APOBEC3 expression. Blood **110:**393-400.
52. **O'Brien WA, Namazi A, Kalhor H, Mao SH, Zack JA, Chen IS.** 1994. Kinetics of human immunodeficiency virus type 1 reverse transcription in blood mononuclear phagocytes are slowed by limitations of nucleotide precursors. J Virol **68:**1258-1263.
53. **Goujon C, Arfi V, Pertel T, Luban J, Lienard J, Rigal D, Darlix JL, Cimarelli A.** 2008. Characterization of simian immunodeficiency virus SIVSM/human immunodeficiency virus type 2 Vpx function in human myeloid cells. J Virol **82:**12335-12345.
54. **Laguette N, Sobhian B, Casartelli N, Ringeard M, Chable-Bessia C, Ségéral E, Yatim A, Emiliani S, Schwartz O, Benkirane M.** 2011. SAMHD1 is the dendritic- and myeloid-cell-specific HIV-1 restriction factor counteracted by Vpx. Nature.
55. **Hrecka K, Hao C, Gierszewska M, Swanson SK, Kesik-Brodacka M, Srivastava S, Florens L, Washburn MP, Skowronski J.** 2011. Vpx relieves inhibition of HIV-1 infection of macrophages mediated by the SAMHD1 protein. Nature **474:**658-661.
56. **Sung TL, Rice AP.** 2009. miR-198 inhibits HIV-1 gene expression and replication in monocytes and its mechanism of action appears to involve repression of cyclin T1. PLoS Pathog **5:**e1000263.
57. **Wang X, Ye L, Hou W, Zhou Y, Wang YJ, Metzger DS, Ho WZ.** 2009. Cellular microRNA expression correlates with susceptibility of monocytes/macrophages to HIV-1 infection. Blood **113:**671-674.
58. **Nasr N, Maddocks S, Turville SG, Harman AN, Woolger N, Helbig KJ, Wilkinson J, Bye CR, Wright TK, Rambukwelle D, Donaghy H, Beard MR, Cunningham AL.** 2012. HIV-1 infection of human macrophages directly induces viperin which inhibits viral production. Blood **120:**778-788.
59. **Orenstein JM, Fox C, Wahl SM.** 1997. Macrophages as a source of HIV during opportunistic infections. Science **276:**1857-1861.

60. **Gonzalez-Perez MP, O'Connell O, Lin R, Sullivan WM, Bell J, Simmonds P, Clapham PR.** 2012. Independent evolution of macrophage-tropism and increased charge between HIV-1 R5 envelopes present in brain and immune tissue. Retrovirology **9:**20.
61. **Hirsch VM, Zack PM, Vogel AP, Johnson PR.** 1991. Simian immunodeficiency virus infection of macaques: end-stage disease is characterized by widespread distribution of proviral DNA in tissues. J Infect Dis **163:**976-988.
62. **Igarashi T, Brown CR, Endo Y, Buckler-White A, Plishka R, Bischofberger N, Hirsch V, Martin MA.** 2001. Macrophage are the principal reservoir and sustain high virus loads in rhesus macaques after the depletion of CD4+ T cells by a highly pathogenic simian immunodeficiency virus/HIV type 1 chimera (SHIV): Implications for HIV-1 infections of humans. Proc Natl Acad Sci U S A **98:**658-663.
63. **Igarashi T, Imamichi H, Brown CR, Hirsch VM, Martin MA.** 2003. The emergence and characterization of macrophage-tropic SIV/HIV chimeric viruses (SHIVs) present in CD4+ T cell-depleted rhesus monkeys. J Leukoc Biol **74:**772-780.
64. **Ortiz AM, Klatt NR, Li B, Yi Y, Tabb B, Hao XP, Sternberg L, Lawson B, Carnathan PM, Cramer EM, Engram JC, Little DM, Ryzhova E, Gonzalez-Scarano F, Paiardini M, Ansari AA, Ratcliffe S, Else JG, Brenchley JM, Collman RG, Estes JD, Derdeyn CA, Silvestri G.** 2011. Depletion of CD4(+) T cells abrogates post-peak decline of viremia in SIV-infected rhesus macaques. J Clin Invest **121:**4433-4445.
65. **Micci L, Alvarez X, Iriele RI, Ortiz AM, Ryan ES, McGary CS, Deleage C, McAtee BB, He T, Apetrei C, Easley K, Pahwa S, Collman RG, Derdeyn CA, Davenport MP, Estes JD, Silvestri G, Lackner AA, Paiardini M.** 2014. CD4 depletion in SIV-infected macaques results in macrophage and microglia infection with rapid turnover of infected cells. PLoS Pathog **10:**e1004467.
66. **Wiley CA, Schrier RD, Nelson JA, Lampert PW, Oldstone MB.** 1986. Cellular localization of human immunodeficiency virus infection within the brains of acquired immune deficiency syndrome patients. Proc Natl Acad Sci U S A **83:**7089-7093.
67. **Cornford ME, Said JW, Vinters HV.** 1991. Immunohistochemical localization of human immunodeficiency virus (HIV) in central nervous system lymphoproliferative disorders of patients with AIDS. Mod Pathol **4:**232-238.
68. **Chakrabarti L, Hurtrel M, Maire MA, Vazeux R, Dormont D, Montagnier L, Hurtrel B.** 1991. Early viral replication in the brain of SIV-infected rhesus monkeys. Am J Pathol **139:**1273-1280.
69. **Kim WK, Alvarez X, Fisher J, Bronfin B, Westmoreland S, McLaurin J, Williams K.** 2006. CD163 identifies perivascular macrophages in normal and viral encephalitic brains and potential precursors to perivascular macrophages in blood. Am J Pathol **168:**822-834.

70. **Hasegawa A, Liu H, Ling B, Borda JT, Alvarez X, Sugimoto C, Vinet-Oliphant H, Kim WK, Williams KC, Ribeiro RM, Lackner AA, Veazey RS, Kuroda MJ.** 2009. The level of monocyte turnover predicts disease progression in the macaque model of AIDS. Blood **114:**2917-2925.
71. **Burdo TH, Soulas C, Orzechowski K, Button J, Krishnan A, Sugimoto C, Alvarez X, Kuroda MJ, Williams KC.** 2010. Increased monocyte turnover from bone marrow correlates with severity of SIV encephalitis and CD163 levels in plasma. PLoS Pathog **6:**e1000842.
72. **Soulas C, Conerly C, Kim WK, Burdo TH, Alvarez X, Lackner AA, Williams KC.** 2011. Recently infiltrating MAC387(+) monocytes/macrophages a third macrophage population involved in SIV and HIV encephalitic lesion formation. Am J Pathol **178:**2121-2135.
73. **Williams K, Burdo TH.** 2012. Monocyte mobilization, activation markers, and unique macrophage populations in the brain: observations from SIV infected monkeys are informative with regard to pathogenic mechanisms of HIV infection in humans. J Neuroimmune Pharmacol **7:**363-371.
74. **Koppensteiner H, Brack-Werner R, Schindler M.** 2012. Macrophages and their relevance in Human Immunodeficiency Virus Type I infection. Retrovirology **9:**82.
75. **Williams K, Westmoreland S, Greco J, Ratai E, Lentz M, Kim WK, Fuller RA, Kim JP, Autissier P, Sehgal PK, Schinazi RF, Bischofberger N, Piatak M, Lifson JD, Masliah E, Gonzalez RG.** 2005. Magnetic resonance spectroscopy reveals that activated monocytes contribute to neuronal injury in SIV neuroAIDS. J Clin Invest **115:**2534-2545.
76. **Nowlin BT, Burdo TH, Midkiff CC, Salemi M, Alvarez X, Williams KC.** 2015. SIV encephalitis lesions are composed of CD163(+) macrophages present in the central nervous system during early SIV infection and SIV-positive macrophages recruited terminally with AIDS. Am J Pathol **185:**1649-1665.
77. **Ancuta P, Kamat A, Kunstman KJ, Kim EY, Autissier P, Wurcel A, Zaman T, Stone D, Mefford M, Morgello S, Singer EJ, Wolinsky SM, Gabuzda D.** 2008. Microbial translocation is associated with increased monocyte activation and dementia in AIDS patients. PLoS One **3:**e2516.
78. **Lyons JL, Uno H, Ancuta P, Kamat A, Moore DJ, Singer EJ, Morgello S, Gabuzda D.** 2011. Plasma sCD14 is a biomarker associated with impaired neurocognitive test performance in attention and learning domains in HIV infection. J Acquir Immune Defic Syndr **57:**371-379.
79. **Kamat A, Lyons JL, Misra V, Uno H, Morgello S, Singer EJ, Gabuzda D.** 2012. Monocyte activation markers in cerebrospinal fluid associated with impaired neurocognitive testing in advanced HIV infection. J Acquir Immune Defic Syndr **60:**234-243.
80. **Burdo TH, Weiffenbach A, Woods SP, Letendre S, Ellis RJ, Williams KC.** 2013. Elevated sCD163 in plasma but not cerebrospinal fluid is a marker of neurocognitive impairment in HIV infection. Aids **27:**1387-1395.

81. **Kaul M, Lipton SA.** 2006. Mechanisms of neuroimmunity and neurodegeneration associated with HIV-1 infection and AIDS. J Neuroimmune Pharmacol **1:**138-151.
82. **Lindl KA, Marks DR, Kolson DL, Jordan-Sciutto KL.** 2010. HIV-Associated Neurocognitive Disorder: Pathogenesis and Therapeutic Opportunities. Journal of Neuroimmune Pharmacology **5:**294-309.
83. **Smythies LE, Sellers M, Clements RH, Mosteller-Barnum M, Meng G, Benjamin WH, Orenstein JM, Smith PD.** 2005. Human intestinal macrophages display profound inflammatory anergy despite avid phagocytic and bacteriocidal activity. J Clin Invest **115:**66-75.
84. **Shen R, Richter HE, Clements RH, Novak L, Huff K, Bimczok D, Sankaran-Walters S, Dandekar S, Clapham PR, Smythies LE, Smith PD.** 2009. Macrophages in Vaginal but Not Intestinal Mucosa Are Monocyte-Like and Permissive to Human Immunodeficiency Virus Type 1 Infection. Journal of Virology **83:**3258-3267.
85. **Shen R, Meng G, Ochsenbauer C, Clapham PR, Grams J, Novak L, Kappes JC, Smythies LE, Smith PD.** 2011. Stromal down-regulation of macrophage CD4/CCR5 expression and NF-kappaB activation mediates HIV-1 non-permissiveness in intestinal macrophages. PLoS Pathog **7:**e1002060.
86. **Brenchley JM, Price DA, Schacker TW, Asher TE, Silvestri G, Rao S, Kazzaz Z, Bornstein E, Lambotte O, Altmann D, Blazar BR, Rodriguez B, Teixeira-Johnson L, Landay A, Martin JN, Hecht FM, Picker LJ, Lederman MM, Deeks SG, Douek DC.** 2006. Microbial translocation is a cause of systemic immune activation in chronic HIV infection. Nature Medicine **12:**1365-1371.
87. **Jiang W, Lederman Michael M, Hunt P, Sieg Scott F, Haley K, Rodriguez B, Landay A, Martin J, Sinclair E, Asher Ava I, Deeks Steven G, Douek Daniel C, Brenchley Jason M.** 2009. Plasma Levels of Bacterial DNA Correlate with Immune Activation and the Magnitude of Immune Restoration in Persons with Antiretroviral-Treated HIV Infection. The Journal of Infectious Diseases **199:**1177-1185.
88. **Epple HJ, Schneider T, Troeger H, Kunkel D, Allers K, Moos V, Amasheh M, Loddenkemper C, Fromm M, Zeitz M, Schulzke JD.** 2009. Impairment of the intestinal barrier is evident in untreated but absent in suppressively treated HIV-infected patients. Gut **58:**220-227.
89. **Estes JD, Harris LD, Klatt NR, Tabb B, Pittaluga S, Paiardini M, Barclay GR, Smedley J, Pung R, Oliveira KM, Hirsch VM, Silvestri G, Douek DC, Miller CJ, Haase AT, Lifson J, Brenchley JM.** 2010. Damaged intestinal epithelial integrity linked to microbial translocation in pathogenic simian immunodeficiency virus infections. PLoS Pathog **6:**e1001052.
90. **Nazli A, Chan O, Dobson-Belaire WN, Ouellet M, Tremblay MJ, Gray-Owen SD, Arsenault AL, Kaushic C.** 2010. Exposure to HIV-1 directly

impairs mucosal epithelial barrier integrity allowing microbial translocation. PLoS Pathog **6:**e1000852.

91. **Sandler NG, Wand H, Roque A, Law M, Nason MC, Nixon DE, Pedersen C, Ruxrungtham K, Lewin SR, Emery S, Neaton JD, Brenchley JM, Deeks SG, Sereti I, Douek DC.** 2011. Plasma Levels of Soluble CD14 Independently Predict Mortality in HIV Infection. Journal of Infectious Diseases **203:**780-790.
92. **Hunt PW, Sinclair E, Rodriguez B, Shive C, Clagett B, Funderburg N, Robinson J, Huang Y, Epling L, Martin JN, Deeks SG, Meinert CL, Van Natta ML, Jabs DA, Lederman MM.** 2014. Gut epithelial barrier dysfunction and innate immune activation predict mortality in treated HIV infection. J Infect Dis **210:**1228-1238.
93. **Somsouk M, Estes JD, Deleage C, Dunham RM, Albright R, Inadomi JM, Martin JN, Deeks SG, McCune JM, Hunt PW.** 2015. Gut epithelial barrier and systemic inflammation during chronic HIV infection. Aids **29:**43-51.
94. **Allers K, Fehr M, Conrad K, Epple HJ, Schurmann D, Geelhaar-Karsch A, Schinnerling K, Moos V, Schneider T.** 2014. Macrophages Accumulate in the Gut Mucosa of Untreated HIV-infected Patients. J Infect Dis **209:**739-748.
95. **Adamson DC, Dawson TM, Zink MC, Clements JE, Dawson VL.** 1996. Neurovirulent simian immunodeficiency virus infection induces neuronal, endothelial, and glial apoptosis. Mol Med **2:**417-428.
96. **Laforge M, Campillo-Gimenez L, Monceaux V, Cumont MC, Hurtrel B, Corbeil J, Zaunders J, Elbim C, Estaquier J.** 2011. HIV/SIV infection primes monocytes and dendritic cells for apoptosis. PLoS Pathog **7:**e1002087.
97. **Kuroda MJ.** 2010. Macrophages: do they impact AIDS progression more than CD4 T cells? Journal of Leukocyte Biology **87:**569-573.
98. **Velilla PA, Hoyos A, Rojas M, Patino PJ, Velez LA, Rugeles MT.** 2005. Apoptosis as a mechanism of natural resistance to HIV-1 infection in an exposed but uninfected population. J Clin Virol **32:**329-335.
99. **Alhetheel A, Yakubtsov Y, Abdkader K, Sant N, Diaz-Mitoma F, Kumar A, Kryworuchko M.** 2008. Amplification of the signal transducer and activator of transcription I signaling pathway and its association with apoptosis in monocytes from HIV-infected patients. Aids **22:**1137-1144.
100. **Dillon SM, Friedlander LJ, Rogers LM, Meditz AL, Folkvord JM, Connick E, McCarter MD, Wilson CC.** 2011. Blood myeloid dendritic cells from HIV-1-infected individuals display a proapoptotic profile characterized by decreased Bcl-2 levels and by caspase-3+ frequencies that are associated with levels of plasma viremia and T cell activation in an exploratory study. J Virol **85:**397-409.
101. **Cosenza MA, Zhao ML, Lee SC.** 2004. HIV-1 expression protects macrophages and microglia from apoptotic death. Neuropathol Appl Neurobiol **30:**478-490.

102. **Giri MS, Nebozhyn M, Showe L, Montaner LJ.** 2006. Microarray data on gene modulation by HIV-1 in immune cells: 2000-2006. Journal of Leukocyte Biology **80:**1031-1043.
103. **Giri MS, Nebozyhn M, Raymond A, Gekonge B, Hancock A, Creer S, Nicols C, Yousef M, Foulkes AS, Mounzer K, Shull J, Silvestri G, Kostman J, Collman RG, Showe L, Montaner LJ.** 2009. Circulating Monocytes in HIV-1-Infected Viremic Subjects Exhibit an Antiapoptosis Gene Signature and Virus- and Host-Mediated Apoptosis Resistance. The Journal of Immunology **182:**4459-4470.
104. **Raymond AD, Gekonge B, Giri MS, Hancock A, Papasavvas E, Chehimi J, Kossevkov AV, Nicols C, Yousef M, Mounzer K, Shull J, Kostman J, Showe L, Montaner LJ.** 2010. Increased metallothionein gene expression, zinc, and zinc-dependent resistance to apoptosis in circulating monocytes during HIV viremia. Journal of Leukocyte Biology **88:**589-596.
105. **Gekonge B, Raymond AD, Yin X, Kostman J, Mounzer K, Collman RG, Showe L, Montaner LJ.** 2012. Retinoblastoma protein induction by HIV viremia or CCR5 in monocytes exposed to HIV-1 mediates protection from activation-induced apoptosis: ex vivo and in vitro study. Journal of Leukocyte Biology **92:**397-405.
106. **Lum JJ, Pilon AA, Sanchez-Dardon J, Phenix BN, Kim JE, Mihowich J, Jamison K, Hawley-Foss N, Lynch DH, Badley AD.** 2001. Induction of cell death in human immunodeficiency virus-infected macrophages and resting memory CD4 T cells by TRAIL/Apo2l. J Virol **75:**11128-11136.
107. **Huang Y, Erdmann N, Peng H, Herek S, Davis JS, Luo X, Ikezu T, Zheng J.** 2006. TRAIL-mediated apoptosis in HIV-1-infected macrophages is dependent on the inhibition of Akt-1 phosphorylation. J Immunol **177:**2304-2313.
108. **Cui M, Huang Y, Zhao Y, Zheng J.** 2008. Transcription factor FOXO3a mediates apoptosis in HIV-1-infected macrophages. J Immunol **180:**898-906.
109. **Zhu DM, Shi J, Liu S, Liu Y, Zheng D.** 2011. HIV infection enhances TRAIL-induced cell death in macrophage by down-regulating decoy receptor expression and generation of reactive oxygen species. PLoS One **6:**e18291.
110. **Saxena M, Busca A, Pandey S, Kryworuchko M, Kumar A.** 2011. CpG protects human monocytic cells against HIV-Vpr-induced apoptosis by cellular inhibitor of apoptosis-2 through the calcium-activated JNK pathway in a TLR9-independent manner. J Immunol **187:**5865-5878.
111. **Busca A, Saxena M, Kumar A.** 2012. Critical role for antiapoptotic Bcl-xL and Mcl-1 in human macrophage survival and cellular IAP1/2 (cIAP1/2) in resistance to HIV-Vpr-induced apoptosis. J Biol Chem **287:**15118-15133.
112. **Herbeuval JP, Boasso A, Grivel JC, Hardy AW, Anderson SA, Dolan MJ, Chougnet C, Lifson JD, Shearer GM.** 2005. TNF-related apoptosis-

inducing ligand (TRAIL) in HIV-1-infected patients and its in vitro production by antigen-presenting cells. Blood **105:**2458-2464.

113. **Huang Y, Walstrom A, Zhang L, Zhao Y, Cui M, Ye L, Zheng JC.** 2009. Type I interferons and interferon regulatory factors regulate TNF-related apoptosis-inducing ligand (TRAIL) in HIV-1-infected macrophages. PLoS One **4:**e5397.
114. **Kim N, Dabrowska A, Jenner RG, Aldovini A.** 2007. Human and simian immunodeficiency virus-mediated upregulation of the apoptotic factor TRAIL occurs in antigen-presenting cells from AIDS-susceptible but not from AIDS-resistant species. J Virol **81:**7584-7597.
115. **Choi HJ, Smithgall TE.** 2004. HIV-1 Nef promotes survival of TF-1 macrophages by inducing Bcl-XL expression in an extracellular signal-regulated kinase-dependent manner. J Biol Chem **279:**51688-51696.
116. **Chugh P, Fan S, Planelles V, Maggirwar SB, Dewhurst S, Kim B.** 2007. Infection of human immunodeficiency virus and intracellular viral Tat protein exert a pro-survival effect in a human microglial cell line. J Mol Biol **366:**67-81.
117. **Abbas W, Khan KA, Kumar A, Tripathy MK, Dichamp I, Keita M, Mahlknecht U, Rohr O, Herbein G.** 2014. Blockade of BFA-mediated apoptosis in macrophages by the HIV-1 Nef protein. Cell Death Dis **5:**e1080.
118. **Busca A, Saxena M, Kryworuchko M, Kumar A.** 2009. Anti-apoptotic genes in the survival of monocytic cells during infection. Curr Genomics **10:**306-317.
119. **Cummins NW, Badley AD.** 2013. Anti-apoptotic mechanisms of HIV: lessons and novel approaches to curing HIV. Cell Mol Life Sci **70:**3355-3363.
120. **Munn DH, Beall AC, Song D, Wrenn RW, Throckmorton DC.** 1995. Activation-induced apoptosis in human macrophages: developmental regulation of a novel cell death pathway by macrophage colony-stimulating factor and interferon gamma. J Exp Med **181:**127-136.
121. **Kiener PA, Davis PM, Starling GC, Mehlin C, Klebanoff SJ, Ledbetter JA, Liles WC.** 1997. Differential induction of apoptosis by Fas-Fas ligand interactions in human monocytes and macrophages. J Exp Med **185:**1511-1516.
122. **Perlman H, Pagliari LJ, Georganas C, Mano T, Walsh K, Pope RM.** 1999. FLICE-inhibitory protein expression during macrophage differentiation confers resistance to fas-mediated apoptosis. J Exp Med **190:**1679-1688.
123. **Lombardo E, Alvarez-Barrientos A, Maroto B, Bosca L, Knaus UG.** 2007. TLR4-mediated survival of macrophages is MyD88 dependent and requires TNF-alpha autocrine signalling. J Immunol **178:**3731-3739.
124. **Herbein G, Gras G, Khan K, Abbas W.** 2010. Macrophage signaling in HIV-1 infection. Retrovirology **7:**34.

125. **Le Douce V, Herbein G, Rohr O, Schwartz C.** 2010. Molecular mechanisms of HIV-1 persistence in the monocyte-macrophage lineage. Retrovirology **7:**32.
126. **Zhang M, Li X, Pang X, Ding L, Wood O, Clouse KA, Hewlett I, Dayton AI.** 2002. Bcl-2 upregulation by HIV-1 Tat during infection of primary human macrophages in culture. J Biomed Sci **9:**133-139.
127. **Zheng L, Yang Y, Guocai L, Pauza CD, Salvato MS.** 2007. HIV Tat Protein Increases Bcl-2 Expression in Monocytes Which Inhibits Monocyte Apoptosis Induced by Tumor Necrosis Factor-Alpha-Related Apoptosis-Induced Ligand. Intervirology **50:**224-228.
128. **Olivetta E, Federico M.** 2006. HIV-1 Nef protects human-monocyte-derived macrophages from HIV-1-induced apoptosis. Experimental Cell Research **312:**890-900.
129. **Guillemard E, Jacquemot C, Aillet F, Schmitt N, Barre-Sinoussi F, Israel N.** 2004. Human immunodeficiency virus 1 favors the persistence of infection by activating macrophages through TNF. Virology **329:**371-380.
130. **Haine V, Fischer-Smith T, Rappaport J.** 2006. Macrophage colony-stimulating factor in the pathogenesis of HIV infection: potential target for therapeutic intervention. J Neuroimmune Pharmacol **1:**32-40.
131. **Swingler S, Mann AM, Zhou J, Swingler C, Stevenson M.** 2007. Apoptotic Killing of HIV-1–Infected Macrophages Is Subverted by the Viral Envelope Glycoprotein. PLoS Pathogens **3:**e134.
132. **Burdo TH, Wood MR, Fox HS.** 2007. Osteopontin prevents monocyte recirculation and apoptosis. J Leukoc Biol **81:**1504-1511.
133. **Norris PJ, Pappalardo BL, Custer B, Spotts G, Hecht FM, Busch MP.** 2006. Elevations in IL-10, TNF-alpha, and IFN-gamma from the earliest point of HIV Type 1 infection. AIDS Res Hum Retroviruses **22:**757-762.
134. **Ambrus JL, Poiesz BJ, Lillie MA, Stadler I, Di Berardino LA, Chadha KC.** 1989. Interferon and interferon inhibitor levels in patients infected with varicella-zoster virus, acquired immunodeficiency syndrome, acquired immunodeficiency syndrome-related complex, or Kaposi's sarcoma, and in normal individuals. Am J Med **87:**405-407.
135. **Stylianou E, Aukrust P, Bendtzen K, Muller F, Froland SS.** 2000. Interferons and interferon (IFN)-inducible protein 10 during highly active anti-retroviral therapy (HAART)-possible immunosuppressive role of IFN-alpha in HIV infection. Clin Exp Immunol **119:**479-485.
136. **Francis ML, Meltzer MS.** 1993. Induction of IFN-alpha by HIV-1 in monocyte-enriched PBMC requires gp120-CD4 interaction but not virus replication. J Immunol **151:**2208-2216.
137. **Cicala C.** 2002. HIV envelope induces a cascade of cell signals in non-proliferating target cells that favor virus replication. Proceedings of the National Academy of Sciences **99:**9380-9385.
138. **Coberley CR, Kohler JJ, Brown JN, Oshier JT, Baker HV, Popp MP, Sleasman JW, Goodenow MM.** 2004. Impact on genetic networks in

human macrophages by a CCR5 strain of human immunodeficiency virus type 1. J Virol **78:**11477-11486.
139. **Woelk CH, Ottones F, Plotkin CR, Du P, Royer CD, Rought SE, Lozach J, Sasik R, Kornbluth RS, Richman DD, Corbeil J.** 2004. Interferon gene expression following HIV type 1 infection of monocyte-derived macrophages. AIDS Res Hum Retroviruses **20:**1210-1222.
140. **Rempel H, Sun B, Calosing C, Pillai SK, Pulliam L.** 2010. Interferon-α drives monocyte gene expression in chronic unsuppressed HIV-1 infection. Aids **24:**1415-1423.
141. **Kim N, Kukkonen S, Martinez-Viedma Mdel P, Gupta S, Aldovini A.** 2013. Tat engagement of p38 MAP kinase and IRF7 pathways leads to activation of interferon-stimulated genes in antigen-presenting cells. Blood **121:**4090-4100.
142. **Zahoor MA, Xue G, Sato H, Murakami T, Takeshima SN, Aida Y.** 2014. HIV-1 Vpr induces interferon-stimulated genes in human monocyte-derived macrophages. PLoS One **9:**e106418.
143. **Pulliam L, Sun B, Rempel H.** 2004. Invasive chronic inflammatory monocyte phenotype in subjects with high HIV-1 viral load. Journal of Neuroimmunology **157:**93-98.
144. **Pulliam L, Rempel H, Sun B, Abadjian L, Calosing C, Meyerhoff DJ.** 2011. A peripheral monocyte interferon phenotype in HIV infection correlates with a decrease in MRS metabolite concentrations. Aids**:**1.
145. **Rempel H, Sun B, Calosing C, Abadjian L, Monto A, Pulliam L.** 2013. Monocyte activation in HIV/HCV coinfection correlates with cognitive impairment. PLoS One **8:**e55776.
146. **Pulliam L.** 2014. Cognitive consequences of a sustained monocyte type 1 IFN response in HIV-1 infection. Curr HIV Res **12:**77-84.
147. **Tilton JC, Johnson AJ, Luskin MR, Manion MM, Yang J, Adelsberger JW, Lempicki RA, Hallahan CW, McLaughlin M, Mican JM, Metcalf JA, Iyasere C, Connors M.** 2006. Diminished Production of Monocyte Proinflammatory Cytokines during Human Immunodeficiency Virus Viremia Is Mediated by Type I Interferons. Journal of Virology **80:**11486-11497.
148. **Li Q, Smith AJ, Schacker TW, Carlis JV, Duan L, Reilly CS, Haase AT.** 2009. Microarray analysis of lymphatic tissue reveals stage-specific, gene expression signatures in HIV-1 infection. J Immunol **183:**1975-1982.
149. **Bosinger SE, Hosiawa KA, Cameron MJ, Persad D, Ran L, Xu L, Boulassel MR, Parenteau M, Fournier J, Rud EW, Kelvin DJ.** 2004. Gene expression profiling of host response in models of acute HIV infection. J Immunol **173:**6858-6863.
150. **Hearps AC, Maisa A, Cheng WJ, Angelovich TA, Lichtfuss GF, Palmer CS, Landay AL, Jaworowski A, Crowe SM.** 2012. HIV infection induces age-related changes to monocytes and innate immune activation in young men that persist despite combination antiretroviral therapy. Aids **26:**843-853.

151. **Martin GE, Gouillou M, Hearps AC, Angelovich TA, Cheng AC, Lynch F, Cheng WJ, Paukovics G, Palmer CS, Novak RM, Jaworowski A, Landay AL, Crowe SM.** 2013. Age-associated changes in monocyte and innate immune activation markers occur more rapidly in HIV infected women. PLoS One **8:**e55279.
152. **Noel N, Boufassa F, Lecuroux C, Saez-Cirion A, Bourgeois C, Dunyach-Remy C, Goujard C, Rouzioux C, Meyer L, Pancino G, Venet A, Lambotte O.** 2014. Elevated IP10 levels are associated with immune activation and low CD4(+) T-cell counts in HIV controller patients. Aids **28:**467-476.
153. **Cozzi-Lepri A, French MA, Baxter J, Okhuysen P, Plana M, Neuhaus J, Landay A.** 2011. Resumption of HIV replication is associated with monocyte/macrophage derived cytokine and chemokine changes: results from a large international clinical trial. Aids**:**1.
154. **van der Kuyl AC, van den Burg R, Zorgdrager F, Groot F, Berkhout B, Cornelissen M.** 2007. Sialoadhesin (CD169) expression in CD14+ cells is upregulated early after HIV-1 infection and increases during disease progression. PLoS One **2:**e257.
155. **Biesen R, Demir C, Barkhudarova F, Grun JR, Steinbrich-Zollner M, Backhaus M, Haupl T, Rudwaleit M, Riemekasten G, Radbruch A, Hiepe F, Burmester GR, Grutzkau A.** 2008. Sialic acid-binding Ig-like lectin 1 expression in inflammatory and resident monocytes is a potential biomarker for monitoring disease activity and success of therapy in systemic lupus erythematosus. Arthritis Rheum **58:**1136-1145.
156. **Pino M, Erkizia I, Benet S, Erikson E, Fernandez-Figueras MT, Guerrero D, Dalmau J, Ouchi D, Rausell A, Ciuffi A, Keppler OT, Telenti A, Krausslich HG, Martinez-Picado J, Izquierdo-Useros N.** 2015. HIV-1 immune activation induces Siglec-1 expression and enhances viral trans-infection in blood and tissue myeloid cells. Retrovirology **12:**37.
157. **York MR, Nagai T, Mangini AJ, Lemaire R, van Seventer JM, Lafyatis R.** 2007. A macrophage marker, Siglec-1, is increased on circulating monocytes in patients with systemic sclerosis and induced by type I interferons and toll-like receptor agonists. Arthritis Rheum **56:**1010-1020.
158. **Rempel H, Calosing C, Sun B, Pulliam L.** 2008. Sialoadhesin expressed on IFN-induced monocytes binds HIV-1 and enhances infectivity. PLoS One **3:**e1967.
159. **Puryear WB, Akiyama H, Geer SD, Ramirez NP, Yu X, Reinhard BM, Gummuluru S.** 2013. Interferon-inducible mechanism of dendritic cell-mediated HIV-1 dissemination is dependent on Siglec-1/CD169. PLoS Pathog **9:**e1003291.
160. **Kim WK, McGary CM, Holder GE, Filipowicz AR, Kim MM, Beydoun HA, Cai Y, Liu X, Sugimoto C, Kuroda MJ.** 2015. Increased Expression of CD169 on Blood Monocytes and Its Regulation by Virus and CD8 T Cells in Macaque Models of HIV Infection and AIDS. AIDS Res Hum Retroviruses **31:**696-706.

161. **Boasso A, Hardy AW, Landay AL, Martinson JL, Anderson SA, Dolan MJ, Clerici M, Shearer GM.** 2008. PDL-1 upregulation on monocytes and T cells by HIV via type I interferon: Restricted expression of type I interferon receptor by CCR5-expressing leukocytes. Clinical Immunology **129:**132-144.
162. **Patro SC, Montaner LJ.** 2011. Editorial: Is HIV-1 induction of macrophage expression of PD-L1 and PD-L2 its weakest or strongest link to disease? HIV-1 plays both sides by augmenting and limiting T cell activation to survive in vivo. J Leukoc Biol **89:**495-498.
163. **Trautmann L, Janbazian L, Chomont N, Said EA, Gimmig S, Bessette B, Boulassel M-R, Delwart E, Sepulveda H, Balderas RS, Routy J-P, Haddad EK, Sekaly R-P.** 2006. Upregulation of PD-1 expression on HIV-specific CD8+ T cells leads to reversible immune dysfunction. Nature Medicine **12:**1198-1202.
164. **Gomez AM, Ouellet M, Tremblay MJ.** 2015. HIV-1-triggered release of type I IFN by plasmacytoid dendritic cells induces BAFF production in monocytes. J Immunol **194:**2300-2308.
165. **Durudas A, Milush JM, Chen HL, Engram JC, Silvestri G, Sodora DL.** 2009. Elevated levels of innate immune modulators in lymph nodes and blood are associated with more-rapid disease progression in simian immunodeficiency virus-infected monkeys. J Virol **83:**12229-12240.
166. **Rotger M, Dalmau J, Rauch A, McLaren P, Bosinger SE, Martinez R, Sandler NG, Roque A, Liebner J, Battegay M, Bernasconi E, Descombes P, Erkizia I, Fellay J, Hirschel B, Miro JM, Palou E, Hoffmann M, Massanella M, Blanco J, Woods M, Gunthard HF, de Bakker P, Douek DC, Silvestri G, Martinez-Picado J, Telenti A.** 2011. Comparative transcriptomics of extreme phenotypes of human HIV-1 infection and SIV infection in sooty mangabey and rhesus macaque. J Clin Invest **121:**2391-2400.
167. **Malim MH, Bieniasz PD.** 2012. HIV Restriction Factors and Mechanisms of Evasion. Cold Spring Harb Perspect Med **2:**a006940.
168. **Strebel K.** 2013. HIV accessory proteins versus host restriction factors. Curr Opin Virol **3:**692-699.
169. **Harris RS, Bishop KN, Sheehy AM, Craig HM, Petersen-Mahrt SK, Watt IN, Neuberger MS, Malim MH.** 2003. DNA deamination mediates innate immunity to retroviral infection. Cell **113:**803-809.
170. **Lu J, Pan Q, Rong L, He W, Liu SL, Liang C.** 2011. The IFITM proteins inhibit HIV-1 infection. J Virol **85:**2126-2137.
171. **Jouvenet N, Neil SJ, Zhadina M, Zang T, Kratovac Z, Lee Y, McNatt M, Hatziioannou T, Bieniasz PD.** 2009. Broad-spectrum inhibition of retroviral and filoviral particle release by tetherin. J Virol **83:**1837-1844.
172. **Goujon C, Moncorge O, Bauby H, Doyle T, Ward CC, Schaller T, Hue S, Barclay WS, Schulz R, Malim MH.** 2013. Human MX2 is an interferon-induced post-entry inhibitor of HIV-1 infection. Nature **502:**559-562.

173. **Teijaro JR, Ng C, Lee AM, Sullivan BM, Sheehan KC, Welch M, Schreiber RD, de la Torre JC, Oldstone MB.** 2013. Persistent LCMV infection is controlled by blockade of type I interferon signaling. Science **340:**207-211.
174. **Wallet MA, Rodriguez CA, Yin L, Saporta S, Chinratanapisit S, Hou W, Sleasman JW, Goodenow MM.** 2010. Microbial translocation induces persistent macrophage activation unrelated to HIV-1 levels or T-cell activation following therapy. Aids **24:**1281-1290.
175. **Rajasuriar R, Booth D, Solomon A, Chua K, Spelman T, Gouillou M, Schlub TE, Davenport M, Crowe S, Elliott J, Hoy J, Fairley C, Stewart G, Cameron P, Lewin SR.** 2010. Biological determinants of immune reconstitution in HIV-infected patients receiving antiretroviral therapy: the role of interleukin 7 and interleukin 7 receptor alpha and microbial translocation. J Infect Dis **202:**1254-1264.
176. **Burdo TH, Lo J, Abbara S, Wei J, DeLelys ME, Preffer F, Rosenberg ES, Williams KC, Grinspoon S.** 2011. Soluble CD163, a novel marker of activated macrophages, is elevated and associated with noncalcified coronary plaque in HIV-infected patients. J Infect Dis **204:**1227-1236.
177. **Burdo TH, Lentz MR, Autissier P, Krishnan A, Halpern E, Letendre S, Rosenberg ES, Ellis RJ, Williams KC.** 2011. Soluble CD163 made by monocyte/macrophages is a novel marker of HIV activity in early and chronic infection prior to and after anti-retroviral therapy. J Infect Dis **204:**154-163.
178. **Lederman MM, Calabrese L, Funderburg NT, Clagett B, Medvik K, Bonilla H, Gripshover B, Salata RA, Taege A, Lisgaris M, McComsey GA, Kirchner E, Baum J, Shive C, Asaad R, Kalayjian RC, Sieg SF, Rodriguez B.** 2011. Immunologic failure despite suppressive antiretroviral therapy is related to activation and turnover of memory CD4 cells. J Infect Dis **204:**1217-1226.
179. **Lichtfuss GF, Cheng WJ, Farsakoglu Y, Paukovics G, Rajasuriar R, Velayudham P, Kramski M, Hearps AC, Cameron PU, Lewin SR, Crowe SM, Jaworowski A.** 2012. Virologically suppressed HIV patients show activation of NK cells and persistent innate immune activation. J Immunol **189:**1491-1499.
180. **Baker JV, Hullsiek KH, Singh A, Wilson E, Henry K, Lichtenstein K, Onen N, Kojic E, Patel P, Brooks JT, Hodis HN, Budoff M, Sereti I.** 2014. Immunologic predictors of coronary artery calcium progression in a contemporary HIV cohort. Aids **28:**831-840.
181. **Krishnan S, Wilson EM, Sheikh V, Rupert A, Mendoza D, Yang J, Lempicki R, Migueles SA, Sereti I.** 2014. Evidence for innate immune system activation in HIV type 1-infected elite controllers. J Infect Dis **209:**931-939.
182. **Kristiansen M, Graversen JH, Jacobsen C, Sonne O, Hoffman HJ, Law SK, Moestrup SK.** 2001. Identification of the haemoglobin scavenger receptor. Nature **409:**198-201.

183. **Hintz KA, Rassias AJ, Wardwell K, Moss ML, Morganelli PM, Pioli PA, Givan AL, Wallace PK, Yeager MP, Guyre PM.** 2002. Endotoxin induces rapid metalloproteinase-mediated shedding followed by up-regulation of the monocyte hemoglobin scavenger receptor CD163. J Leukoc Biol **72:**711-717.
184. **Walker JA, Sulciner ML, Nowicki KD, Miller AD, Burdo TH, Williams KC.** 2014. Elevated numbers of CD163+ macrophages in hearts of simian immunodeficiency virus-infected monkeys correlate with cardiac pathology and fibrosis. AIDS Res Hum Retroviruses **30:**685-694.
185. **Romero-Sanchez M, Gonzalez-Serna A, Pacheco YM, Ferrando-Martinez S, Machmach K, Garcia-Garcia M, Alvarez-Rios AI, Vidal F, Leal M, Ruiz-Mateos E.** 2012. Different biological significance of sCD14 and LPS in HIV-infection: importance of the immunovirology stage and association with HIV-disease progression markers. J Infect **65:**431-438.
186. **Gekonge B, Giri MS, Kossenkov AV, Nebozyhn M, Yousef M, Mounzer K, Showe L, Montaner LJ.** 2012. Constitutive gene expression in monocytes from chronic HIV-1 infection overlaps with acute Toll-like receptor induced monocyte activation profiles. PLoS One **7:**e41153.
187. **Meier A, Bagchi A, Sidhu HK, Alter G, Suscovich TJ, Kavanagh DG, Streeck H, Brockman MA, LeGall S, Hellman J, Altfeld M.** 2008. Upregulation of PD-L1 on monocytes and dendritic cells by HIV-1 derived TLR ligands. Aids **22:**655-658.
188. **Baruchel S, Wainberg MA.** 1992. The role of oxidative stress in disease progression in individuals infected by the human immunodeficiency virus. J Leukoc Biol **52:**111-114.
189. **Martensen PM, Justesen J.** 2004. Small ISGs coming forward. J Interferon Cytokine Res **24:**1-19.
190. **Cheriyath V, Leaman DW, Borden EC.** 2011. Emerging Roles of FAM14 Family Members (G1P3/ISG 6–16 and ISG12/IFI27) in Innate Immunity and Cancer. Journal of Interferon & Cytokine Research **31:**173-181.
191. **Tahara E, Tahara H, Kanno M, Naka K, Takeda Y, Matsuzaki T, Yamazaki R, Ishihara H, Yasui W, Barrett JC, Ide T, Tahara E.** 2005. G1P3, an interferon inducible gene 6-16, is expressed in gastric cancers and inhibits mitochondrial-mediated apoptosis in gastric cancer cell line TMK-1 cell. Cancer Immunology, Immunotherapy **54:**729-740.
192. **Cheriyath V, Glaser KB, Waring JF, Baz R, Hussein MA, Borden EC.** 2007. G1P3, an IFN-induced survival factor, antagonizes TRAIL-induced apoptosis in human myeloma cells. J Clin Invest **117:**3107-3117.
193. **Rosebeck S, Leaman DW.** 2008. Mitochondrial localization and pro-apoptotic effects of the interferon-inducible protein ISG12a. Apoptosis **13:**562-572.
194. **Daniel-Carmi V, Makovitzki-Avraham E, Reuven E-M, Goldstein I, Zilkha N, Rotter V, Tzehoval E, Eisenbach L.** 2009. The human1-8Dgene (IFITM2) is a novelp53independent pro-apoptotic gene. International Journal of Cancer **125:**2810-2819.

195. **Lu MY, Liao F.** 2010. Interferon-stimulated gene ISG12b2 is localized to the inner mitochondrial membrane and mediates virus-induced cell death. Cell Death and Differentiation **18:**925-936.
196. **Brass AL, Huang IC, Benita Y, John SP, Krishnan MN, Feeley EM, Ryan BJ, Weyer JL, van der Weyden L, Fikrig E, Adams DJ, Xavier RJ, Farzan M, Elledge SJ.** 2009. The IFITM Proteins Mediate Cellular Resistance to Influenza A H1N1 Virus, West Nile Virus, and Dengue Virus. Cell **139:**1243-1254.
197. **Li M.** 2000. Apoptosis Induced by Cadmium in Human Lymphoma U937 Cells through Ca2+-calpain and Caspase-Mitochondria- dependent Pathways. Journal of Biological Chemistry **275:**39702-39709.
198. **Galan A.** 2000. Stimulation of p38 Mitogen-activated Protein Kinase Is an Early Regulatory Event for the Cadmium-induced Apoptosis in Human Promonocytic Cells. Journal of Biological Chemistry **275:**11418-11424.
199. **Miguel BG, Rodriguez ME, Aller P, Martinez AM, Mata F.** 2005. Regulation of cadmium-induced apoptosis by PKCδ in U937 human promonocytic cells. Biochimica et Biophysica Acta (BBA) - Molecular Cell Research **1743:**215-222.
200. **Sancho P, Fernández C, Yuste VJ, Amrán D, Ramos AM, de Blas E, Susin SA, Aller P.** 2006. Regulation of apoptosis/necrosis execution in cadmium-treated human promonocytic cells under different forms of oxidative stress. Apoptosis **11:**673-686.
201. **Walker JA, Sulciner ML, Misgen KD, Miller AD, Burdo TH, Williams K.** 2014. Elevated Numbers of CD163+ Macrophages in Hearts of SIV Infected Monkeys Correlates with Cardiac Pathology and Fibrosis. AIDS Res Hum Retroviruses.
202. **Haupt Y, Rowan S, Oren M.** 1995. p53-mediated apoptosis in HeLa cells can be overcome by excess pRB. Oncogene **10:**1563-1571.
203. **Shinohara H, Zhou J, Yoshikawa K, Yazumi S, Ko K, Yamaoka Y, Mizukami T, Yoshida T, Akinaga S, Tamaoki T, Motoda H, Benedict WF, Takahashi R.** 2000. Retinoblastoma protein-initiated cellular growth arrest overcomes the ability of cotransfected wild-type p53 to induce apoptosis. Br J Cancer **83:**1039-1046.
204. **Jiang X, Wang X.** 2004. Cytochrome C-mediated apoptosis. Annu Rev Biochem **73:**87-106.
205. **Youle RJ, Strasser A.** 2008. The BCL-2 protein family: opposing activities that mediate cell death. Nat Rev Mol Cell Biol **9:**47-59.
206. **Ow YP, Green DR, Hao Z, Mak TW.** 2008. Cytochrome c: functions beyond respiration. Nat Rev Mol Cell Biol **9:**532-542.
207. **Chipuk JE, Moldoveanu T, Llambi F, Parsons MJ, Green DR.** 2010. The BCL-2 family reunion. Mol Cell **37:**299-310.
208. **Ola MS, Nawaz M, Ahsan H.** 2011. Role of Bcl-2 family proteins and caspases in the regulation of apoptosis. Mol Cell Biochem **351:**41-58.

209. **Malcolm KC, Worthen GS.** 2003. Lipopolysaccharide stimulates p38-dependent induction of antiviral genes in neutrophils independently of paracrine factors. J Biol Chem **278:**15693-15701.
210. **Rustagi A, Gale M, Jr.** 2014. Innate antiviral immune signaling, viral evasion and modulation by HIV-1. J Mol Biol **426:**1161-1177.
211. **Bukh AR, Melchjorsen J, Offersen R, Jensen JM, Toft L, Stovring H, Ostergaard L, Tolstrup M, Sogaard OS.** 2011. Endotoxemia is associated with altered innate and adaptive immune responses in untreated HIV-1 infected individuals. PLoS One **6:**e21275.
212. **Yan J, Sabbaj S, Bansal A, Amatya N, Shacka JJ, Goepfert PA, Heath SL.** 2013. HIV-specific CD8+ T cells from elite controllers are primed for survival. J Virol **87:**5170-5181.
213. **Hearps AC, Martin GE, Angelovich TA, Cheng WJ, Maisa A, Landay AL, Jaworowski A, Crowe SM.** 2012. Aging is associated with chronic innate immune activation and dysregulation of monocyte phenotype and function. Aging Cell **11:**867-875.
214. **Funderburg N, Kalinowska M, Eason J, Goodrich J, Heera J, Mayer H, Rajicic N, Valdez H, Lederman MM.** 2010. Effects of maraviroc and efavirenz on markers of immune activation and inflammation and associations with CD4+ cell rises in HIV-infected patients. PLoS One **5:**e13188.
215. **Wilkin TJ, Lalama CM, McKinnon J, Gandhi RT, Lin N, Landay A, Ribaudo H, Fox L, Currier JS, Mellors JW, Gulick R, Tenorio AR.** 2012. A pilot trial of adding maraviroc to suppressive antiretroviral therapy for suboptimal CD4(+) T-cell recovery despite sustained virologic suppression: ACTG A5256. J Infect Dis **206:**534-542.
216. **Gutierrez C, Diaz L, Vallejo A, Hernandez-Novoa B, Abad M, Madrid N, Dahl V, Rubio R, Moreno AM, Dronda F, Casado JL, Navas E, Perez-Elias MJ, Zamora J, Palmer S, Munoz E, Munoz-Fernandez MA, Moreno S.** 2011. Intensification of antiretroviral therapy with a CCR5 antagonist in patients with chronic HIV-1 infection: effect on T cells latently infected. PLoS One **6:**e27864.
217. **Hunt PW, Shulman NS, Hayes TL, Dahl V, Somsouk M, Funderburg NT, McLaughlin B, Landay AL, Adeyemi O, Gilman LE, Clagett B, Rodriguez B, Martin JN, Schacker TW, Shacklett BL, Palmer S, Lederman MM, Deeks SG.** 2013. The immunologic effects of maraviroc intensification in treated HIV-infected individuals with incomplete CD4+ T-cell recovery: a randomized trial. Blood **121:**4635-4646.
218. **Rusconi S, Vitiello P, Adorni F, Colella E, Foca E, Capetti A, Meraviglia P, Abeli C, Bonora S, D'Annunzio M, Di Biagio A, Di Pietro M, Butini L, Orofino G, Colafigli M, d'Ettorre G, Francisci D, Parruti G, Soria A, Buonomini AR, Tommasi C, Mosti S, Bai F, Di Nardo Stuppino S, Morosi M, Montano M, Tau P, Merlini E, Marchetti G.** 2013. Maraviroc as intensification strategy in HIV-1 positive patients with

deficient immunological response: an Italian randomized clinical trial. PLoS One **8:**e80157.

219. **Romero-Sanchez MC, Alvarez-Rios AI, Bernal-Morell E, Genebat M, Vera F, Benhnia MR, Bravo-Urbieta J, Galera-Penaranda C, de Pablo-Bernal RS, Abad-Carrillo MA, Leal M, Ruiz-Mateos E.** 2014. Maintenance of virologic efficacy and decrease in levels of beta2-microglobulin, soluble CD40L and soluble CD14 after switching previously treated HIV-infected patients to an NRTI-sparing dual therapy. Antiviral Res **111:**26-32.
220. **Puertas MC, Massanella M, Llibre JM, Ballestero M, Buzon MJ, Ouchi D, Esteve A, Boix J, Manzardo C, Miro JM, Gatell JM, Clotet B, Blanco J, Martinez-Picado J.** 2014. Intensification of a raltegravir-based regimen with maraviroc in early HIV-1 infection. Aids **28:**325-334.
221. **Sierra-Madero JG, Ellenberg SS, Rassool MS, Tierney A, Belaunzarán-Zamudio PF, López-Martínez A, Piñeirúa-Menéndez A, Montaner LJ, Azzoni L, Benítez CR, Sereti I, Andrade-Villanueva J, Mosqueda- Gómez JL, Rodriguez B, Sanne I, Lederman MM.** 2014. Effect of the CCR5 antagonist maraviroc on the occurrence of immune reconstitution inflammatory syndrome in HIV (CADIRIS): a double-blind, randomised, placebo-controlled trial. The Lancet HIV **1:**e60-e67.
222. **Lee C, Tomkowicz B, Freedman BD, Collman RG.** 2005. HIV-1 gp120-induced TNF-{alpha} production by primary human macrophages is mediated by phosphatidylinositol-3 (PI-3) kinase and mitogen-activated protein (MAP) kinase pathways. J Leukoc Biol **78:**1016-1023.
223. **Cheung R, Ravyn V, Wang L, Ptasznik A, Collman RG.** 2008. Signaling mechanism of HIV-1 gp120 and virion-induced IL-1beta release in primary human macrophages. J Immunol **180:**6675-6684.
224. **Moniuszko M, Kowal K, Rusak M, Pietruczuk M, Dabrowska M, Bodzenta-Lukaszyk A.** 2006. Monocyte CD163 and CD36 expression in human whole blood and isolated mononuclear cell samples: influence of different anticoagulants. Clin Vaccine Immunol **13:**704-707.
225. **Patro SC, Pal S, Bi Y, Lynn K, Mounzer KC, Kostman JR, Davuluri RV, Montaner LJ.** 2015. Shift in monocyte apoptosis with increasing viral load and change in apoptosis-related ISG/Bcl2 family gene expression in chronically HIV-1-infected subjects. J Virol **89:**799-810.
226. **Fjaerli HO, Bukholm G, Krog A, Skjaeret C, Holden M, Nakstad B.** 2006. Whole blood gene expression in infants with respiratory syncytial virus bronchiolitis. BMC Infect Dis **6:**175.
227. **Budhu A, Chen Y, Kim JW, Forgues M, Valerie K, Harris CC, Wang XW.** 2007. Induction of a unique gene expression profile in primary human hepatocytes by hepatitis C virus core, NS3 and NS5A proteins. Carcinogenesis **28:**1552-1560.
228. **Qi Y, Li Y, Zhang Y, Zhang L, Wang Z, Zhang X, Gui L, Huang J.** 2015. IFI6 Inhibits Apoptosis via Mitochondrial-Dependent Pathway in Dengue Virus 2 Infected Vascular Endothelial Cells. PLoS One **10:**e0132743.

229. **Dill MT, Duong FH, Vogt JE, Bibert S, Bochud PY, Terracciano L, Papassotiropoulos A, Roth V, Heim MH.** 2011. Interferon-induced gene expression is a stronger predictor of treatment response than IL28B genotype in patients with hepatitis C. Gastroenterology **140:**1021-1031.
230. **Onomoto K, Morimoto S, Kawaguchi T, Toyoda H, Tanaka M, Kuroda M, Uno K, Kumada T, Matsuda F, Shimotohno K, Fujita T, Murakami Y.** 2011. Dysregulation of IFN system can lead to poor response to pegylated interferon and ribavirin therapy in chronic hepatitis C. PLoS One **6:**e19799.
231. **Okumura A, Lu G, Pitha-Rowe I, Pitha PM.** 2006. Innate antiviral response targets HIV-1 release by the induction of ubiquitin-like protein ISG15. Proc Natl Acad Sci U S A **103:**1440-1445.
232. **Pincetic A, Kuang Z, Seo EJ, Leis J.** 2010. The interferon-induced gene ISG15 blocks retrovirus release from cells late in the budding process. J Virol **84:**4725-4736.
233. **Morales DJ, Lenschow DJ.** 2013. The antiviral activities of ISG15. J Mol Biol **425:**4995-5008.
234. **Smidt KC, Hansen LL, Sogaard TM, Petersen LK, Knudsen UB, Martensen PM.** 2003. A nine-nucleotide deletion and splice variation in the coding region of the interferon induced ISG12 gene. Biochim Biophys Acta **1638:**227-234.
235. **Steube KG, Teepe D, Meyer C, Zaborski M, Drexler HG.** 1997. A model system in haematology and immunology: the human monocytic cell line MONO-MAC-1. Leuk Res **21:**327-335.
236. **Genois N, Robichaud GA, Tremblay MJ.** 2000. Mono Mac 1: a new in vitro model system to study HIV-1 infection in human cells of the mononuclear phagocyte series. J Leukoc Biol **68:**854-864.
237. **Zhuang J, Cohen GM.** 1998. Release of mitochondrial cytochrome c is upstream of caspase activation in chemical-induced apoptosis in human monocytic tumour cells. Toxicol Lett **102-103:**121-129.
238. **Hileman CO, Kinley B, Scharen-Guivel V, Melbourne K, Szwarcberg J, Robinson J, Lederman MM, McComsey GA.** 2015. Differential Reduction in Monocyte Activation and Vascular Inflammation With Integrase Inhibitor-Based Initial Antiretroviral Therapy Among HIV-Infected Individuals. J Infect Dis **212:**345-354.
239. **Funderburg NT, Jiang Y, Debanne SM, Storer N, Labbato D, Clagett B, Robinson J, Lederman MM, McComsey GA.** 2014. Rosuvastatin treatment reduces markers of monocyte activation in HIV-infected subjects on antiretroviral therapy. Clin Infect Dis **58:**588-595.
240. **Funderburg NT, Jiang Y, Debanne SM, Labbato D, Juchnowski S, Ferrari B, Clagett B, Robinson J, Lederman MM, McComsey GA.** 2015. Rosuvastatin reduces vascular inflammation and T-cell and monocyte activation in HIV-infected subjects on antiretroviral therapy. J Acquir Immune Defic Syndr **68:**396-404.

241. **Cory TJ, Schacker TW, Stevenson M, Fletcher CV.** 2013. Overcoming pharmacologic sanctuaries. Curr Opin HIV AIDS **8:**190-195.
242. **Kumar A, Abbas W, Herbein G.** 2014. HIV-1 latency in monocytes/macrophages. Viruses **6:**1837-1860.